

12/19/88

JGM

(2)

DR-0460-X

WAPD-TM-1600  
DOE RESEARCH AND  
DEVELOPMENT REPORT

**WATER COOLED BREEDER PROGRAM  
SUMMARY REPORT  
(LWBR Development Program)**

**DO NOT MICROFILM  
COVER**

**OCTOBER 1987**

**CONTRACT DE-AC11-76PN00014**

**DISTRIBUTION OF THIS DOCUMENT IS UNLIMITED**

**BETTIS ATOMIC POWER LABORATORY  
WEST MIFFLIN, PENNSYLVANIA 15122-0079**

**Operated for the U. S. Department of Energy by  
WESTINGHOUSE ELECTRIC CORPORATION**



## **DISCLAIMER**

**This report was prepared as an account of work sponsored by an agency of the United States Government. Neither the United States Government nor any agency Thereof, nor any of their employees, makes any warranty, express or implied, or assumes any legal liability or responsibility for the accuracy, completeness, or usefulness of any information, apparatus, product, or process disclosed, or represents that its use would not infringe privately owned rights. Reference herein to any specific commercial product, process, or service by trade name, trademark, manufacturer, or otherwise does not necessarily constitute or imply its endorsement, recommendation, or favoring by the United States Government or any agency thereof. The views and opinions of authors expressed herein do not necessarily state or reflect those of the United States Government or any agency thereof.**

## **DISCLAIMER**

**Portions of this document may be illegible in electronic image products. Images are produced from the best available original document.**

WAPD-TM--1600

DE88 010121

WAPD-TM-1600  
Distribution Category UC-78

WATER COOLED BREEDER PROGRAM  
SUMMARY REPORT

(LWBR Development Program)

Prepared by members of the LWBR staff

R. Atherton, Coordinator

Contract No. DE-AC11-76PN00014

October 1987

Printed in the United States of America  
Available from the  
National Technical Information Service  
U. S. Department of Commerce  
5285 Port Royal Road  
Springfield, Virginia 22161

This report was prepared as an account of work sponsored by an agency of the United States Government. Neither the United States Government nor any agency thereof, nor any of their employees, makes any warranty, express or implied, or assumes any legal liability or responsibility for the accuracy, completeness, or usefulness of any information, apparatus, product, or process disclosed, or represents that its use would not infringe privately owned rights. Reference herein to any specific commercial product, process, or service by trade name, trademark, manufacturer, or otherwise does not necessarily constitute or imply its endorsement, recommendation, or favoring by the United States Government or any agency thereof. The views and opinions of authors expressed herein do not necessarily state or reflect those of the United States Government or any agency thereof.

**DISCLAIMER**

NOTE

This document is an interim memorandum prepared primarily for internal reference and does not represent a final expression of the opinion of Westinghouse. When this memorandum is distributed externally, it is with the express understanding that Westinghouse makes no representation as to completeness, accuracy, or usability of information contained therein.

Bettis Atomic Power Laboratory

Operated for the U.S. Department of Energy by  
WESTINGHOUSE ELECTRIC CORPORATION

West Mifflin, PA 15122-0079

**MASTER**

DISTRIBUTION OF THIS DOCUMENT IS UNLIMITED

#### NOTICE

This report was prepared as an account of work sponsored by the United States Government. Neither the United States, nor the United States Department of Energy, nor any of their employees, nor any of their contractors, subcontractors, or their employees, makes any warranty, express or implied, or assumes any legal liability or responsibility for the accuracy, completeness or usefulness of any information, apparatus, product or process disclosed, or represents that its use would not infringe privately owned rights.

## FOREWORD

The Shippingport Atomic Power Station located in Shippingport, Pennsylvania was the first large-scale, central-station nuclear power plant in the United States and the first plant of such size in the world operated solely to produce electric power. This program was started in 1953 to confirm the practical application of nuclear power for large-scale electric power generation. It has provided much of the technology being used for design and operation of the commercial, central-station nuclear power plants now in use.

Subsequent to development and successful operation of the Pressurized Water Reactor in the Atomic Energy Commission (now Department of Energy, DOE) owned reactor plant at the Shippingport Atomic Power Station, the Atomic Energy Commission in 1965 undertook a research and development program to design and build a Light Water Breeder Reactor core for operation in the Shippingport Station.

The objective of the Light Water Breeder Reactor (LWBR) program has been to develop a technology that would significantly improve the utilization of the nation's nuclear fuel resources employing the well-established water reactor technology. To achieve this objective, work has been directed toward analysis, design, component tests, and fabrication of a water-cooled, thorium oxide-uranium oxide fuel cycle breeder reactor for installation and operation at the Shippingport Station. The LWBR core started operation in the Shippingport Station in the Fall of 1977 and finished routine power operation on October 1, 1982. After End-of-Life core testing, the core was removed and the spent fuel shipped to the Naval Reactors Expended Core Facility for detailed examination to verify core performance including an evaluation of breeding characteristics.

In 1976, with fabrication of the Shippingport LWBR core nearing completion, the Energy Research and Development Administration, now DOE, established the Advanced Water Breeder Applications (AWBA) program to develop and disseminate technical information which would assist U. S. industry in evaluating the LWBR concept for commercial-scale applications. The AWBA program, which was concluded in September, 1982, explored some of the problems that would be faced by industry in adopting technology confirmed in the LWBR program. Information developed includes concepts for commercial-scale prebreeder cores which would produce uranium-233 for light water breeder cores while producing electric power, improvements for breeder cores based on the technology developed to fabricate and operate the Shippingport LWBR core, and other information and technology to aid in evaluating commercial-scale application of the LWBR concept.

All three development programs (Pressurized Water Reactor, Light Water Breeder Reactor, and Advanced Water Breeder Applications) have been conducted under the technical direction of the Office of the Deputy Assistant Secretary for Naval Reactors of DOE.

Technical information developed under the Shippingport, LWBR, and AWBA programs has been published in technical memoranda, one of which is this present report.

## TABLE OF CONTENTS

	<u>Page</u>
List of Figures.....	xi
List of Tables.....	xii
1 INTRODUCTION.....	3
1.1 Objective.....	3
1.2 Breeder Reactor Concept.....	4
1.3 Importance of Breeding.....	6
1.4 Use of the Shippingport Plant.....	9
1.5 Water Cooled Breeder Contributions to Reactor Technology.....	11
2 LWBR REACTOR DESIGN.....	15
2.1 General Description.....	15
2.2 LWBR Fuel.....	15
2.3 Fuel Module Design.....	19
2.4 Variable Geometry Control.....	19
2.5 Simulating a Large Breeder in the Shippingport Reactor Vessel.....	22
2.6 Design Features.....	22
3 MANUFACTURE OF THE LWBR CORE.....	31
3.1 Fuel Pellets.....	31
3.1.1 Fuel Pellet Design.....	31
3.1.2 Fuel Pellet Fabrication.....	33
3.1.2.1 Background.....	33
3.1.2.2 Process Description.....	34
3.1.3 Fuel Fabrication Facility Description.....	38
3.1.4 Additional Information.....	38
3.2 Fuel Rods.....	38
3.2.1 Introduction.....	38
3.2.2 Fuel Element Design.....	39

TABLE OF CONTENTS (Cont)

	<u>Page</u>
3.2.3    Fuel Rod Fabrication Process Outline.....	43
3.2.3.1    Component Preparation.....	43
3.2.3.2    Tube Assembly Processing.....	43
3.2.3.3    Processing and Inspection of Fuel Rods.....	44
3.2.4    Additional Information.....	45
3.3    Fabrication of Fuel Rod Support Grids for the Shippingport LWBR.....	45
3.3.1    Introduction.....	45
3.3.2    Description of LWBR Grids.....	46
3.3.3    Materials Used in Grid Construction.....	46
3.3.3.1    AM-350 Precipitation Hardening Stainless Steel.....	46
3.3.3.2    Braze Alloy.....	50
3.3.4    Manufacturing Operations.....	50
3.3.4.1    General Process Outline.....	50
3.3.4.1.1    Sheet Metal Stamped Components.....	50
3.3.4.1.2    Machined Components.....	50
3.3.4.1.3    Grid Component Assembly Pins.....	51
3.3.4.2    Component Assembly.....	51
3.3.4.3    Furnace Brazing of Grids.....	51
3.3.4.4    Decarburization.....	51
3.3.4.5    Dimensional Inspection and Adjustment.....	51
3.3.4.6    Grid Tempering.....	52
3.3.4.7    Post-Temper Dimensional Inspection and Adjustment.....	52
3.3.4.8    Grid Preconditioning.....	52
3.3.4.9    Final Inspection and Adjustment of Grid Dimensions and Attributes.....	52
3.3.5    Additional Information.....	53

TABLE OF CONTENTS (Cont)

	<u>Page</u>
3.4 Fuel Module Fabrication.....	53
3.4.1 Preassembly.....	53
3.4.2 Fuel Rod Installation.....	54
3.4.3 Final Assembly.....	54
3.4.4 Inspection.....	54
3.4.5 Additional Information.....	55
4 PLANT MODIFICATIONS MADE PRIOR TO LWBR OPERATION.....	57
4.1 Introduction.....	57
4.2 Plant Modifications or Upgradings Accomplished.....	57
4.2.1 Incorporation of the Auxiliary Control Room.....	57
4.2.2 Incorporation of the Containment Isolation System.....	58
4.2.3 Addition of Flywheel Generators to Main Coolant Pump Circuitry .....	59
4.2.4 Replacement of the 1A and 1D Steam Generator Heat Exchangers .....	59
4.2.5 Additional Information .....	60
5 INSTALLATION OF THE LIGHT WATER BREEDER REACTOR.....	61
6 OPERATION OF THE LWBR CORE IN THE SHIPPINGPORT ATOMIC POWER STATION.....	63
6.1 Introduction.....	63
6.2 Nuclear Performance.....	63
6.3 Thermal Performance.....	64
6.4 Hydraulic Performance.....	65
6.4.1 Flow and Pressure Drop.....	65
6.5 Reactor Coolant Chemistry.....	65
6.5.1 Reactor Coolant Water Conditions.....	65
6.5.2 Base and Operational Radionuclide Levels.....	66
6.5.2.1 Base Level Fission and Activation Products.....	66
6.5.2.2 Routinely Monitored Radionuclides.....	66

## TABLE OF CONTENTS (Cont)

	<u>Page</u>
6.6 Plant Operating Experience.....	67
6.6.1 Introduction.....	67
6.6.2 Maintenance.....	68
6.6.3 Additional Information.....	68
7 DEFUELING AND SHIPMENT OF THE LWBR CORE FUEL.....	69
7.1 Introduction.....	69
7.2 Defueling Safety.....	69
7.3 Summary of Defueling Operations.....	70
7.4 Disassembly of LWBR Fuel Modules.....	71
7.5 Loading and Shipping Operations.....	71
7.5.1 Additional Information.....	72
8 END-OF-LIFE EVALUATION.....	73
8.1 Introduction.....	73
8.2 The Two-Stage Stratified Random Sampling Plan Objectives.....	73
8.2.1 Objectives.....	73
8.2.2 Simulation Studies Used to Develop the Sampling Plan.....	74
8.2.3 Selection of Twelve Proof-of-Breeding Modules.....	74
8.2.4 Selection of Five Hundred Proof-of-Breeding Rods.....	75
8.2.5 Selection of Twenty-Four Additional Rods.....	76
8.2.6 Selection of Seventeen Rods for Destructive Assay.....	76
8.2.7 Additional Information.....	76
8.3 Proof of Breeding.....	77
8.3.1 Introduction.....	77
8.3.2 Sample Selection.....	77
8.3.3 Nondestructive Assay Techniques.....	80
8.3.4 Assay Results.....	80

## TABLE OF CONTENTS (Cont)

	<u>Page</u>
8.3.4.1 General.....	80
8.3.4.2 Destructive Versus Nondestructive Results.....	83
8.3.4.3 Symmetry Results.....	83
8.3.4.4 Final Results.....	85
8.3.5 Additional Information.....	88
8.4 Core Component Examination.....	88
8.4.1 Introduction.....	88
8.4.2 Major Assembly Examination.....	88
8.4.3 Additional Information.....	90
8.5 Nondestructive Examination of LWBR Fuel Rods.....	90
8.5.1 Introduction.....	90
8.5.2 Examinations Performed.....	91
8.5.3 Examination Results and Conclusions.....	92
8.5.4 Additional Information.....	96
8.6 Destructive Examination of LWBR Fuel Rods.....	97
8.6.1 Introduction.....	97
8.6.2 Iodine and Cesium Analysis of the Fuel and Cladding.....	97
8.6.3 Tensile Testing of the Cladding.....	98
8.6.4 Summary and Conclusions.....	99
8.6.5 Additional Information.....	103
8.7 Examination of LWBR Grids and Other Module Structural Components.....	103
8.7.1 Introduction.....	103
8.7.2 Components and Materials Selected for EOL Examination and Examination Results.....	103
8.7.2.1 Grids.....	103
8.7.2.2 Results of Examinations of Grids.....	105
8.7.2.3 Bolts, Screws, and Washers.....	105

## TABLE OF CONTENTS (Cont)

		<u>Page</u>
	8.7.2.4      Results of Examination of Bolts, Screws, and Washers.....	106
	8.7.2.5      Plates and Shells.....	106
	8.7.2.6      Results of Examinations of Plates and Shells.....	106
	8.7.2.7      Tubes.....	106
	8.7.2.8      Results of Examinations of Tubes.....	107
	8.7.2.9      Shear Keys and Struts.....	107
	8.7.2.10     Results of Examination of Shear Keys and Struts.....	107
	8.7.2.11     Posts and Shafts.....	107
	8.7.2.12     Results of Examinations of Posts and Shafts.....	107
	8.7.3      Additional Information.....	107
9	LONG TERM FUEL STORAGE.....	109
9.1	Introduction.....	109
9.2	Fuel Shipment Operations.....	109
9.3	Idaho Chemical Processing Plant Facility and Fuel Storage.....	111
9.3.1	Additional Information.....	113
10	SUMMARY OF ADVANCED WATER BREEDER APPLICATIONS WORK.....	115
10.1	Introduction.....	115
10.2	Advanced Breeder Concepts.....	116
10.2.1	LWBR Scale-Up Concept.....	116
10.2.2	Movable Thorium Finger Rod Controlled Breeder Concept.....	117
10.2.3	Advanced Movable Fuel Breeder Concept.....	119
10.2.4	Seed-Blanket Prebreeder/Breeder System Concept....	121
10.2.5	Additional Information.....	122

TABLE OF CONTENTS (Cont)

	<u>Page</u>
APPENDIX A SUMMARY OF PUBLISHED LWBR TECHNICAL MEMORANDA.....	A-1
APPENDIX B SUMMARY OF PUBLISHED AWBA TECHNICAL MEMORANDA.....	B-1

## LIST OF FIGURES

<u>Figure</u>	<u>Title</u>	<u>Page</u>
1	Neutron Yield Per Neutron Absorbed, $n$ , Versus Energy of Neutron Absorbed.....	5
2	Energy Potential Comparison.....	7
3	Effect of Fissile Inventory Ratio at End of Core Life on Fuel Utilization for a Typical Light Water Breeder Reactor.....	8
4	LWBR Core in Shippingport Reactor Vessel.....	16
5	LWBR Core Cross Section.....	17
6	Typical LWBR Fuel Module Cross Section.....	18
7	Variable Geometry Nuclear Control Concept.....	21
8	LWBR Blanket Module, Vertical View; LWBR Seed Balance Piston Assembly, Cutaway View.....	24
9	LWBR Core Control Drive Mechanism.....	25
10	Typical LWBR Seed Rod Support Grid.....	26
11	Typical LWBR Blanket Rod Support Grid.....	27
12	Typical LWBR Blanket Grid.....	28
13	General Dimensions and Components of Seed Fuel Rods.....	40
14	General Dimensions and Components of Reflector Fuel Elements.....	41
15	General Dimensions and Components of Blanket Fuel Rods.....	42
16	Seed Rod Support Grid.....	47
17	Blanket Rod Support Grid (Type I).....	48
18	Reflector Rod Support Grid (Type IV).....	49
19	Sample Modules for LWBR Core.....	78
20	Rod Sampling for Blanket III-6 Modules.....	79
21	PIFAG Schematic Diagram.....	81

## LIST OF TABLES

<u>Table</u>	<u>Title</u>	<u>Page</u>
1	Core and Plant Parameters for the LWBR Core in Shippingport.....	30
2	Regular Blanket III-6 Fissile Loadings in Grams .....	82
3	Comparison of Module Loadings for Symmetric Modules .....	84
4	Nondestructive Assay Results for 12 LWBR Fuel Modules .....	86
5	Total Fissile Fuel Loadings and FIR for the LWBR Core .....	87

## ABSTRACT

The purpose of the Department of Energy Water Cooled Breeder Program was to demonstrate practical breeding in a uranium-233/thorium fueled core while producing electrical energy in a commercial water reactor generating station. A demonstration Light Water Breeder Reactor (LWBR) was successfully operated for more than 29,000 effective full power hours in the Shippingport Atomic Power Station. The reactor operated with an availability factor of 76 percent and had a gross electrical output of 2,128,943,470 kilowatt hours.

Following operation, the expended core was examined and no evidence of any fuel element defects was found. Nondestructive assay of 524 fuel rods determined that 1.39 percent more fissile fuel was present at the end of core life than at the beginning, proving that breeding had occurred. This demonstrates the existence of a vast source of electrical energy using plentiful domestic thorium potentially capable of supplying the entire national need for many centuries.

To build on the successful design and operation of the Shippingport Breeder Core and to provide the technology to implement this concept, several reactor designs of large breeders and prebreeders were developed for commercial-sized plants of 900 to 1000 Mw(e) net.

This report summarizes the Water Cooled Breeder Program from its inception in 1965 to its completion in 1987. Four hundred thirty-six technical reports are referenced which document the work conducted as part of this program. This work demonstrated that the Light Water Breeder Reactor is a viable alternative as a PWR replacement in the next generation of nuclear reactors. This transition would only require a minimum of change in design and fabrication of the reactor and operation of the plant.

(Intentionally Blank)

WATER COOLED BREEDER PROGRAM  
SUMMARY REPORT

(LWBR Development Program)

SECTION 1 - INTRODUCTION

1.1 - OBJECTIVE

The objective of the Department of Energy (DOE) Light Water Breeder Reactor (LWBR) Program, begun in December 1965, was to develop the technology to breed in a light water reactor and to expand nuclear fuel resources vastly for water thermal reactors. To achieve this objective, technology was developed by designing, fabricating, and operating a breeder reactor in the existing DOE-owned pressurized water reactor plant in Shippingport, Pennsylvania.

The objective of the Shippingport Atomic Power Station was to make available for the nation's use the basic pressurized light water reactor technology, including the development and testing of advanced design reactor concepts. Operation of the LWBR core in the Shippingport plant was an extension of the development work that had been carried out at this facility since its initial operation in 1957. After five years of core operation, the reactor was defueled and the expended core was shipped to the Expendable Core Facility for core examination and proof of breeding. There it was determined that the fissile fuel inventory was 1.39 percent greater than the fissile fuel inventory at the beginning of core life. This proof of breeding is discussed in WAPD-TM-1612, October 1987, listed in Section 1-H of Appendix A to this document.

The Light Water Breeder Reactor used a fertile material, thorium, that is in plentiful supply and for which there has been no other major energy-related use. All but one of the commercial power reactors currently in operation in this country are of the light water type. The operation of the LWBR core in the Shippingport Atomic Power Station has confirmed breeding in a pressurized light water reactor using the thorium/uranium-233 fuel system in a seed-blanket core configuration. This reactor was designed to breed more fissile fuel from thorium than it consumed, while producing electrical energy. This means that an LWBR replacement core could be produced from the expended fuel

of a previous LWBR without requiring further mining and enrichment of uranium. The LWBR effort was directed toward developing a demonstration core for operation in the Shippingport pressurized water reactor, and development work confirmed that similar cores could be used in any pressurized water reactor. No inherent limitations were discovered that would prevent application of the LWBR concept to boiling light water reactor plants.

## 1.2 - BREEDER REACTOR CONCEPT

A breeder reactor produces more fissile nuclear fuel than it consumes while it is producing energy for the generation of electricity. When fissile fuel, such as uranium-233, undergoes fission in a breeder reactor, the amount of new fissile fuel produced from non-fissile but "fertile" thorium in the reactor exceeds the amount of fissile fuel depleted in producing energy.

Each atom that fissions after absorbing a neutron ejects two or three more neutrons, averaging about 2.5 neutrons per fission. One of these neutrons is required to cause another fission and to keep the chain reaction going. A fraction of a neutron is captured parasitically in fissile fuel and in other reactor materials. The remaining neutrons are available for absorption by atoms of fertile materials, causing conversion to fissile material. Calculations show that it is not possible to breed in a light water reactor fueled with  $^{235}\text{U}$  and thorium because not enough neutrons are produced in fission. However,  $^{233}\text{U}$  releases enough additional neutrons during fission and has a small enough parasitic capture of neutrons to make it feasible to breed in a light water reactor (see Figure 1).

Most reactors designed and built to date have utilized  $^{235}\text{U}$  as the fissile material since it is the only naturally occurring fissile material. However, the amount of  $^{235}\text{U}$  available is quite limited, representing only 0.7 percent of naturally occurring uranium. The total energy potentially available from reasonably assured U.S. reserves of economically recoverable  $^{235}\text{U}$  is substantially less than the energy potentially available from known U.S. fossil fuel reserves. Thus, long-range plans for a nuclear power industry that would make a significant contribution to total energy resources have looked to two fertile materials:  $^{238}\text{U}$ , which makes up over 99 percent of all natural

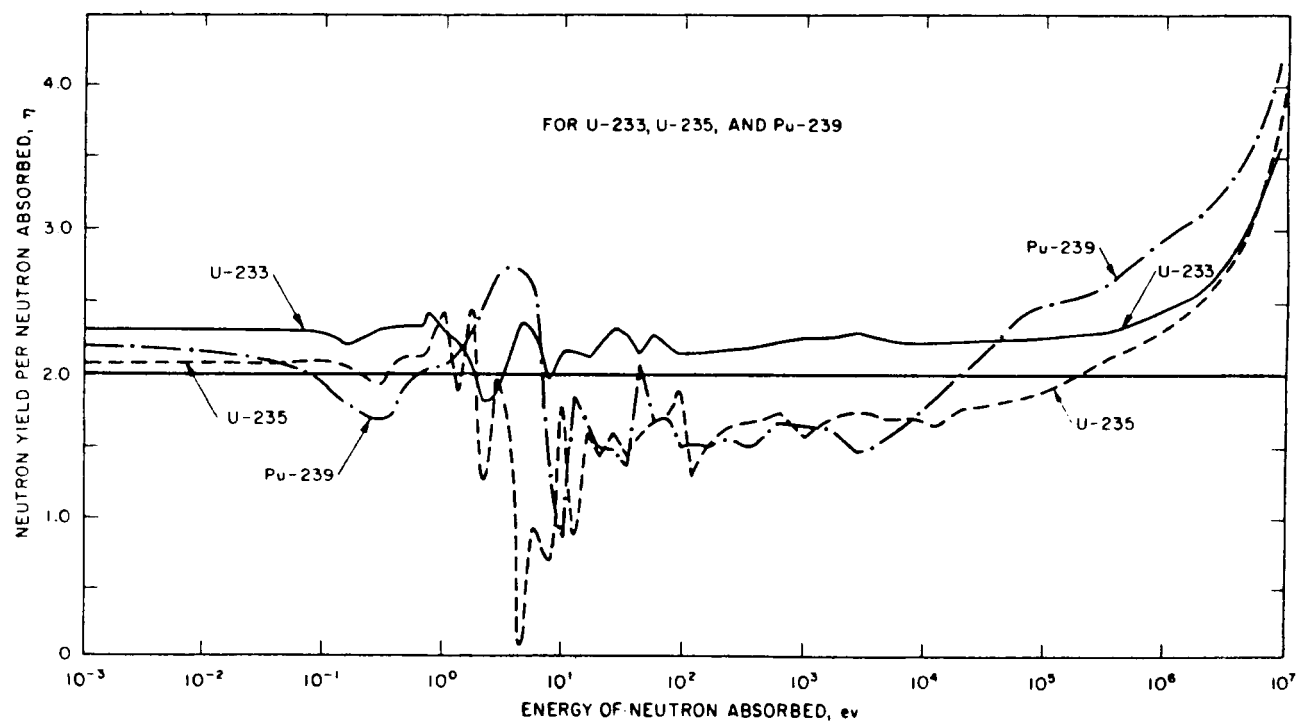
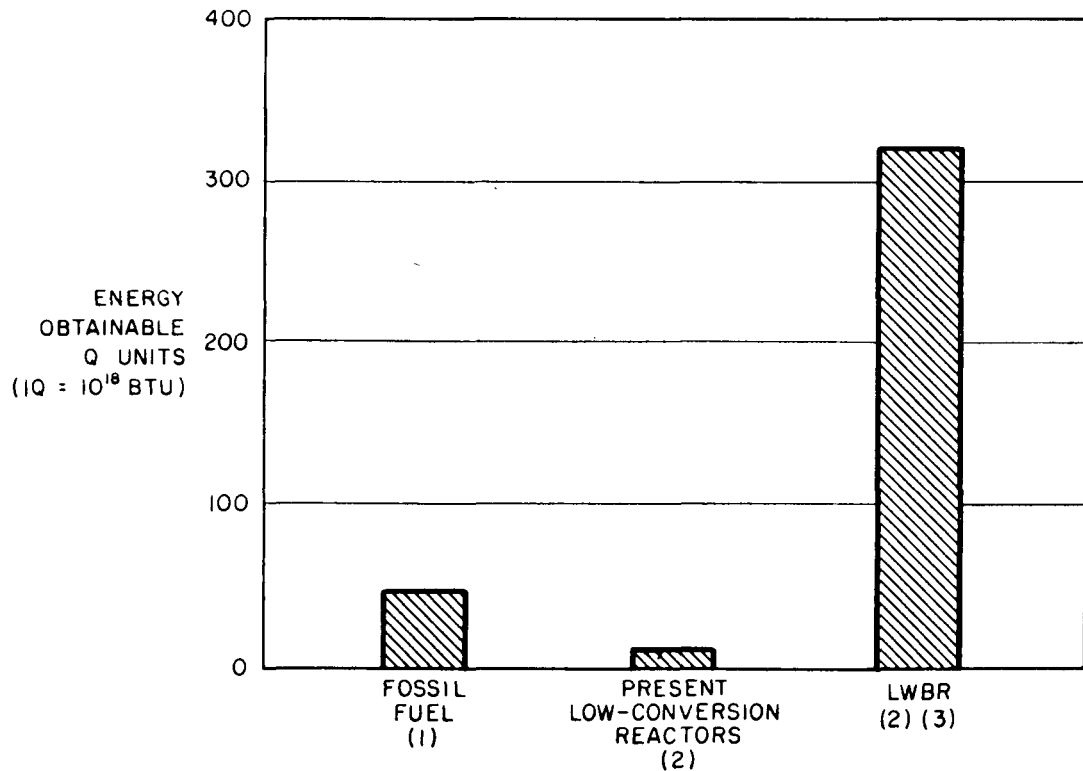


Figure 1. Neutron Yield Per Neutron Absorbed,  $\eta$ , Versus Energy of Neutron Absorbed

uranium, and thorium. While these materials themselves cannot be used to produce a nuclear chain reaction, they can (under irradiation) be converted into the fissile fuels  $^{239}\text{Pu}$  and  $^{233}\text{U}$ , respectively. In the neutron energy spectrum of light water reactors,  $^{239}\text{Pu}$  captures too many neutrons parasitically to permit breeding. Uranium-233 does emit enough neutrons per fission and parasitically captures few enough neutrons in a water reactor to permit breeding. As shown in Figure 2, the energy potentially available from the fertile material thorium is many times greater than the energy potential of either fossil fuel resources or uranium fuel resources using present low-conversion reactors. To appreciate the significance of this figure, one must realize that current national energy requirement is about 1.0 Q per year.

### 1.3 - IMPORTANCE OF BREEDING

The importance of breeding is further illustrated in Figure 3. This figure, which plots fuel utilization (the percent of mined fuel that is fissioned to obtain useful thermal energy) for typical light water breeder reactor parameters as a function of the fissile inventory ratio at the end of core life, also shows the effect of losses assumed in recycling the fuel to a new core loading. The fissile inventory ratio at any point in core life is the ratio of the amount of fissile fuel in the core at that time to that at the beginning of life. All breeder reactors, including the light water breeder, require reprocessing of expended cores and refabrication of the recovered fuel material in subsequent cores. It is evident from Figure 3 that if the Fissile Inventory Ratio at end of core life exceeds unity by enough to compensate for an assumed 1 percent recycle loss (both reprocessing and refabrication), about 50 percent of the total thorium resources could ultimately be converted to  $^{233}\text{U}$  and fissioned to produce electric power. Figure 3 further shows that when the Fissile Inventory Ratio is less than 1.00 plus the assumed recycling losses, the percent of available fuel that is fissioned to obtain useful energy is drastically reduced. The primary reason for this abrupt decrease in fuel utilization is that when the cycle is not self-sustaining in terms of fissile inventory, makeup fissile material (ultimately  $^{235}\text{U}$ ) must be mined and enriched. For every unit of  $^{235}\text{U}$  required, about 200 units of natural uranium



NOTES:

- (1) BASED ON U.S. GEOLOGICAL SURVEY PROFESSIONAL PAPER 820, (1973), AND BUREAU OF MINES BULLETIN 650, (1970).
- (2) BASED ON WASH-1097, (1969) AND "OUTLOOK FOR URANIUM," J.A. PATTERSON, USAEC 17 TH MINERALS SYMPOSIUM (CASPER, WYOMING), (1974).
- (3) BASED ON WASH-1097, (1969), AND WASH-1535 (PROPOSED FINAL), (1974), ASSUMING 1% FUEL LOSSES DURING RECYCLE OPERATIONS.

Figure 2. Energy Potential Comparison

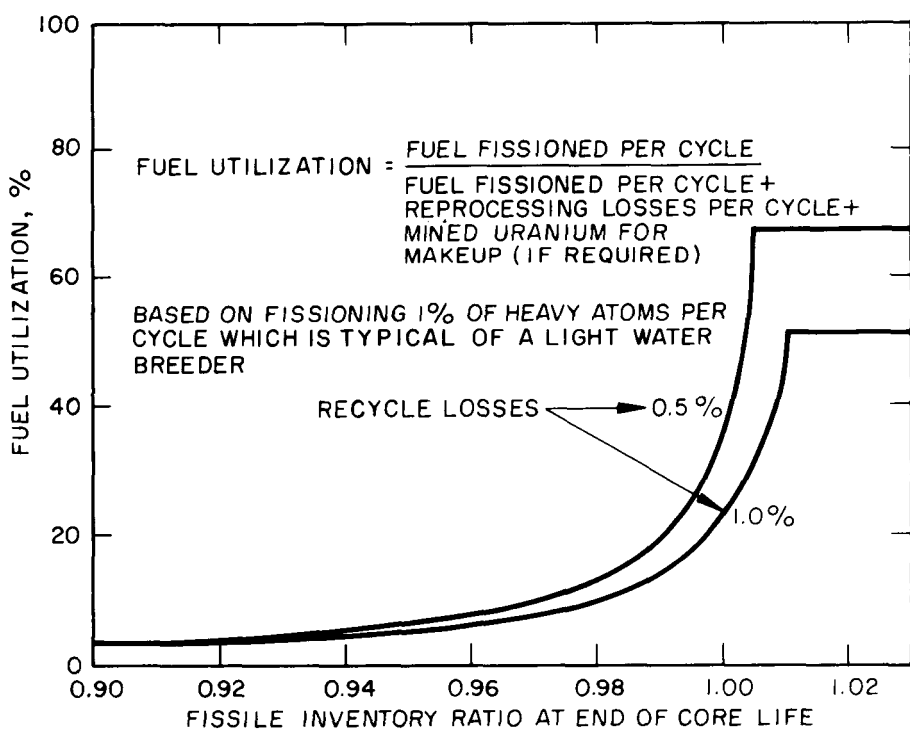


Figure 3. Effect of Fissile Inventory Ratio at End of Core Life on Fuel Utilization for a Typical Light Water Breeder Reactor

must be mined and enriched, and this leads to the great drop in fuel utilization shown in Figure 3. Present light water reactors have a Fissile Inventory Ratio in the range of 0.5 to 0.7 at the end of life.

Breeding to the extent of recovering the original fuel inventory plus recycling losses is of the utmost importance if nuclear fuel is to be a significant energy resource. Once the Fissile Inventory Ratio is high enough to avoid the need for makeup fissile material, nearly all the fertile material can eventually be fissioned except that lost in reprocessing. The overall fuel utilization will then depend only on the fractional depletion obtained in each core reloading cycle and the reprocessing loss each time the fuel is recycled. A high Fissile Inventory Ratio above that required for self-sustaining breeding will increase the fissile fuel supply, but will not affect the fuel utilization.

#### 1.4 - USE OF THE SHIPPINGPORT PLANT

On July 16, 1953, the Atomic Energy Commission (AEC) decided to construct the United States' first large-scale central station nuclear power plant using a pressurized light water reactor (PWR). This project was started to confirm the practicability of nuclear power for civilian purposes and to provide the technology necessary for design and operation of large-scale central station nuclear power plants. Because of its extensive naval work with pressurized light water reactors, Naval Reactors was assigned the responsibility for the PWR Project, under which the Shippingport Atomic Power Station was constructed. From its inception, the Shippingport Atomic Power Station was a joint project of the AEC and subsequently DOE, and the Duquesne Light Company of Pittsburgh, Pennsylvania. The DOE owned the reactor plant portion of the station, which was designed and developed by Bettis Atomic Power Laboratory under the technical direction of Naval Reactors. The Bettis Atomic Power Laboratory is operated for DOE by Westinghouse Electric Corporation.

The Shippingport reactor achieved criticality December 2, 1957 on the 15th anniversary of criticality of the world's first reactor under the University of Chicago West Stand. Shippingport produced electrical power for the first time on December 18, 1957, and 5 days later reached its full power of

60 Mw(e) net. The objective of the Shippingport Station was advancement of basic pressurized light water reactor technology by operation of reactor cores. Numerous tests were conducted in the highly instrumented nuclear plant to evaluate the reactor plant, as well as core design and performance. The first core, PWR-Core I, operated from December 2, 1957 to February 13, 1964, and PWR-Core II operated from April 30, 1965 to February 4, 1974. Data obtained from the operation of the Shippingport Station has been widely disseminated in over 2000 published reports, and has played a major role in the development of the commercial nuclear power industry.

The third reactor to be operated at Shippingport was LWBR. The LWBR core was installed in the Shippingport plant and began operation in 1977. The LWBR Program confirmed the breeding potential of the LWBR concept by operation of a breeder reactor core in an existing light water reactor plant. It included development of the supporting technologies required for the successful operation of a breeder reactor including: (1) the development of a thorough understanding of the nuclear and material characteristics of the thorium/uranium-233 fuel system, (2) the analytical and experimental development supporting improved performance of Zircaloy-clad thorium oxide fuel, (3) the engineering design of a practical variable geometry control system which accomplished all normal control functions without parasitic loss of neutrons, and (4) the design of a reliable fuel rod support system with minimum detrimental effect on neutron economy.

The LWBR core design was based on the use of the Shippingport Station because of Bettis and Naval Reactors experience with the detailed plant design characteristics. No major changes to the Shippingport reactor plant were required to accommodate the LWBR core. The principal new components were the LWBR reactor core with associated reactor vessel head and control drive mechanisms, and four flywheel generators. The 20-year old station was upgraded to reflect then current standards of the Nuclear Regulatory Commission. Because of the technological soundness and conservatism of the original design of Shippingport, this required the addition of only four new structures and associated system changes as discussed in Section 4.

The LWBR provided about 5 years of power operation at Shippingport. During this time, the reactor core fissile fuel inventory grew to 1.39 percent more fissile fuel than at the beginning of life. Subsequent to the end of operation, special examinations and tests were performed to confirm the predicted breeding performance. These examinations and tests are discussed in Section 8.

#### 1.5 - WATER COOLED BREEDER CONTRIBUTIONS TO REACTOR TECHNOLOGY

The operation of the LWBR core at Shippingport was intended primarily to accomplish three things. First, it was to prove that breeding could be achieved in a light water nuclear power plant. Second, it was to confirm a practical way to use a source of fuel (thorium) in plentiful supply and with no other major energy-related use. Third, it was to show that a light water breeder reactor utilizing thorium fuel could be installed directly into an existing pressurized water nuclear power plant using the same pressure vessel, heat exchangers, piping systems, etc., with few modifications. These three objectives were accomplished.

The LWBR Program also provided important contributions to general reactor technology, the same as developmental work for the original Shippingport Project provided basic technology to the then emerging commercial nuclear power industry. The technology developed in the LWBR program has potential applicability not only to the present light water reactor nuclear industry, but also to the development of new reactor types.

The LWBR program began at a time when the technical information about the thorium fuel cycle was very limited and inaccurate. An important part of the technology development was to vastly expand the knowledge about the thorium fuel cycle in the areas of nuclear, physical, thermal, mechanical, and metallurgical properties. In addition, extensive work was done in the area of fuel rod design and irradiation testing. This technology has been published in a book, "ThO<sub>2</sub> Thorium Dioxide - Properties and Nuclear Applications" and printed by the Government Printing Office. Extensive development was also done in rod support grid design and manufacture, in control drive mechanism design and

in design of a movable fuel reactivity control balancing system. All of these technology developments are documented in the technical memoranda indexed in Appendix A.

Prior to operating the Light Water Breeder Reactor in Shippingport, a final environmental statement, ERDA 1541 dated June 1976, was issued. This report included a comprehensive evaluation of environmental impact of not only the LWBR demonstration at Shippingport but also of the impact of implementing this technology in a large industry of breeders. This five volume statement therefore provides a comprehensive summary of all aspects of implementation of the LWBR for large scale generation of electric power.

The Advanced Water Breeder Applications (AWBA) Program, established in 1976, was a part of the DOE Water Cooled Breeder Program. To build on the successful design and operation of the Shippingport breeder core and to provide the technology to implement this concept for improved fuel utilization, Bettis Atomic Power Laboratory developed three self-sustaining breeder concepts and Knolls Atomic Power Laboratory (KAPL) developed one concept for commercial-sized plants of 900 to 1000 Mw(e) net. The first of the breeder concepts, called the "scale-up" concept, used the same fuel assembly and control system designs as the Shippingport core. This concept was developed to identify and resolve any potential technical concerns related to extrapolating the small Shippingport LWBR to a larger, commercial-size core. The second Bettis concept employed movable thoria finger rods (analogous to the poison rods of commercial cores) for reactivity control, rather than the large movable fuel assemblies of the scale-up concept. This concept, which employed fuel management with annual refueling shutdowns, provided reduced power peaking factors, thus increasing core power density. The third Bettis concept, a batch-loaded concept, utilized smaller fuel assembly sizes for simpler reprocessing plant disassembly (shearing) equipment, was capable of being assembled remotely using high radiation level recycle fuel, and provided additional margin for breeding in the equilibrium cycle. The fourth breeder concept, developed by KAPL, incorporated a stationary seed-blanket core arrangement plus

movable thoria shim rods in combination with a typical commercial PWR reactivity control system. This work demonstrated the flexibility of the LWBR concept.

To provide the initial fuel loading for a commercial breeder, prebreeder reactors would be necessary to use enriched natural uranium ( $^{238}\text{U}$  and  $^{235}\text{U}$ ) and thorium to produce electrical energy and to produce  $^{233}\text{U}$  from the thorium. After sufficient  $^{233}\text{U}$  is accumulated to fuel a self-sustaining breeder core, no further prebreeder operation would be necessary to support the breeder, and no further mining of uranium ore to produce  $^{235}\text{U}$  would be necessary. The prebreeder could be in a separate reactor plant, or the initial prebreeder and subsequent breeder reactors could be integrated into a single plant concept. The AWBA work included the development of conceptual designs for such commercial-sized prebreeder cores.

These AWBA developments had the objectives of: (1) verifying that utilization of the LWBR technology on a commercial scale was feasible, and (2) identifying the more important aspects of LWBR technology that could be modified to incorporate standard commercial PWR design features, thus making the breeder concept more economically attractive. This work demonstrated that the light water breeder was a viable alternative as a PWR replacement in the next generation of nuclear reactors and that the transitions would require a minimum of change in design and fabrication of the reactor and operation of the plant. Details on these developments are summarized in Section 10. Appendix B lists the 68 detailed reports issued on the AWBA program.

(Intentionally Blank)

## SECTION 2 - LWBR REACTOR DESIGN

### 2.1 - GENERAL DESCRIPTION

The LWBR core was developed for reactor operation within the constraints of the Shippingport plant. The interior modules were designed so that they could be used directly in a large LWBR core. The design provided a good simulation of a large LWBR core environment in the interior of the core, and permitted net breeding in the entire core. In the reactor (Figure 4), hexagonal modules were arranged in a symmetric array surrounded by a reflector region (Figure 5). Filler units were arranged outside of the reflector region to take up space between the reflector and the core barrel.

Figure 4 shows the arrangement of the new reactor core components in the Shippingport reactor vessel. Each of the 12 hexagonal fuel modules contained an identical central movable seed surrounded by a stationary blanket as shown in Figure 5. Each of these assemblies contained a lattice of rod-type fuel elements arranged in a hexagonal pattern as shown in Figure 6.

Each central movable seed region was attached to, moved by, and supported by a control drive mechanism which, in turn, was attached to the reactor vessel head. The head provided the cover for the vessel and was bolted to the vessel as shown in Figure 4.

Water entered the vessel through four inlet nozzles at the bottom of the reactor vessel (only two inlet and two outlet nozzles are shown in Figure 4; actually, there are inlet and outlet nozzles for each of the four reactor coolant loops). The water was heated as it flowed upward through the modules past the fuel elements, and exited the vessel through the outlet nozzles after a single pass through the core.

### 2.2 - LWBR FUEL

The LWBR fuel was in the form of cylindrically shaped ceramic fuel pellets, which were loaded into cylindrical tubes or rods whose ends were capped and sealed shut by welding after the rod was backfilled with helium. The

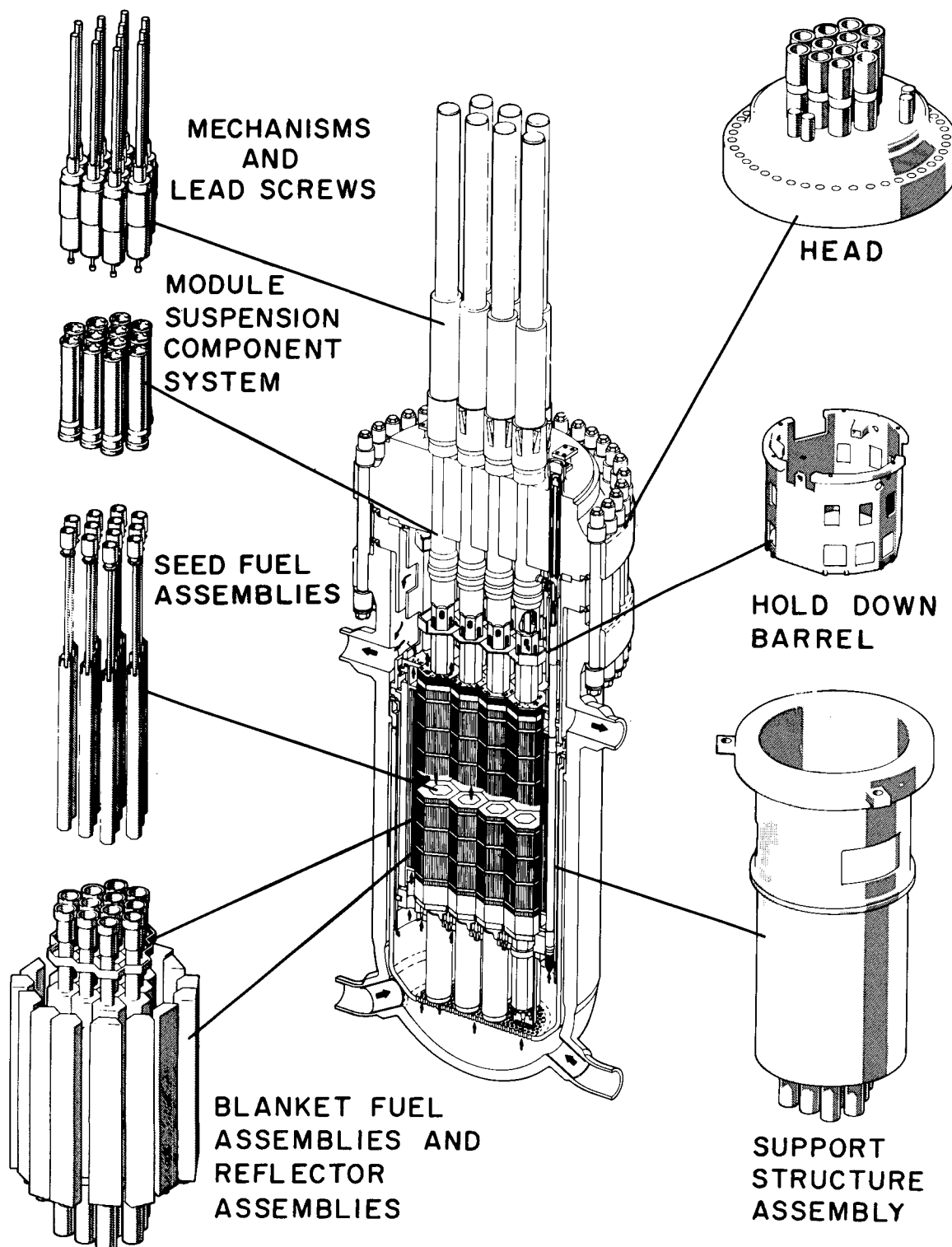


Figure 4. LWBR Core in Shippingport Reactor Vessel

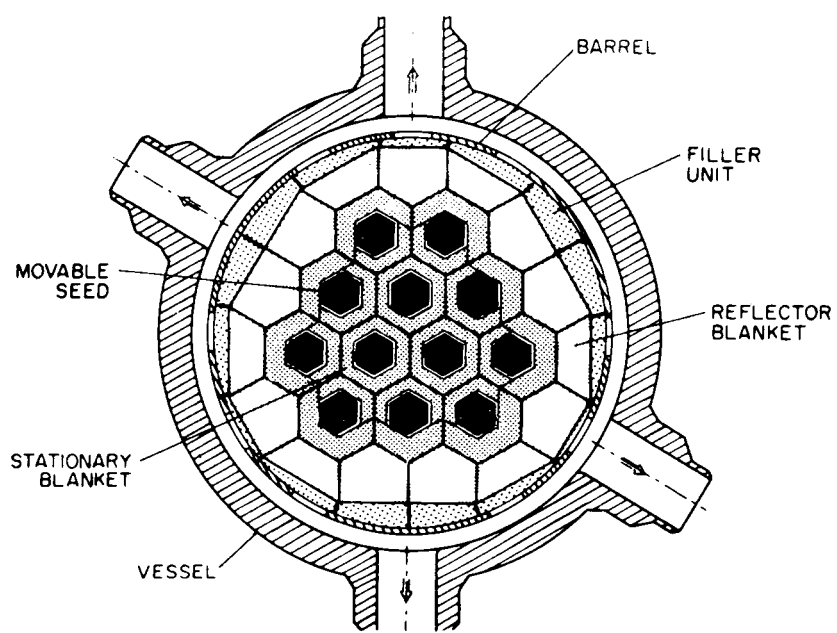


Figure 5. LWBR Core Cross Section

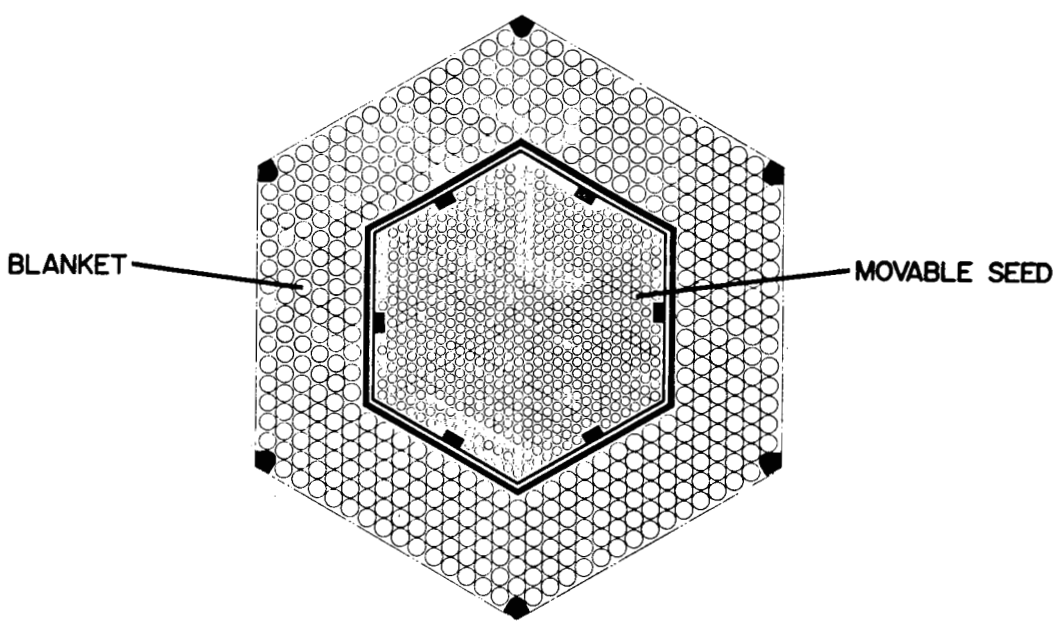


Figure 6. Typical LWBR Fuel Module Cross Section

tubes were made of Zircaloy-4, an alloy of zirconium, which has good heat transfer and corrosion resistance properties and a low probability for capturing neutrons.

In the seed and blanket regions, the fuel pellets contained a mixture of  $^{233}\text{U}$  and thorium, both in oxide form (i.e., urania ( $\text{UO}_2$ ) and thoria ( $\text{ThO}_2$ )). In the seed region, the  $^{233}\text{U}$  loading was about 5 to 6 weight percent (w/o) of uranium oxide in the thoria. In the blanket, the  $^{233}\text{U}$  loading was about 1.5 to 3 w/o uranium oxide. In the reflector region and in regions at the top and bottom of the seed and blanket, the pellets contained only thorium with no uranium at the beginning of life.

### 2.3 - FUEL MODULE DESIGN

A typical fuel module cross section is shown in Figure 6. Each module contained a central, axially movable, hexagonal seed and a stationary, annular, hexagonal blanket. The seed was made up of fuel rods about 0.3 inch in diameter. The blanket fuel rods were about 0.6 inch in diameter. The length of the fuel in the seed and blanket fuel rods was about 8.7 feet, which included a region of thoria pellets above and below the  $\text{ThO}_2/\text{UO}_2$  loaded pellets. The seed and blanket rods also contained gas plenums above the stack of fuel pellets to accommodate fission gas release and compression springs to maintain pellet stack continuity during reactor operation.

### 2.4 - VARIABLE GEOMETRY CONTROL

The variable geometry control concept was based on changing the position of the movable seed fuel assembly, relative to the stationary blanket assembly, to control core reactivity without parasitic neutron loss. Changing the position of the seed assembly relative to the blanket assembly changed the relative amounts of neutron absorptions in the fissile ( $^{233}\text{U}$ ) and fertile (Th) fuel materials to maintain criticality and to shut down the reactor when desired.

The LWBR nuclear design was such that the more highly loaded seed had a neutron multiplication ( $k_{\infty}$ ) greater than one, and the lower loaded blanket had a  $k_{\infty}$  less than one. Reactivity was controlled by varying the leakage of

neutrons from the high  $k_{\infty}$  seed regions into the low  $k_{\infty}$  blanket regions. This was achieved by axially positioning the seed section of the core to change core geometry, rather than by using conventional parasitic neutron-absorbing poisons. With this method of control, which was enhanced by the seed-blanket concept, no neutrons are wasted in control rods or soluble poisons. Rather, any excess neutrons are absorbed in fertile thorium material, and good neutron economy is achieved. Neutron economic reactivity control, thorium-uranium-233 fuel, and closely spaced fuel rods were three essential features to make breeding possible. The reactivity worth of the movable seed was increased by using various lengths of natural thoria in a stepped arrangement in some of the seed and blanket rods as shown in Figure 7.

When the reactor was shut down, the seed assemblies were aligned below the rest of the fuel in the core as shown in Figure 7. To start up the reactor, the operator raised the seed assemblies in a uniform bank by remote control.

By raising the seed fuel, more nearly into alignment with the rest of the core, the operator brought the  $^{233}\text{U}$  bearing parts of the fuel closer together. This increased the likelihood that some of the excess neutrons would cause fission in  $^{233}\text{U}$  atoms. This enabled the operator to start the controlled chain reaction and control reactivity. The movable-fuel control system was designed so that, under any operating condition, when the movable seed fuel assembly was lowered relative to the stationary blanket the reactivity of the core always decreased.

During normal power operation, all seeds were aligned as a uniform bank. At the beginning of core life, critical operation occurred with the seeds located about 2 feet lower than the stationary blanket. As the core operated, the seed assemblies were moved gradually upward toward a position about 2 feet higher than the stationary blanket at the end of core life. The operation of the movable fuel control system was similar in many respects to that of the movable poison rod control used in many light water reactors.

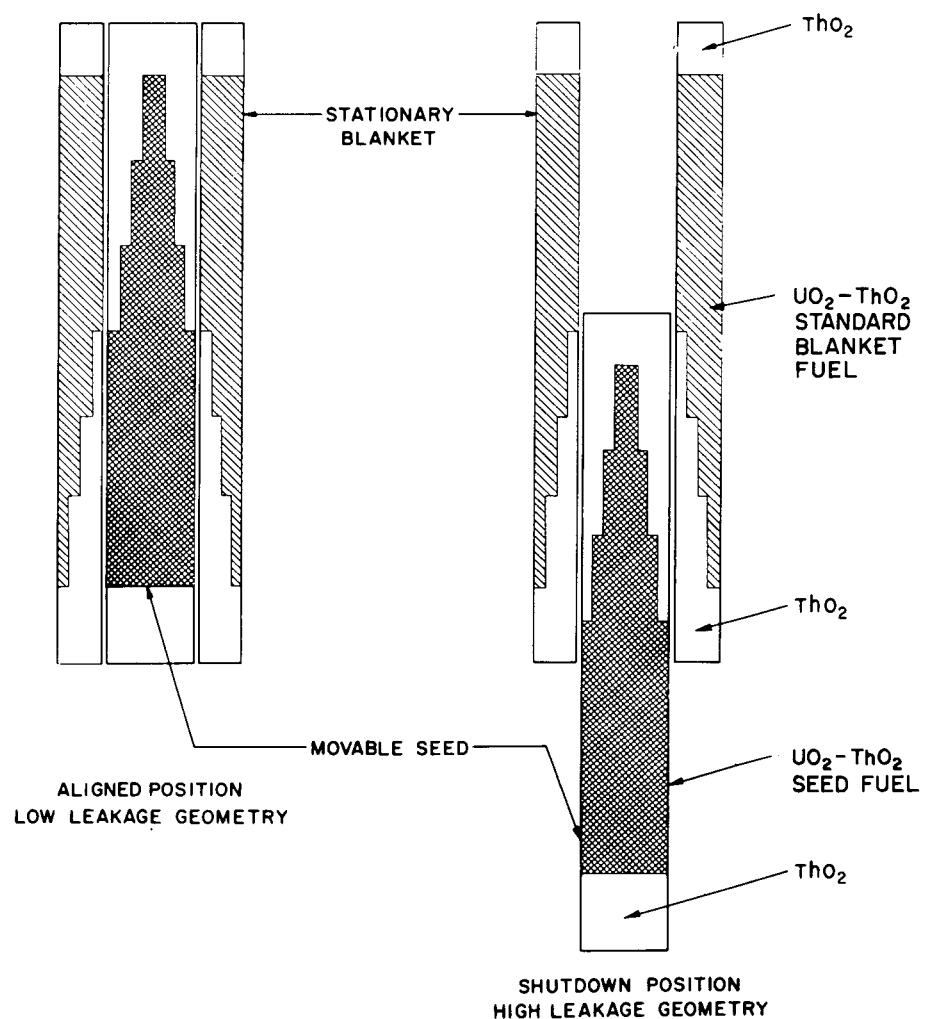


Figure 7. Variable Geometry Nuclear Control Concept

## 2.5 - SIMULATING A LARGE BREEDER IN THE SHIPPINGPORT REACTOR VESSEL

The three central fuel modules of the LWBR core were identical and symmetrical. These modules were designed to be typical of those to be used in a large central station reactor plant. The nine modules surrounding the central modules had a larger outer blanket region that was fueled with a higher  $^{233}\text{U}$  content and smaller rod diameter than the blanket regions of the inner modules (Figure 6). Use of this more highly loaded blanket region and lower metal to water ratio produced a relatively uniform power distribution within the interior of the core, thereby better simulating the breeding environment of a large (1000 Mw(e)) core. This power flattening increased the relative  $^{233}\text{U}$  loading required for the small core used in Shippingport by about 30 percent.

Surrounding the 12 hexagonal fuel modules in LWBR was an annular region, about 8 inches thick, made up of 15 reflector blanket modules. These modules did not contain  $^{233}\text{U}$  fuel initially, but instead contained  $\text{ThO}_2$  pellets in rods about 0.8 inch in diameter. The purpose of the reflector blanket region was to limit neutron losses from the core to less than about 0.8 percent of all neutrons, simulating the neutron leakage of a large (about 500 Mw(e)) LWBR core. The result was an estimated end-of-life fissile inventory ratio of 1.012 for the LWBR core at Shippingport. Larger light water breeder cores can be designed with neutron losses of 0.1 percent or less, thereby achieving even better breeding performance than the LWBR core at Shippingport.

## 2.6 - DESIGN FEATURES

The reactor was cooled by pressurized light water flowing in a single pass through the core. Flow was orificed to distribute it to the seed, blanket, and reflector regions in accordance with heat transfer requirements.

Axial positioning of the individual movable seeds was accomplished by a collapsible-rotor, reluctance-type control drive mechanism similar to those used successfully during operation of the first two Shippingport cores. When energized, the LWBR mechanism was connected to a drive screw that supported the seed. Safety shutdown was accomplished by deenergizing the control drive mechanism stator, thus collapsing the rotor and releasing the drive screw. This permitted the movable fuel to move to its least reactive position. A

continually engaged out-motion latch was incorporated in the mechanism to provide positive prevention of any unsignaled up-motion of a seed. A net downward force on the seed was achieved under all conditions of flow by the use of a balance piston within each module to counterbalance the upward flow of coolant through the seed. A portion of the inlet flow was bypassed around the core and directed to the top of the balance piston, thus balancing the upward flow force on the movable seed module. A buffer region was incorporated to prevent excessive forces on the movable assemblies as they came to rest following scram. Figure 8 shows the overall module, including the balance piston; Figure 9 shows the control drive mechanism.

A feature of the fuel assembly design was that each fuel rod was attached at one end to a support plate. In addition, the fuel rods were held in position laterally by a series of grids with springs that provided enough force on a fuel rod to hold it firmly, yet with not so much force as to prevent axial movement or to induce bowing of the rod. The design accommodated the effects of elongation of individual rods during irradiation as well as irradiation- or pressure-induced shrinkage of the rod. In addition, the design accommodated growth of the fuel pellets during irradiation as well as the tendency of the springs to "relax" and lose a portion of their spring force at high temperature and extended exposure to neutrons. Typical grid support system concepts for the seed and blanket rods are shown in Figures 10 and 11.

Figure 12 shows a typical grid designed to provide lateral support for the fuel rods in LWBR. These grids, which were made of AM-350 stainless steel, were positioned at several locations axially in each fuel region.

The in-core instrumentation included means for measuring neutron flux, coolant flow, and selected coolant temperature. The in-core instrumentation was used only to provide design confirmation information about the behavior of the core during its life since this instrumentation was not required for operational or reactor protection purposes. Other instrumentation was installed in the plant to provide the operational and protective functions.

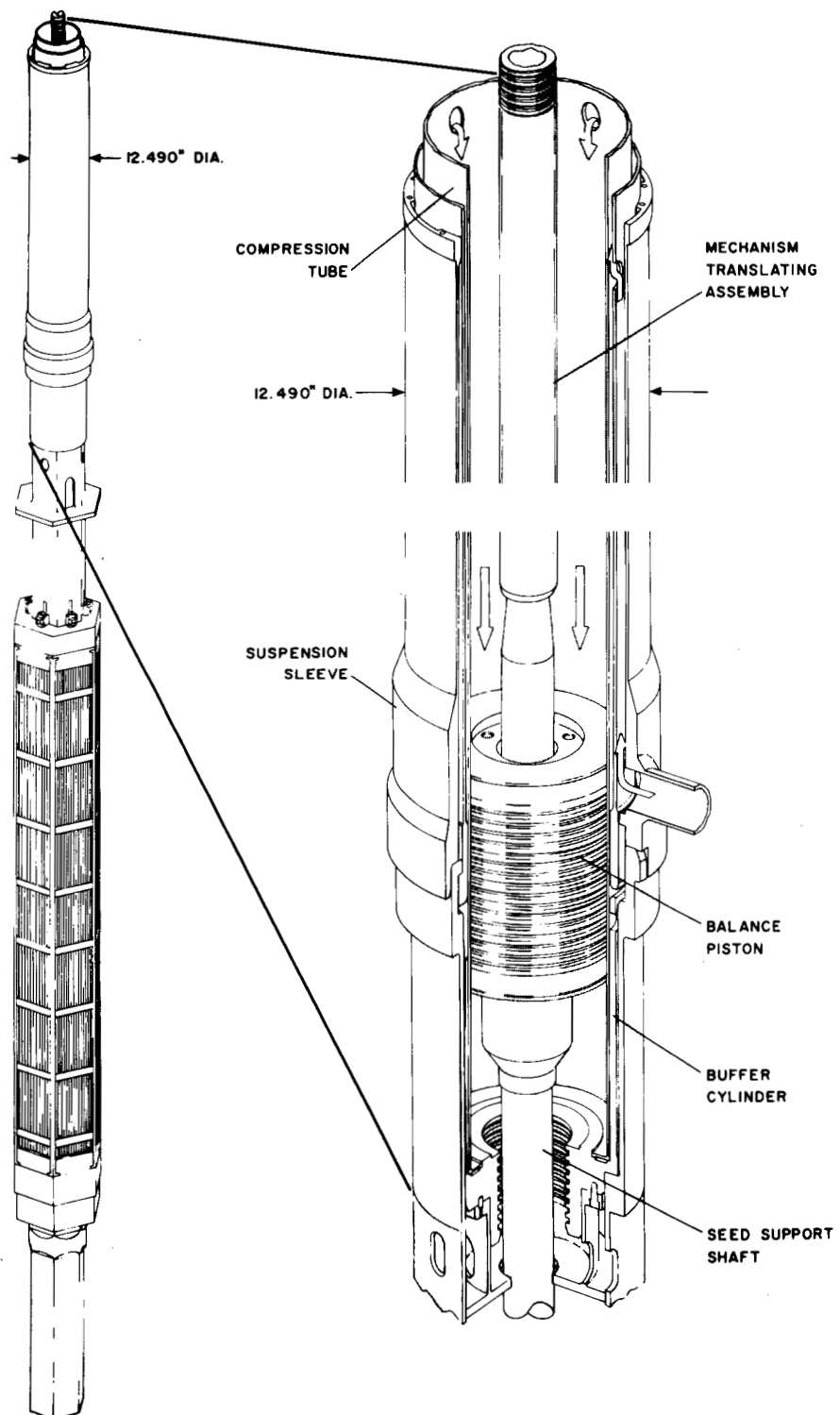


Figure 8. LWBR Blanket Module, Vertical View; LWBR Seed Balance Piston Assembly, Cutaway View

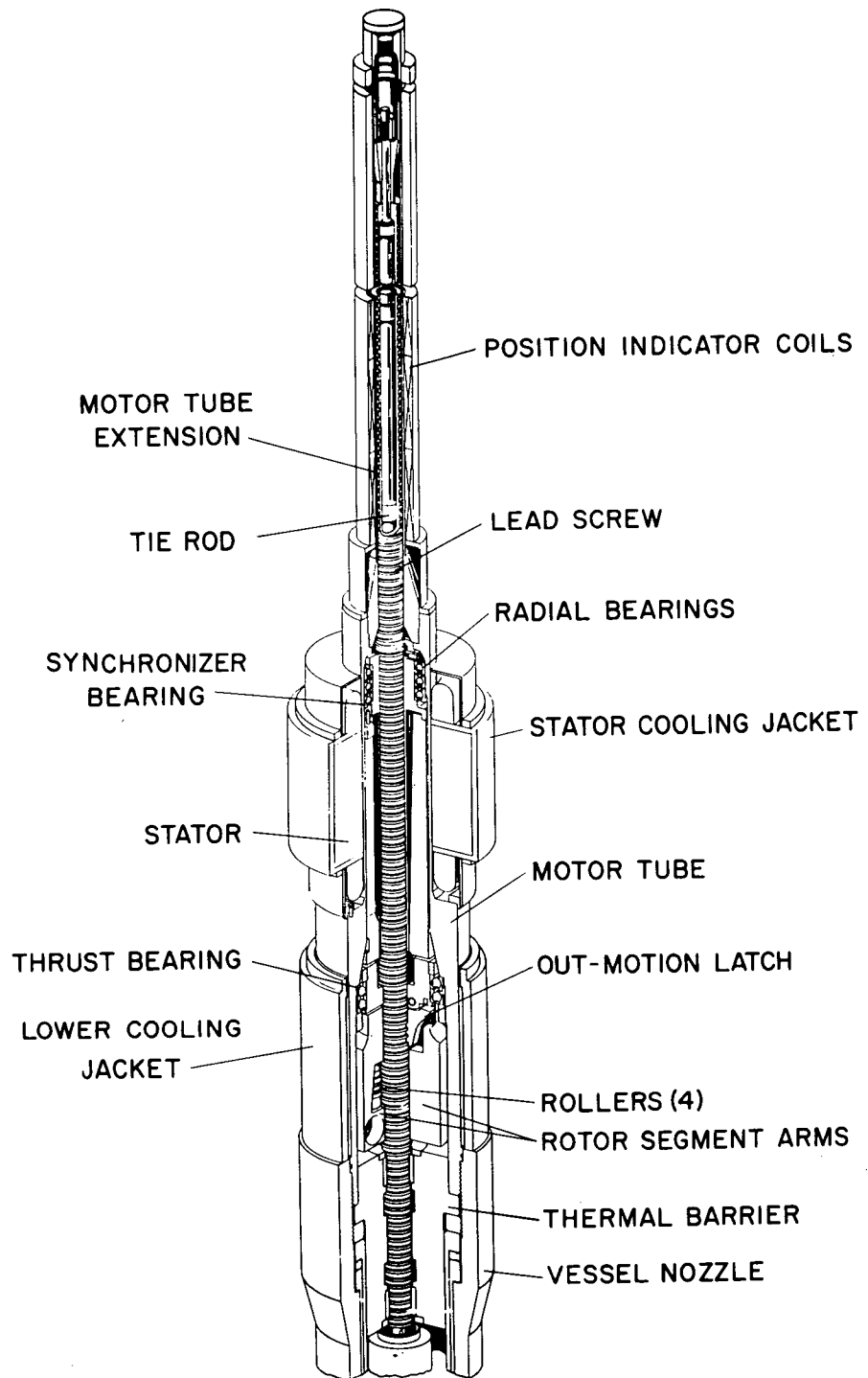


Figure 9. LWBR Core Control Drive Mechanism

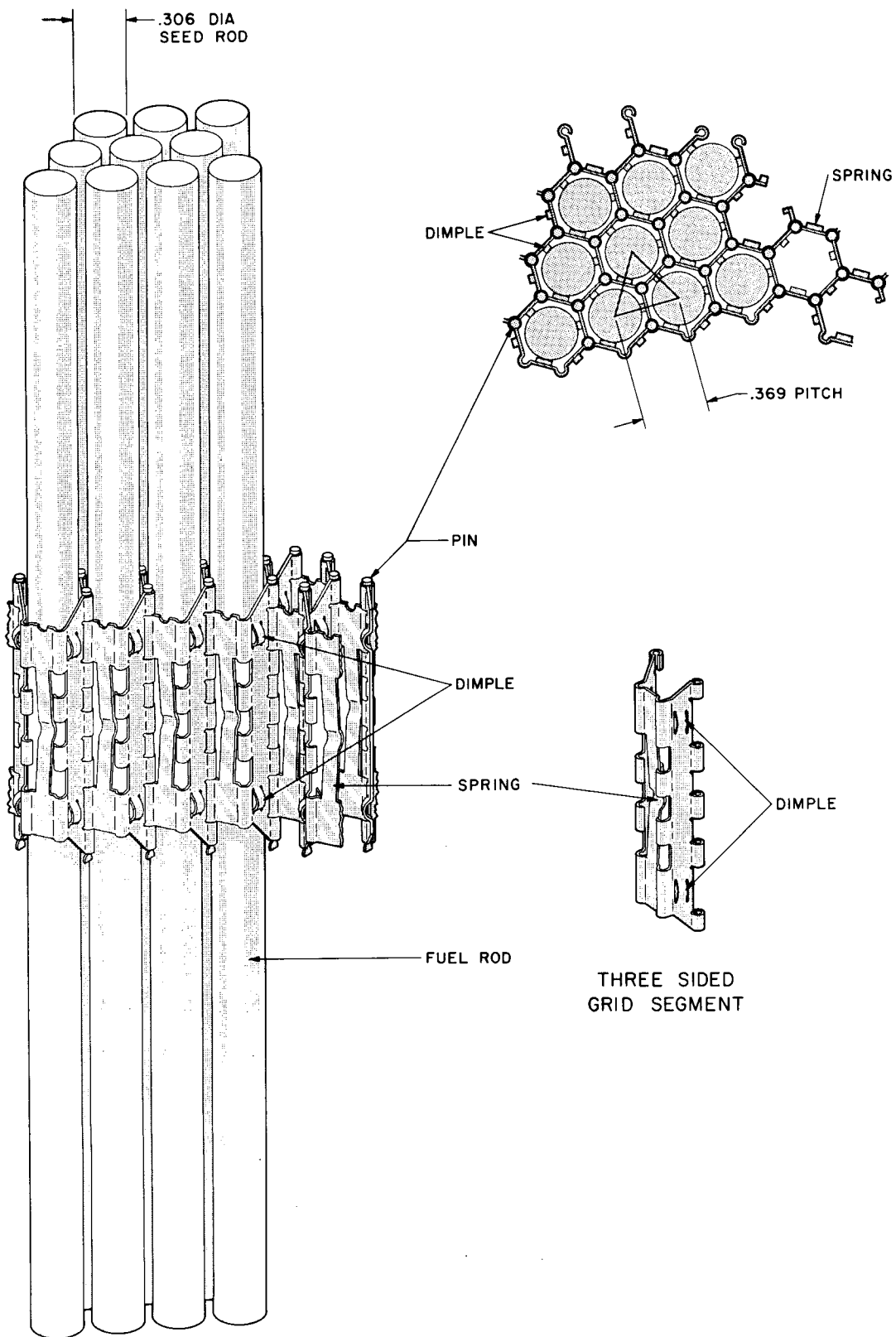


Figure 10. Typical LWBR Seed Rod Support Grid

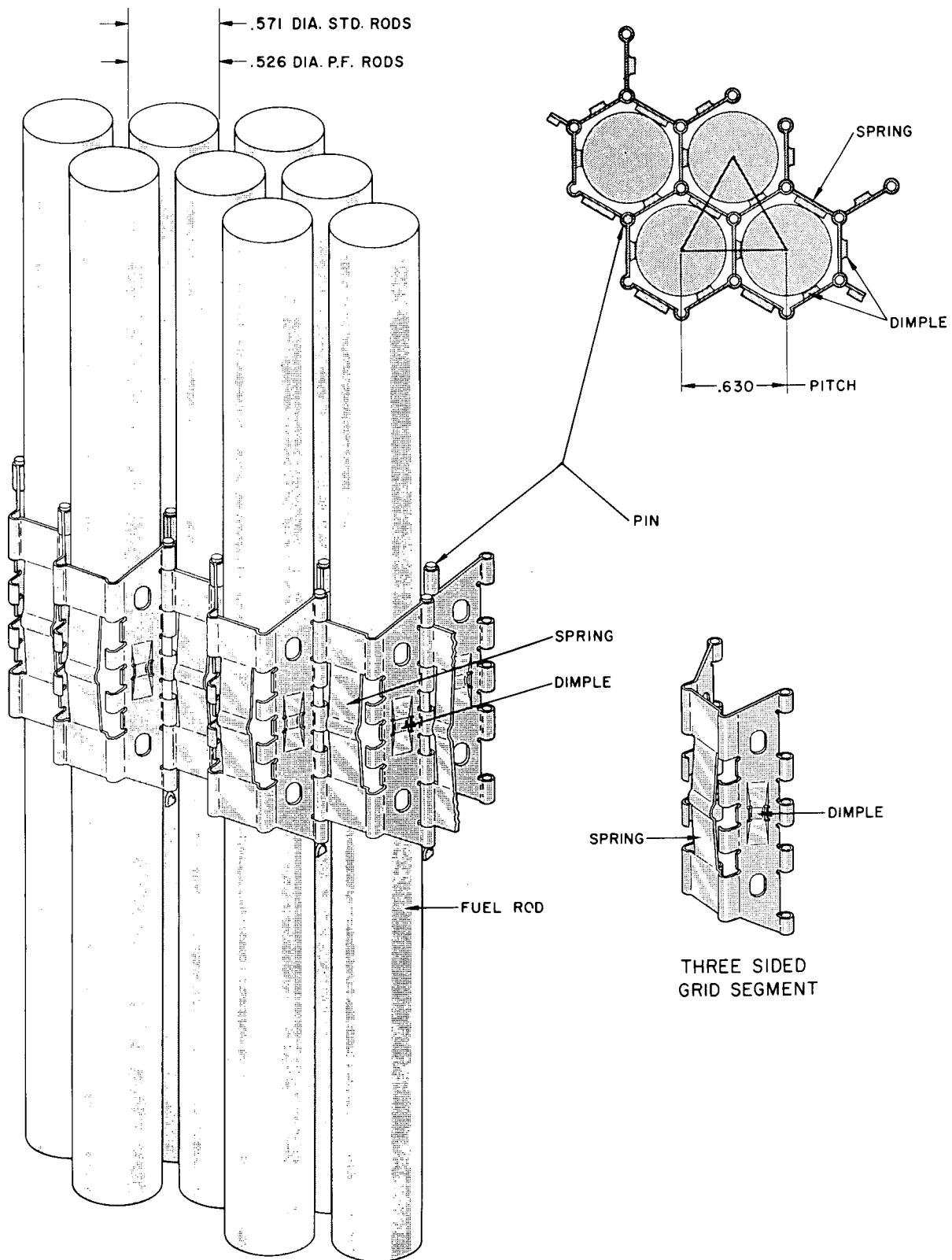
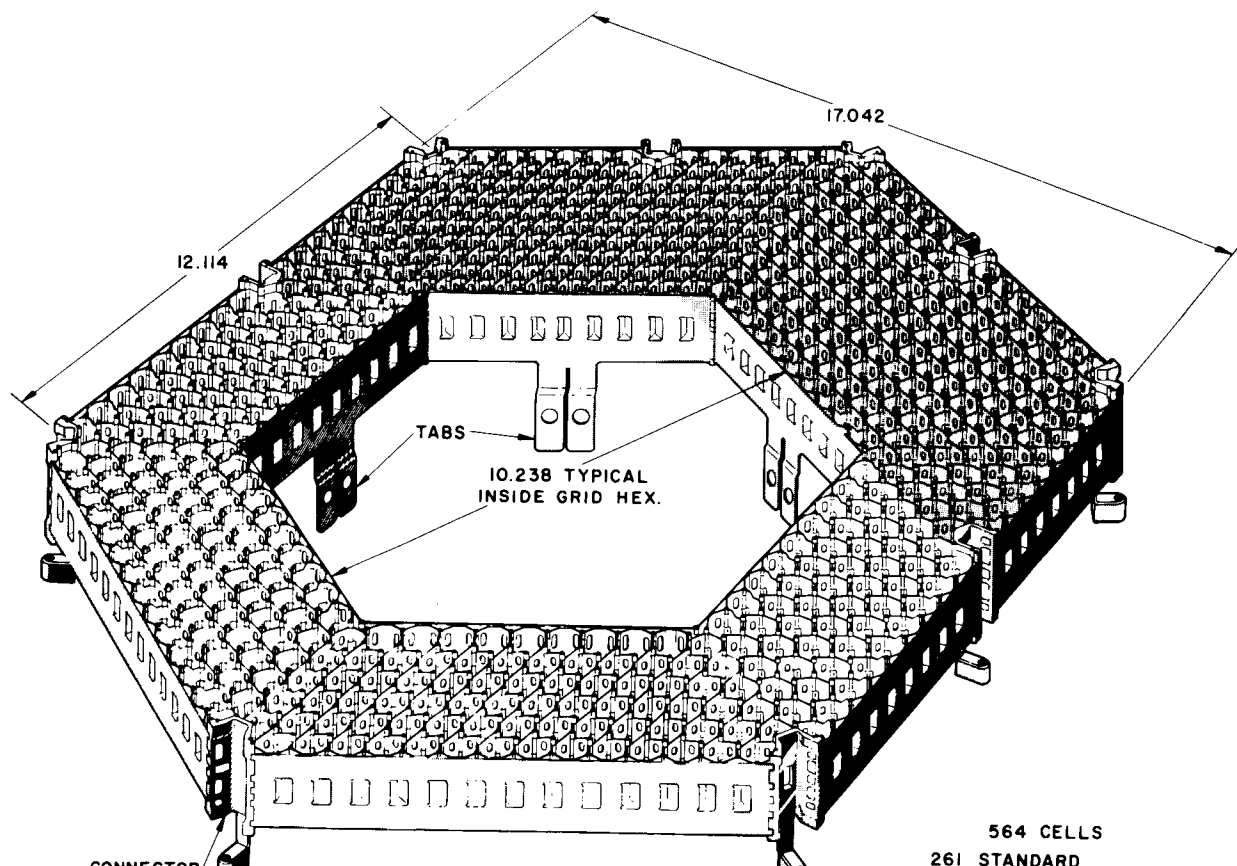


Figure 11. Typical LWBR Blanket Rod Support Grid



TABS: GRID-TO-GUIDE TUBE ATTACHMENTS (12 REQUIRED)  
 CONNECTORS: GRID-TO-SUPPORT POST CORNER CONNECTIONS (6 REQUIRED)  
 GRID-TO-SUPPORT POST SIDE CONNECTIONS (4 REQUIRED)

**LWBR**  
**BLANKET TYPE II**  
**ROD SUPPORT GRID**

STANDARD CELLS   
 POWER FLATTENING CELLS 

Figure 12. Typical LWBR Blanket Grid

Table 1 lists the major core and plant parameters for the LWBR core operation at Shippingport.

Operation of the LWBR demonstration core is reported in Section 6.

Table 1 - Core and Plant Parameters for the LWBR Core in Shippingport

POWER PLANT

Gross electrical output, Mw(e)	72
Net station output, Mw(e)	60
Net station heat rate, Btu/kw-hr	13,450
Steam pressure, psia:	
Full load at steam generator	744
No load at steam generator	895
Number of loops	4
Average reactor pressure drop, psi	67.6
Coolant piping OD, inches	18
Coolant piping ID, inches	15
Coolant velocity, main piping, ft/sec	35

REACTOR CORE

Type	Pressurized light water cooled and moderated seed and blanket
Total reactor heat output, Mw(t)	At least 204
Average total coolant flow rate, $10^6$ lb/hr	30.6
Reactor coolant inlet temperature at 204 Mw(t), F	521*
Reactor coolant outlet temperature at 204 Mw(t), F	541*
Average coolant temperature, nominal, F	531*
Primary system pressure, nominal, psia	1815 to 2000*
Nominal core height, including	
ThO <sub>2</sub> reflector, ft	8.7
Mean core diameter, ft	7.5
End-of-life Fissile Inventory Ratio (FIR), Nominal	1.012
Design	
Fuel loading (thorium and uranium), metric tons	About 42
Fuel material:	
Seed	<sup>233</sup> UO <sub>2</sub> -ThO <sub>2</sub> ; ThO <sub>2</sub>
Blanket	<sup>233</sup> UO <sub>2</sub> -ThO <sub>2</sub> ; ThO <sub>2</sub>
Reflector	ThO <sub>2</sub>
Fuel cladding material	
Seed, blanket, and reflector	Zircaloy-4

\*For LWBR core operation at 80-percent power following the Fall 1980 semi-annual shutdown, these parameters became:

Coolant inlet temperature, F	512
Coolant exit temperature, F	530
Average coolant temperature, F	521
Coolant pressure, psia	1615

## SECTION 3 - MANUFACTURE OF THE LWBR CORE

### 3.1 - FUEL PELLETS

#### 3.1.1 - Fuel Pellet Design

The fuel pellets were thoria ( $\text{ThO}_2$ ), or thoria with a low weight percent (1 to 6) of uranium dioxide ( $^{233}\text{UO}_2\text{-ThO}_2$ ). These ceramic fuel materials are similar to  $\text{UO}_2$ , but have higher melting temperatures, more creep resistance at high temperature, better corrosion stability if exposed to reactor coolant, and release less fission gas, including iodine. The seed fuel pellets were dished on both ends and chamfered on the edges; the blanket fuel pellets were dished on both ends and tapered at the edges.

The fuel pellets were basically right circular cylinders, modified as noted below. Fuel pellet dimensions and shape were specified to optimize performance, considering limits imposed by fuel-rod cladding mechanical interaction and fuel pellet temperatures. Small radial gaps between the fuel and cladding could close during power operation, leading to fuel-cladding contact. The resulting circumferential and axial cladding strains had to be limited to maintain cladding integrity. Large radial gaps effectively reduced heat transfer capability and increased fuel temperature, which had to be limited to avoid undesirable fuel structural changes or melting and the subsequent risk of cladding failure.

All pellets were fabricated with a concave dish in the center of each end except for the top pellet in each fuel rod, which had one end ground flat to provide a bearing surface for the plenum spring. In the finished pellet, the dish diameter was approximately 75 percent of the pellet diameter, with a nominal depth of 0.009 to 0.014 inch, depending on the pellet size and fuel composition.

At power, the temperature distribution in a fuel pellet with flat ends would change the flat contour to convex. This convex shape would increase the axial thermal expansion of the fuel stack and, in combination with fuel-cladding interaction, increase cladding axial strain and fuel rod length. By

dishing the ends of the pellets, the convex contour was eliminated, minimizing axial expansion and fuel-clad interaction.

The flat portion of the pellet end, referred to as the end land, was sized to carry axial pellet-to-pellet bearing forces that could be imposed by the cladding on the fuel stack. By limiting pellet-to-pellet contact to the end land area where temperatures were low, axial expansion of the fuel stack was minimized.

Blanket binary pellets contained a shallow taper at each end of a pellet, extending radially inward at the pellet end from 0.001 to 0.004 inch and extending axially from the pellet end 0.100 to 0.200 inch. A pellet taper was specified for the binary blanket pellets due to the nonfreestanding blanket cladding which resulted in radial fuel-cladding contact early in core life. Axial pellet-to-pellet contact forces and the temperature distribution in an untapered fuel pellet at power would produce an hourglass shape (i.e., the pellet would be larger in diameter at its ends than at its midsection). This hourglass pellet shape would produce nonuniform fuel-cladding contact forces, causing a local ridge in the cladding at pellet interfaces. Such a ridge was a region of increased circumferential cladding strain combined with an axial bending strain.

The utilization of the taper avoided the pellet hourglass shape, thus minimizing cladding ridging. The manufacturing tolerance bands noted above were specified such that the minimum taper was sufficient to avoid ridging. At the maximum dimensions, a gentle grooving of the cladding occurred at the pellet interfaces, with a corresponding minor perturbation to the cladding strain distribution.

The reflector region of the core and the blanket thoria pellets operated at lower power, and the seed regions had relatively thicker cladding; thus, these regions were not sensitive to this consideration and had fuel pellets without a taper.

All seed pellets and blanket thoria pellets had a small chamfer at the pellets ends. The chamfer had a nominal angle of 45 degrees and nominal linear dimensions of 0.006 or 0.015 inch, depending on the pellet type.

Reflector pellets were not chamfered because of the low power demand in this region of the core.

Chamfers and perpendicularity control were required to minimize the force needed to accommodate relative motion between the fuel and cladding. The chamfers also minimized the formation of chips during rod loading which, if present in the rod, would have increased local cladding strains.

All pellet types had limits placed on the perpendicularity of the plane of the pellet end face relative to the axial center line of the cylinder. The limit was related to the length and diameter of the pellet and the radial clearance of the pellet to the inside diameter of that type of fuel rod.

The pellet length was specified to provide a control over pellet loading density. Thus, radiographs of finished fuel rods could confirm that the correct pellet loading was in the fuel element.

### 3.1.2 - Fuel Pellet Fabrication

#### 3.1.2.1 - Background

Fabrication of fuel pellets for the LWBR core was based on the single-fire process (sintering). This process was straightforward for ceramic fuel of a single oxide, but required development for the binary fuel system to produce fuel pellets with satisfactory uranium homogeneity and density. Previously, PWR Core 1 and 2 fuel was fabricated using a double-fire technique, with comminution of initial-fired granules and subsequent compaction and sintering of fuel pellets. However, the advantages with a single-fire process for radioactive fuel material were less radiation exposure of personnel and the need for less processing equipment. This development resulted in a process utilizing a micronizer to comminute the powder and homogenize the binary composition. This micronizing produced the required uranium homogeneity and the high density of green fuel pellets. Micronizing was also used for the thoria pellet process because it was a low-impurity approach to breaking up the powder agglomerates to achieve powder uniformity.

### 3.1.2.2 - Process Description

The key operations for fabrication of high structural integrity, high density  $\text{ThO}_2$  and  $\text{ThO}_2\text{-UO}_2$  fuel pellets were: (1) micronizing, (2) agglomeration, (3) compaction, and (4) pretreatment and sintering.

Fuel fabrication consisted of processing small discrete quantities designated as batches and blends. The batch/blend sizes specified for the binary fuel fabrication were controlled on the basis of  $\text{UO}_2$  content with associated criticality limits, assuming the worst-case condition of double loading. Final blend sizes for binary compositions were 25 kilograms (seed) and 100 kilograms (blanket). Each blend was composed of batches to be consistent with the particular equipment employed. The blend size for thoria was 50 kilograms, based primarily on the preproduction experience since no criticality limits were required.

The individual steps of the fabrication process were as follows:

#### 1. Blending

The fabrication of a binary composition fuel pellet first required blending the as-received thoria and urania powders to a mixed feed material suitable for further intermixing and processing.

The preblend can was rotated on a rotary arm blender and then non-destructively assayed using a fissile uranium assay gage to verify the uranium mix and composition within the can to  $\pm 10$  percent. Several preblend batches were combined in a larger blender to form a primary blend of 25 kilograms, which was blended. The blended powder was then unloaded in either 4.5- or 8.5-kilogram increments for seed and blanket compositions, respectively, and was ready for the next operation, micronizing.

#### 2. Micronizing

Micronizing, powder comminution, and mixing were performed on the fuel powder primarily to activate the as-received calcined powder to a level suitable for meeting final sintered density (greater than 96.5 percent on the blend average), microstructural requirements, and

uranium homogeneity. Activation in this context refers to increasing the surface area of the powder by decreasing the particle size. Micronization of thoria-urania powder mixtures was also required to ensure meeting the stringent uranium homogeneity requirements. It served as a highly efficient mixing or homogenizing operation for the product.

Micronization was particularly attractive for powder processing because it was essentially self-commminuting, which limited impurity pickups, and the mills were small enough to be readily enclosed within a glovebox.

### 3. Secondary Blending

Secondary blending was performed on comicronized thoria-urania powder batches to homogenize the powder batches into a blend, thereby minimizing potential product variability. A blend served as the inspection sampling unit for most of the product final certification. After the operation was complete, representative samples were obtained from the homogenized powder and surface area analyses were performed to confirm the required activity of the powder.

### 4. Agglomeration

The purpose of the agglomeration process was to transform the finely divided, micronized powder into a freely flowing, compactible press feed spherical in shape. The process input was the secondary blender powder. The agglomerates were formed by the addition of a carbowax-oxylene binder in solution with a solvent. The binder-solvent solution was introduced as a spray during tumbling of the powder in the twin-shell blender. This step resolved two of the major problems associated with compaction of a finely divided powder: nonuniform filling of the die, and the formation of circumferential cracks in the green pellets. The spherical agglomerates flowed more easily and consistently into the die and, by being higher in bulk density than micronized powder, resulted in less entrapped air and associated cracks during compaction.

5. Granule Drying

Granule drying was performed on the agglomerated product after granulation to volatilize the retained oxylene from the granules, to provide a dry press feed suitable for compaction.

6. Final Blending

The various agglomeration batches comprising each blend were final blended to remix the blend.

7. Lubricant Addition

A dry powdered lubricant (Sterotex) was added to the agglomerated powder prior to compaction to minimize interparticle and die-wall-to-pellet friction. This minimized pressing loads during pellet compaction as well as the forces required to eject the pellet from the die cavity, thereby minimizing the internal pellet stresses which tended to cause cracks and other associated pellet defects.

8. Compacting

The purpose of the compacting operation was to form fuel pellets by cold pressing the feed powder. The forces of compaction established the interparticle contacts in the powder which were necessary for pellet densification and microstructure development in the sintering operation. The compaction parameters determined the density level, density distribution, dimensional uniformity, and pellet shrinkage during subsequent sintering. In addition, close control of compaction conditions was mandatory because flaws or faults in the pressed pellet were not correctable in later pellet processing steps. For these reasons, the compacting operation was of critical importance.

9. Pretreatment

Before compacted pellets were introduced into the sintering furnace for densification (sintering), the pellets were exposed to a thermal pretreatment for the removal of the carbowax (Sterotex) additives.

This pretreatment process required the pellets be subjected to a controlled environment (time, temperature, heatup rate, and atmosphere) for effective additive removal.

10. Sintering

Sintering was performed on compacted (and pretreated) pellets at a maximum temperature of 1790C to obtain a high-density product (typically 97 to 98 percent of theoretical) meeting all finished product microstructural requirements. In the binary compositions, sintering had the added objective of forming a homogeneous solid solution of the mixed and blended thoria and urania powder.

11. Pellet Grinding

The final geometric shape and size of the sintered pellet was attained by a two-stage centerless grinding procedure. This operation produced pellets with a configuration which satisfied dimensional design requirements.

12. Cleaning and Drying

Following the grinding operation, fuel pellets were cleaned to remove remaining particulate matter. To ensure that the cleaning process itself left no unacceptable residue, the cleaning fluid was limited to deionized Grade A water aided by the use of ultrasonic agitation.

13. Degassing of Pellets Prior to Loading

Before being loaded into fuel rods, fuel pellets were subjected to a high-temperature vacuum degassing operation to remove any absorbed moisture, any other surface contaminants, and any residual gases within the fuel. These gases, which consisted predominantly of CO and H<sub>2</sub> with minor amounts of CO<sub>2</sub> and various hydrocarbons, were formed during the pretreatment and sintering steps in the fuel manufacture.

### 3.1.3 - Fuel Fabrication Facility Description

In addition to providing the required fabrication capability, the manufacturing facility for the production of LWBR binary fuel had to be designed and constructed to incorporate features to preclude inadvertent criticality, to control the escape of contamination, to provide for the security of material, and to minimize the radiation exposure of personnel. A prime consideration in designing this facility was that the binary fuel contain low levels (less than 10 ppm) of the beta/gamma emitting  $^{232}\text{U}$ , which required a shielded facility and procedures to minimize radiation exposure. A continuous system of shielded gloveboxes connected by short tunnels and similar enclosures was employed.

Since the processing of thoria powder involved only low levels of alpha radiation, processing thoria powder into thoria pellets permitted this work to be performed by the use of hoods or other exhaust-controlled containment areas relatively free from shielding.

### 3.1.4 - Additional Information

Section 1D of Appendix A lists available reports on the development of fuel pellet technology. Section 2A of Appendix A lists the available reports concerning fuel powder and fuel pellet manufacture.

## 3.2 - FUEL RODS

### 3.2.1 - Introduction

A total of 17,290 rods were assembled into the LWBR core. Each fuel rod was composed of a Zircaloy-4 seamless tube filled with oxide fuel and thoria pellets. The nominal diameters were 0.306 inch for seed rods, 0.571 inch for standard blanket rods, 0.526 inch for power-flattening blanket rods, and 0.832 inch for reflector rods. All fuel rods were approximately 10 feet long. A plenum region at the top of each rod provided void volume to accommodate released fission gas and a helical coiled spring to exert pressure on the pellets to keep the stack together.

The fabrication procedure consisted of:

1. Sizing and cleaning the metallic components.
2. Welding an end closure to the bottom end of the cladding tube to form a tube assembly.
3. Loading the pellets and plenum hardware into the tube assembly to form a fuel assembly.
4. Welding (in a helium atmosphere to provide a helium environment inside the fuel rod after welding) the top end closure to seal the fuel and plenum hardware in the cladding to form a fuel rod.
5. Pickling the rod to final diameter and applying a corrosion film to all surfaces.
6. Inspecting the finished fuel rod for external and internal attributes, including the integrity and proper placement of the fuel pellets.

Because an objective of LWBR was to demonstrate breeding capability, the level of process control, quality assurance, and documentation of manufacturing and inspection data during core fabrication was very rigorous. All rods were individually identified and documentation was maintained to permit traceability of material, manufacturing history, and inspection data for all components. The number of variations in rod and fuel pellet types required the implementation of controls during loading and overchecks of finished rods to assure that all rods were correctly loaded.

### 3.2.2 - Fuel Element Design

Schematics of the seed, reflector, and blanket fuel rods are shown in Figures 13 through 15, respectively.

The fuel rod tubing (cladding) was Zircaloy-4. The final tubing processing and heat treatment differed between those tubes used for seed fuel rods and those used for blanket and reflector fuel rods. The blanket and reflector tubing was highly cold-worked and stress-relief annealed. This treatment resulted in a high-strength cladding early in the irradiation lifetime. The seed tubing was recrystallized annealed which provided more creep resistance during irradiation. The reduced strength of recrystallized annealed tubing

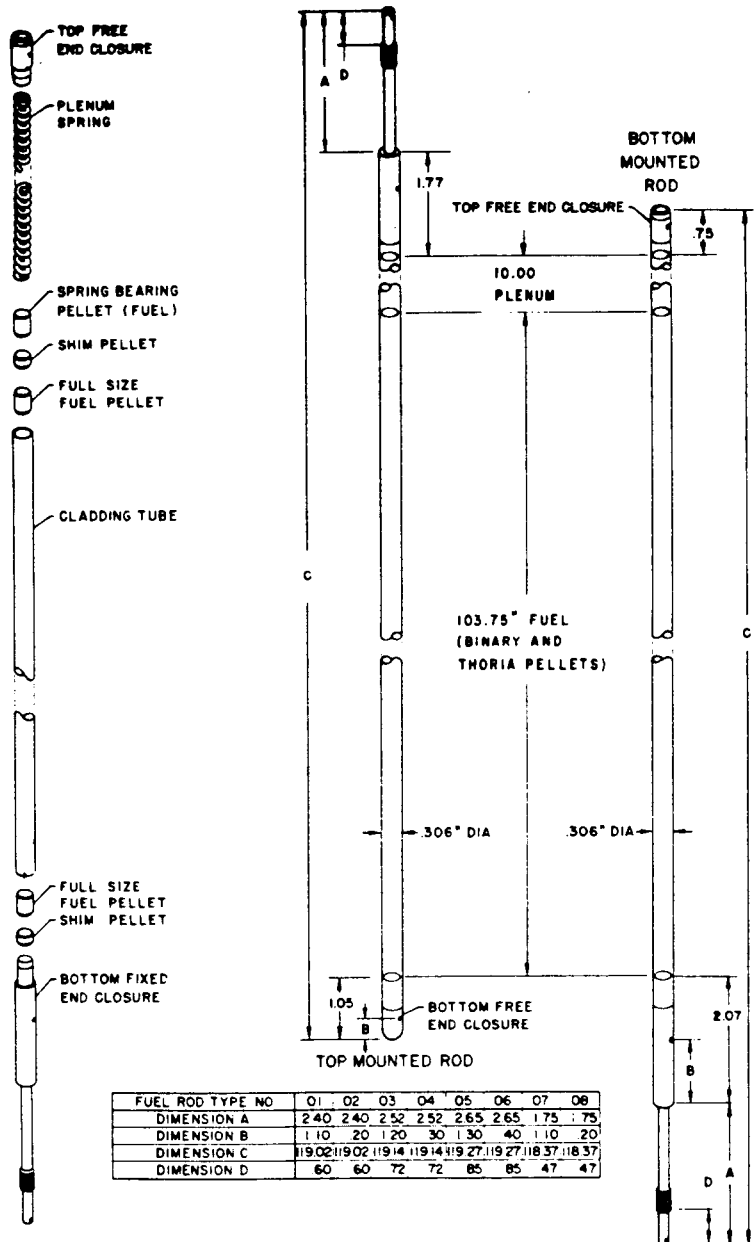


Figure 13. General Dimensions and Components of Seed Fuel Rods

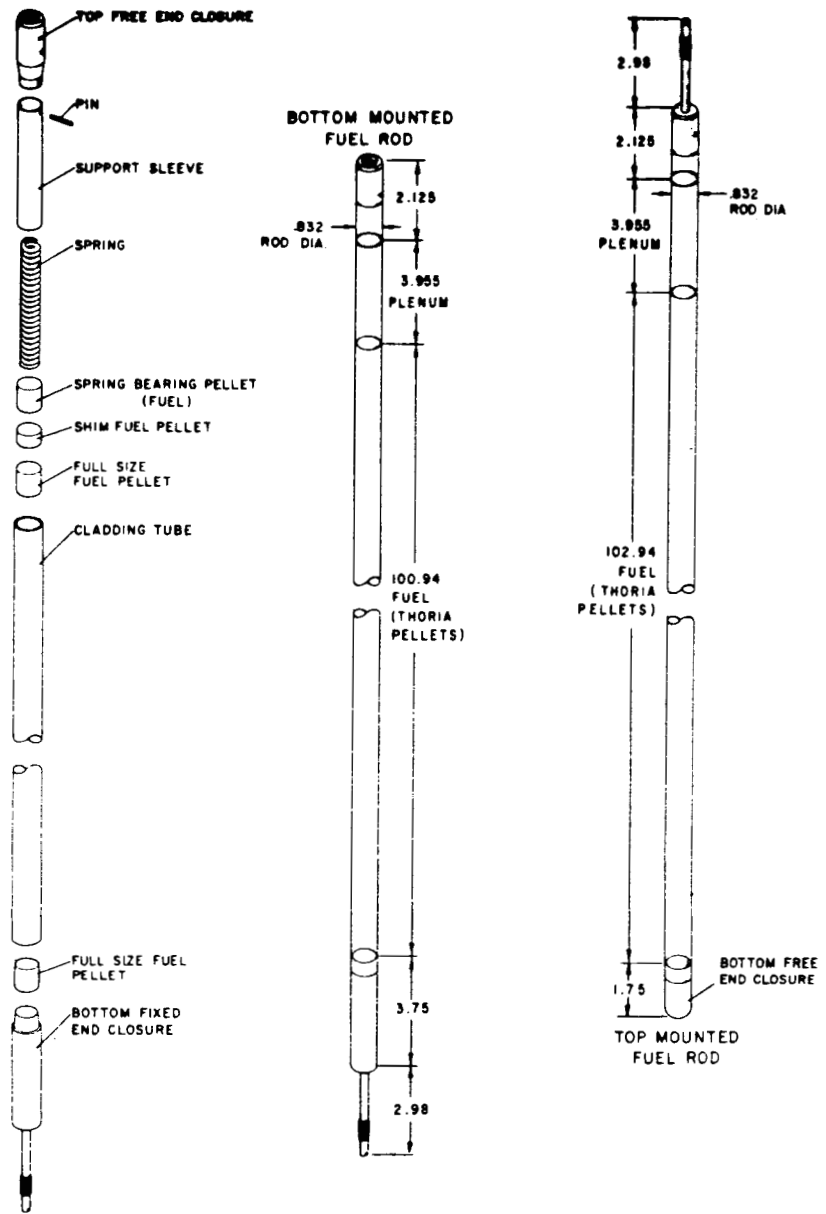
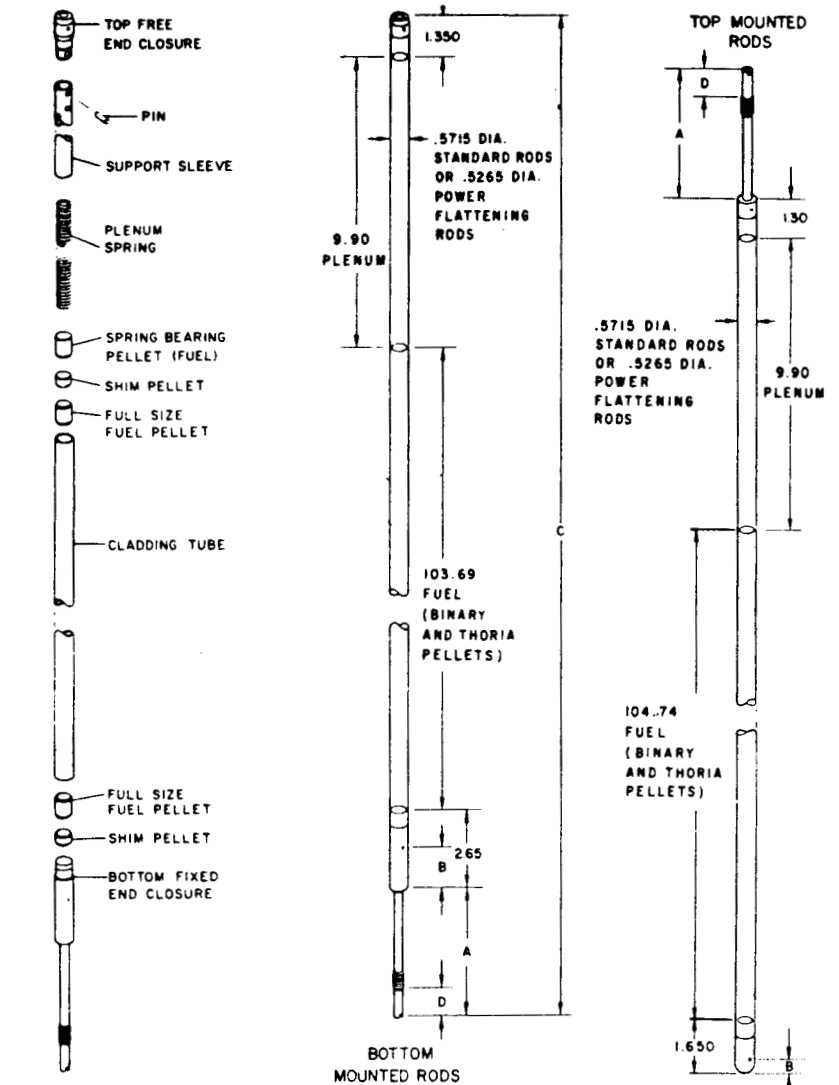


Figure 14. General Dimensions and Components of Reflector Fuel Elements



FUEL ROD TYPE NO	11	12	13	14	15	16	21	22	23	24	25	26	27
DIMENSION - A	4.23	4.23	4.35	4.35	4.47	4.47	4.23	4.23	4.35	4.35	4.47	4.47	4.60
DIMENSION - B	1.40	.50	1.50	.60	1.60	.70	1.70	.80	1.80	.90	1.90	1.00	2.00
DIMENSION - C ± .07	121.9	121.9	122.0	122.0	122.1	122.1	121.9	121.9	122.0	122.0	122.1	122.1	122.3
DIMENSION - D	.78	.78	.90	.90	1.03	1.03	.78	.78	.90	.90	1.03	1.03	1.16

Figure 15. General Dimensions and Components of Blanket Fuel Rods

early in irradiation lifetime was acceptable for seed fuel rods because the large fuel-cladding clearance delayed fuel-cladding interaction until the clad had experienced considerable irradiation hardening. The blanket and reflector fuel rods had higher diameter-to-thickness ratios than the seed fuel rods to minimize the volume of Zircaloy and enhance breeding. This was feasible because the blanket experienced only half the burnup requirements of the seed rods.

The plenum hardware, as indicated in Figures 13 through 15, consisted of a helically coiled spring of nickel-iron-chromium Alloy X-750 that was used in all types of rods, and a support sleeve of stainless steel that was used only in the blanket and reflector rods.

### 3.2.3 - Fuel Rod Fabrication Process Outline

The fuel rod fabrication process was divided into three main stages: (1) preparation of components, (2) fabrication of tube assemblies, and (3) processing and inspection of fuel rods. No fuel was involved in the first two stages. The third stage began with the loading of the fuel pellets into a tube assembly and included all the subsequent processing and inspection operations required to release the finished rod for module assembly.

#### 3.2.3.1 - Component Preparation

The plenum hardware (i.e., spring, plenum sleeve, and plenum pin) was obtained from suppliers in the finished condition and required only cleaning prior to use in a fuel rod. The end closures and tubes were procured oversize to allow control of the mating surfaces for welding. The fuel pellets were previously inspected and released for loading. They were vacuum degassed immediately prior to loading as part of the pellet processing. The operations involved in the preparation of the nonfuel components are described below.

#### 3.2.3.2 - Tube Assembly Processing

A tube assembly was made by joining a prepared bottom end closure to a cladding tube by gas tungsten arc (GTA) welding. Each welded assembly was

evaluated to ensure that it was acceptable prior to loading with fuel pellets. These operations were performed in the nonfuel areas of the fabrication facility.

The bottom end closure and the tube were initially assembled by pressing the end closure insert into the bottom end (unidentified end) of the tube. Groups of these assemblies were loaded into the weld box, making up a weld lot, and welded individually to form tube assemblies. Each weld was machined and polished flush with the tube surface, then inspected by both radiographic and ultrasonic techniques for internal defects. Welds rejected by either of these inspections were repair welded, and the machining and inspection operations were repeated. Assemblies with acceptable welds continued to be processed through a dimensional inspection; this included weld bead depression, end closure concentricity, fixed end closure end face perpendicularity, and local tube ovality. Out-of-tolerance weld and end closure dimensions were repaired by either rewelding or remachining. If repair welding was necessary, all of the above operations were repeated. A pressurized helium leak check of the welds, and measurement and visual inspection of the internal length completed the normal processing of tube assemblies.

### 3.2.3.3 - Processing and Inspection of Fuel Rods

Prior to loading of fuel pellets, the welded tube assembly, the end closure assembly, and the plenum spring were vacuum-dried to remove surface moisture. The vacuum-degassed and inspected pellets were assembled into the required stack length in the gloveboxes. Upon completion of stacking, the tube assembly end was inserted into the glovebox and the fuel was loaded into the tube. Loaded assemblies and their hardware were stored under vacuum in the welding equipment until a weld lot was accumulated. Top end closure welding was performed using equipment and procedures similar to those for bottom end welding. After welding, the end closures were machined and inspected ultrasonically for internal defects. Acceptable welds were rinsed in a cold nitric acid solution to remove surface contamination, and transferred to the rod processing facility. Rejected welds were rewelded for repair, and the machining and evaluation process was repeated.

Before any further manufacturing operations were performed, the rods were in-motion radiographed to confirm pellet loading. The top end closure was radiographically evaluated for weld integrity and inspected for dimensional requirements by the same procedures performed on the bottom end. Acceptable rods were brought to their finished condition by vapor blasting the surface in preparation for pickling to final size and corrosion testing. The remaining operations consisted of inspections to evaluate the rod for all required attributes prior to final release. The corrosion film evaluation was performed after corrosion testing, the final visual inspection was performed as close to the end of the processing as possible, and in-motion radiography for internal evaluation was performed last.

Released rods were cleaned, coated with Neolube (an assembly lubricant), then packaged and shipped to the module assembly area.

### 3.2.4 - Additional Information

Section 1D of Appendix A lists available reports on the development of fuel rod technology. Section 2B of Appendix A lists the available reports concerning fuel rod manufacture.

## 3.3 - FABRICATION OF FUEL ROD SUPPORT GRIDS FOR THE SHIPPINGPORT LWBR

### 3.3.1 - Introduction

The fuel rod support system (grids) design for LWBR created a close-packed, triangular pitch fuel rod arrangement in which the rod-to-rod spacing was about 0.060 inch. The close spacing for LWBR rods was necessary to achieve a high fuel-to-water ratio and was one of the requirements imposed on a breeder reactor grid system to facilitate the production of neutrons and achieve neutron economy.

The hexagonal-shaped "honeycomb" cell structure of each grid was formed by assembling precision-stamped AM-350 stainless steel sheet metal components and connecting members machined from AM-350 bar stock with the aid of wire pins, then permanently joining all components by brazing. Brazing was selected instead of welding because the complex design of the grid honeycomb structure required a process that would provide precise dimensional control

and metallurgical properties that result in good corrosion resistance and uniform high strength. The boundary straps and end plates supporting the honeycomb were joined by welding (see Section 3.3.4.2.2).

### 3.3.2 - Description of LWBR Grids

The function of a fuel rod support grid is to provide lateral support along the length of the rod to assure that rods do not touch throughout the operating life of the core. Rod-to-rod (or unintended rod-to-grid contact) was undesirable because of the possible detrimental effect on rod integrity. In LWBR, there were three basic types of grids that corresponded to the three types of fuel assemblies in the core.

To illustrate the physical appearance of the LWBR grids, each grid type (seed, blanket, and reflector) is shown in Figures 16 through 18. Figure 16 illustrates one of the 108 seed grids required for the LWBR core. Each grid had 619 cells. Figure 17 presents one type of blanket grid. Each type had a hexagonal, annular construction with the central opening sized to accommodate the movable seed fuel assembly. The Type I grid in Figure 17 accommodated 444 standard blanket fuel rods. Figure 18 shows one type of reflector grid. The pentagonal shaped Type IV grid held 228 rods.

Unlike square lattice grids which utilize two springs and two dimples per cell to position and hold fuel rod, lateral spacing in the LWBR hexagonal grid cells was provided by a flexible support spring located on one of the six cell walls and by rigid reaction dimples located on walls 120-degrees circumferentially from the spring. The spring and dimple orientations are illustrated in Figures 10 (seed) and 11 (blanket). The seed cells had reaction dimples at both the top and bottom of the cells (a total of four per cell), whereas the blanket (and reflector) had two reaction dimples per cell located at the same elevation as the spring (see Figure 11).

### 3.3.3 - Materials Used in Grid Construction

#### 3.3.3.1 - AM-350 Precipitation Hardening Stainless Steel

The selection of AM-350 stainless steel as the construction material for LWBR grids was based on its low level of stress relaxation during irradiation.

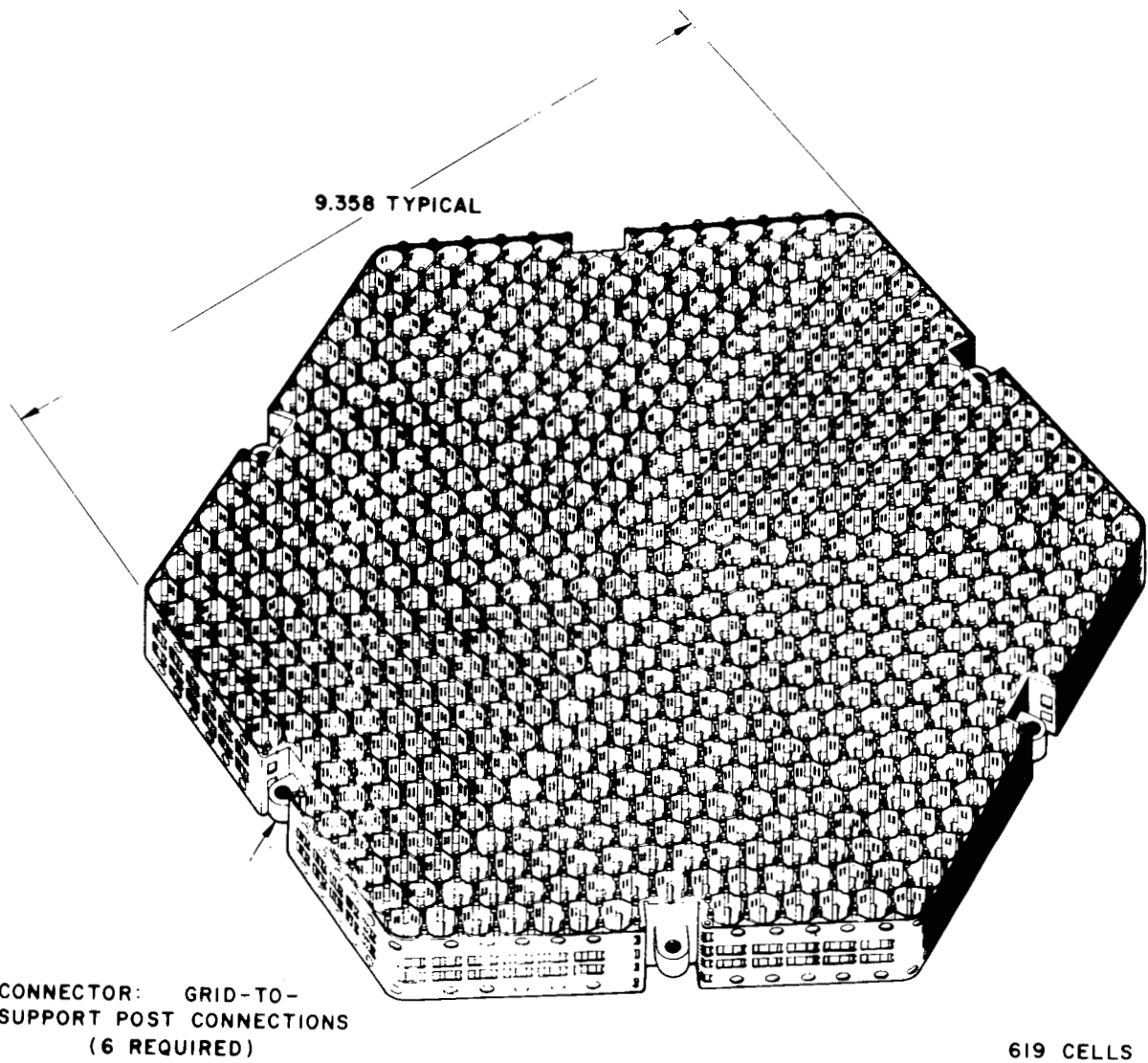


Figure 16. Seed Rod Support Grid

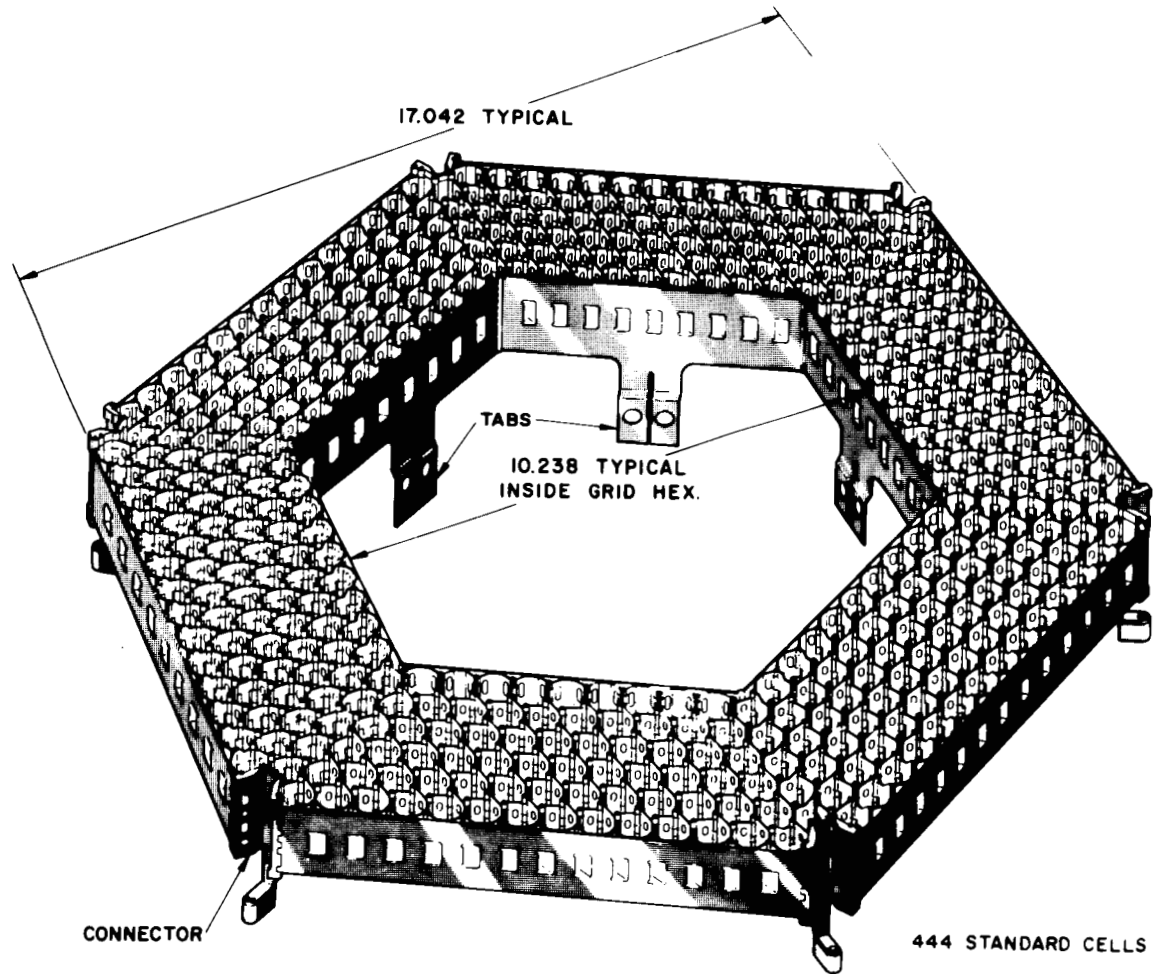


Figure 17. Blanket Rod Support Grid (Type I)

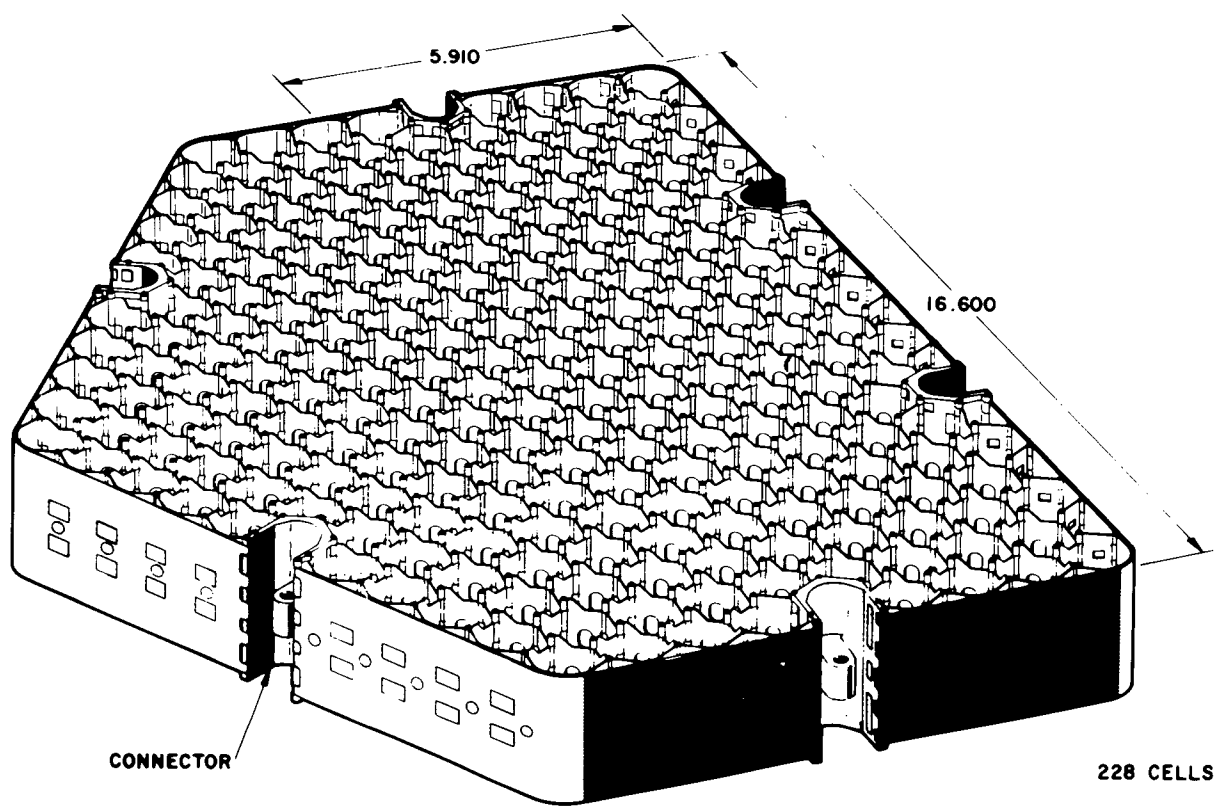


Figure 18. Reflector Rod Support Grid (Type IV)

This minimized concern over flow-induced vibratory cladding wear and fuel rod bow under conditions where the rod would be loose in the grid cell due to relaxation of spring force. This material property was judged to be of such importance as to override the higher neutron capture cross section of AM-350 as compared with Zircaloy-4.

### 3.3.3.2 - Braze Alloy

A special filler metal for grid brazing was developed because standard brazing filler metals did not possess adequate corrosion resistance in the reference LWBR environment. The resulting alloy (a brazing filler metal containing nominally 60-percent nickel, 30-percent chromium, 10-percent silicon) was superior to the other alloys because it forms basically a two-phase microstructure with AM-350 when heated to the brazing temperature of 2100F. Corrosion studies had revealed that the poor corrosion behavior of the braze filler metals lower in chromium was related to the presence of a third, chromium-depleted phase.

## 3.3.4 - Manufacturing Operations

### 3.3.4.1 - General Process Outline

#### 3.3.4.1.1 - Sheet Metal Stamped Components

Sheet metal grid components were manufactured from sheet stock which was first sheared to a specific width, pierced to form internal cutouts and external boundary configurations, then formed by either single or multiple die striking operations to produce the desired final components.

#### 3.3.4.1.2 - Machined Components

The only components manufactured in this category were the grid-support post connectors. The complex shape of each connector required precision machining, including the machining of hinge curls to mate with the formed curls on the sheet metal components. Low carbon AM-350 bar stock was utilized for the thicker cross-section components such as the grid-support post connectors.

#### 3.3.4.1.3 - Grid Component Assembly Pins

The assembly pins were manufactured from AM-350 wire by a combination cold heading and length shearing cycle comparable to that utilized for producing nails. A tapered point was ground on each pin to preclude fissuring when the nonheaded end was mechanically crimped after assembly.

#### 3.3.4.2 - Component Assembly

The typical procedure for grid assembly consisted of the following operations.

1. Cleaning the components,
2. Welding boundary straps and end plates,
3. Applying a protective inhibiting slurry to restrict brazing filler metal flow,
4. Assembling components and applying braze alloy slurry.

#### 3.3.4.3 - Furnace Brazing of Grids

To impart dimensional stability and rotational rigidity to the grid structure, the pieces were vacuum brazed at 2100F using relatively massive fixturing to maintain grid dimensions. Because AM-350 is relatively soft at this temperature, rigid brazing fixtures were developed to control dimensions. These fixtures were made from NiCrFe Alloy 600 because the thermal expansion and contraction, anisotropy, and dimensional stability characteristics of Alloy 600 were compatible with those of AM-350.

#### 3.3.4.4 - Decarburization

Decarburization of AM-350 fuel rod support grids to a carbon range of 0.02 to 0.06 weight percent was required to develop optimum corrosion resistance while retaining adequate strength. Decarburization was performed by heating the grid to 1900F in a wet hydrogen atmosphere for a prescribed time period that was dependent on size of charge and the hydrogen flow rate.

#### 3.3.4.5 - Dimensional Inspection and Adjustment

At this stage in the manufacturing process, each grid was inspected to assess the adequacy of the individual cell and overall grid dimensions. The

required grid dimensions were obtained with a Cordax Coordinate Measuring Machine (CMM). In the LWBR grid program, the CMM was coupled with an integral PDP-8 minicomputer to provide a rapid data collection and analysis system. On an average, the complete inspection of a grid yielded in excess of 3000 recorded data points.

#### 3.3.4.6 - Grid Tempering

Light Water Breeder Reactor fuel rod support grids were then subjected to a thermal tempering cycle to reduce residual stresses from the prior martensite phase transformation. Tempering was employed to maximize the material's corrosion resistance in high-temperature water.

#### 3.3.4.7 - Post-Temper Dimensional Inspection and Adjustment

The second complete dimensional inspection was performed subsequent to the grid tempering operation. This inspection was also done on the CMM; its purpose was to identify the cells with residual dimensional violations which required correction by spring, dimple, or panel adjustment.

#### 3.3.4.8 - Grid Preconditioning

Preconditioning the grid surfaces to have a dense, uniform, tightly adherent surface oxide film was then accomplished by corrosion testing the grids in an autoclave for 3 days in 600F ammoniated water. This test also provided an overcheck of the material quality in a grid after the completion of all manufacturing thermal treatments to assure no degradation of corrosion properties had occurred.

#### 3.3.4.9 - Final Inspection and Adjustment of Grid Dimensions and Attributes

Following post-temper cell adjustments and connector machining, each grid was subjected to a final complete CMM inspection of the cell dimensions and grid boundary to verify that the attributes were within the design requirements. This inspection afforded the last opportunity to "fine tune" the cell dimensions to the design requirements.

### 3.3.5 - Additional Information

Section 1G of Appendix A lists available reports on the development of fuel rod support grids. Section 2C of Appendix A lists the available reports concerning grid manufacture.

## 3.4 - FUEL MODULE FABRICATION

Fuel module fabrication was accomplished in four stages. Each stage was the same for each module type, although variations in the module designs required adaptations of the sequence in which detailed assembly steps were performed. The four stages are:

1. Preassembly - assembly of the module frame structure in preparation for rod insertion.
2. Fuel Rod Installation - operations to install and secure the fuel rods to the module frame assembly.
3. Final Assembly - installation of remaining module hardware.
4. Preparation for Shipment - packaging and loading the modules for shipment to Shippingport.

The following sections present an overview of these operations.

### 3.4.1 - Preassembly

Module preassembly was initiated by preparing a frame assembly, consisting of grids connected by support posts (seed and reflector) or a guide tube (blanket). The frame positioned and supported fuel rods in the core. Because the frame was flexible, a rigid supporting fixture was used to maintain the correct grid and frame alignment. Prior to initiating any assembly operations, however, the main structural members of the modules (i.e., grids, support posts, shells, guide tubes, etc.) were dimensionally evaluated and assigned to specific modules to ensure optimum fit and alignment when the components were assembled into modules. An example of this process was the selection of fuel rod support grids for a module based on the computerized

evaluation of all of the grid cell coordinates. This analysis allowed grids with the most similar grid cell arrays to be used together to optimize rod straightness and spacing.

The preassembly process was similar for the seed and reflector modules since the frame assembly was constructed by attaching the support posts to the outer boundary of the fuel rod support grids. For blanket modules, however, the grids also had an internal boundary which required attachment to a guide tube.

#### 3.4.2 - Fuel Rod Installation

With the frame assembly constructed and aligned, the next stage in the manufacture of a module was to install the fuel rods in the appropriate cell location and attach them to the baseplates. Rod pulling was accomplished in special stations composed of a cage that held the assembly, a rod-pulling mechanism installed above the assembly, a shielded manlift, concrete shielding, a communication system, and auxiliary components unique to each type of module assembly.

#### 3.4.3 - Final Assembly

In final assembly operations, the remaining module hardware was attached to the rodded fuel assemblies, and measurements and adjustments were made to this hardware so that the critical module boundary envelope dimensions were achieved. This module hardware consisted of components designed for structural support of the fuel in the assembled core and for flow control of the coolant water flowing through this core.

#### 3.4.4 - Inspection

Inspection during fuel module assembly was performed with conventional equipment. For example, grid alignment (grid-to-grid so that grid cells would provide a straight path for rod pulling) was measured by an optical scope focusing on optical targets. The optical system was also used to measure grid levelness and the module assembly envelope. Dimensional inspections of clearances such as rod-to-rod, rod-to-post, and rod-to-grid were made by feeler

gages. A special gage made for the measurement of the seed shell outer envelope and the blanket module guide tube inner boundary consisted of a hexagonal frame with a dial gage mounted on each of the six faces of the frame. These measurements were used in the selective assembly of shells and grids and, later, the selection of mating seed and blanket modules.

#### 3.4.5 - Additional Information

Section 2D of Appendix A lists WAPD-TM-1317 concerning fuel module assembly.

(Intentionally Blank)

## SECTION 4 - PLANT MODIFICATIONS MADE PRIOR TO LWBR OPERATION

### 4.1 - INTRODUCTION

The Shippingport Atomic Power Station primary plant coolant system could accommodate the LWBR core with only minor modifications. However, additional plant modifications were undertaken to comply with the intent of current regulatory guides and 10CFR50, Appendix A, Design Criteria, which had evolved since the original construction of Shippingport. These additional modifications dealt principally with the engineered safety systems, which were provided to mitigate the consequences of postulated accidents, and various system and component upgradings. The 1A and 1D (straight-through-tube type) steam generator heat exchangers were replaced.

New safety related structures and equipment were provided to support LWBR operations at Shippingport. These structures and equipment were designed to more stringent requirements than were used in the original Shippingport design, including seismic analyses required of conventional nuclear power plants. Examples of structures, equipment, and controls in this category included the new safety injection system equipment and pump house, the new diesel generators and their foundation, the new containment isolation valves, the new auxiliary control room, auxiliary d-c control system, and the a-c on-site emergency power system. Also, seismic instrumentation was provided to shut the plant down automatically on a low-level tremor, so that any damage to the shutdown instrumentation from subsequent tremors would not comprise plant safety. Three of these examples are discussed below.

### 4.2 - PLANT MODIFICATIONS OR UPGRADINGS ACCOMPLISHED

#### 4.2.1 - Incorporation of the Auxiliary Control Room

The new design criteria stated in part that a control room shall be provided from which the nuclear plant can be operated safely under normal conditions and can be maintained in a safe condition under accident conditions including loss-of-coolant accidents. Adequate radiation protection is to be

provided to protect personnel from receiving radiation exposures in excess of 5 Rem whole body or its equivalent to any part of the body for the duration of the accident.

The main control room at the Shippingport Atomic Power Station did not meet these requirements. Therefore, a normally unmanned auxiliary control room (ACR) which would meet current requirements was provided for LWBR operations. This ACR was equipped with sufficient instrumentation and controls to safely proceed to a controlled reactor plant cooldown, and to control and monitor the engineered safeguard systems required to cope with loss-of-coolant accidents. In addition, the room provided sufficient shielding to limit the exposure of occupants to 5 Rem over a 30-day period for the worst case external conditions predicted for a design basis loss-of-coolant accident.

The ACR was designed to withstand the effects of natural phenomena such as earthquakes, tornadoes, and the Shippingport design basis flood without the loss of the capability to perform its design functional requirements. The foundation was designed to accommodate the soil properties of the ground below and that immediately surrounding the ACR.

The ACR included equipment to provide habitability of the room for a maximum period of 30 days by four operating personnel. It was also assumed for purpose of design that supplies and equipment would not be replenished during the 30-day period. The life support system included shielding, a controlled (slightly positive) atmosphere/ventilation system, sanitation and food and water supply for the 30 days.

#### 4.2.2 - Incorporation of the Containment Isolation System

The reactor plant container was designed to prevent escape of radioactivity to the environment in the event of accidents. Two accidents of major concern were the loss-of-coolant accident and the steam line rupture accident, both of which would result in an increase of pressure in the container.

The function of the new containment isolation system was to isolate the penetrations into the reactor plant container in the event of high pressure within the containment. Isolation was accomplished by automatically shutting

designated valves in the operating fluid system lines which penetrate the containment and by locking shut designated manual valves in the nonoperating fluid system lines which penetrate the containment.

#### 4.2.3 - Addition of Flywheel Generators to Main Coolant Pump Circuitry

For LWBR, a flywheel generator was used with each reactor coolant pump to improve the pump flow coastdown characteristics and to permit the core to sustain a complete loss of flow accident at maximum power operation. One flywheel generator was connected to each pump power circuit to provide, in electrical energy, the equivalent inertia of 13,000 lb-ft<sup>2</sup> at the pump rotor if the 2.4-kv bus power to the pump were lost. As the energy from the flywheel was used, the generator speed and frequency decreased. Although generator voltage varies as the square of the speed, the voltage was sufficient to hold the pump motor in synchronism with the generator as the speed decreased, and the current demand was held within the capability of both machines during the coastdown.

#### 4.2.4 - Replacement of the 1A and 1D Steam Generator Heat Exchangers

Because of detectable primary-to-secondary leakage during PWR Core 2 operations, the straight-through-tube 1A and 1D heat exchangers (including tube bundles) were removed and replaced with spare units. The removal of the heat exchangers consisted of cutting all connections and clearing obstructions in the heat exchanger removal path. Disconnection of the heat exchangers consisted of cutting the risers and downcomers to the steam drums, the inlet and outlet connections to the main coolant lines, and the primary and secondary vent and blowdown lines. To clear the heat exchanger removal path, spool pieces were cut out of the main coolant lines, and five of the 10 short risers, the two long crossover risers, and the six downcomers between the steam drum and the heat exchanger were removed. Also, the instrument lines on the forward end of the steam drums were removed. The back end of the heat exchangers were lowered, the front ends raised, and the heat exchangers lifted forward, up, and around the steam drums and out the top of the boiler chambers. Installation of the spare heat exchangers reversed this process. After

rewelding, the units were hydrostatically tested satisfactorily and made available for plant operation. No tube leakage was experienced in these units during LWBR operation.

#### 4.2.5 - Additional Information

WAPD-TM-1542, listed in Section 1A of Appendix A, discusses the modification of the Shippingport Station for LWBR.

## SECTION 5 - INSTALLATION OF THE LIGHT WATER BREEDER REACTOR

The Light Water Breeder Reactor (LWBR) core was installed into the existing pressurized water reactor vessel of the Shippingport Atomic Power Station. The installation was accomplished using specially designed handling equipment to minimize the risk of damage to the components of the reactor.

During installation, a rigorous quality assurance program was followed which included third party verification of proper installation of all components. In many cases, verification of proper installation was obtained by remote indicators on the tooling since the components being installed were within the reactor and could not be observed.

The LWBR installation occurred in five distinct phases:

1. Preparatory Phase - Following removal of the previous reactor core (which left only the thermal shield in the open reactor vessel), a remote visual inspection of the reactor vessel was performed. Pre-conditioning and filtering of the entire primary system were then performed to provide a protective oxide film on the plant new primary system surfaces and to remove loose corrosion products from the system. Concurrent with preparing the reactor vessel for the new core, the assembly of the LWBR core barrel was completed in a clean room environment. Training of personnel, checkout of equipment, and receipt of the seed and reflector fuel assemblies also occurred during this period.
2. Phase I - The assembled core barrel was inserted into the reactor vessel, and the pressure boundary seal between the core barrel support flange and reactor vessel was welded. As a method of criticality control, the reactor vessel was drained of water and the blanket, seed, and reflector assemblies (in that order) were then installed in the core barrel. The holdown barrel was installed onto the reflector assemblies.
3. Phase II - The closure head was placed on the reactor vessel and the suspension system components that engage and lock onto the blanket

fuel assemblies were installed to suspend the blanket fuel assemblies from the closure head. The pressure boundary seal between the core barrel support flange and the underside of the closure head was welded.

4. Phase III - Control drive mechanism components were installed, and the motor tube omega seals on the mechanisms were welded. Thermo-couples and flux wire thimbles (dry wells) were installed and welded on the mechanism ports. Initial fill of the reactor vessel was completed.
5. Phase IV - Remaining head area components were installed and electrical cables connected. Final fill and venting of the reactor was completed and the reactor chamber dome installed. A hydrostatic test of the reactor vessel was performed, completing the installation of LWBR.

WAPD-TM-1342, listed in Section 4 of Appendix A, describes LWBR installation in detail.

## SECTION 6 - OPERATION OF THE LWBR CORE IN THE SHIPPINGPORT ATOMIC POWER STATION

### 6.1 - INTRODUCTION

During most of LWBR core lifetime, the Shippingport Atomic Power Station was operated as a base load station (100-percent power). However, during the first 2 years of operation, the station operated part of the time in load following operation (swing load) to demonstrate the capability of the LWBR core fuel elements in this operating mode as well as under base load. The station experienced 204 load follow cycles distributed nearly uniformly throughout the 2-year period. During LWBR core lifetime, 29,047 equivalent full power hours (EFPH) were accumulated. The total electrical gross output for LWBR was 2,128,943,470 kilowatt hours.

### 6.2 - NUCLEAR PERFORMANCE

The nuclear performance of the LWBR core during its lifetime agreed well with predicted behavior. Performance analysis during power operation showed that the core was slightly more reactive than calculated at full power. Reactivity bias during power operation ranged from a minimum of 0.18 percent  $\Delta\rho$  more reactive than predicted near beginning of life to a maximum of 0.54 percent  $\Delta\rho$  more reactive than predicted late in core life. Following the third periodic shutdown at 10,771 EFPH, the measured core reactivity at power was observed to have decreased from 0.38-percent  $\Delta\rho$  to 0.26-percent  $\Delta\rho$  more reactive than predicted. This loss of reactivity is consistent with the larger-than-expected flow coefficient of reactivity observed at the same shutdown. This flow coefficient is thought to be caused by small physical movement of fuel assemblies as discussed in WAPD-TM-1546. Operation of LWBR to 29,047 EFPH exceeded the design lifetime of 15,000 EFPH by nearly 100 percent.

Breeding performance of LWBR was also evaluated throughout core life. Fuel depletion calculations which approximated the actual power operations indicated that more fissile fuel was produced in the core than was consumed. The calculated best estimate of final fissile fuel content was 1.35 percent greater than the initial fissile fuel inventory. Final measured fissile fuel

content of the LWBR core was 1.39 percent greater than the initial fissile fuel inventory, with a lower 95 percent confidence bound of 1.15 percent greater than initial fissile fuel inventory.

Periodic tests were performed during core operation to confirm the adequacy of the LWBR nuclear design, to qualify the calculational model used to predict LWBR nuclear performance, and to confirm core symmetry. Agreement between measured test results and calculations using the core follow nuclear analysis model was generally good throughout the LWBR core lifetime. The predicted reactivity was well within the uncertainty allowance of  $\pm 1$  percent used in predicting the lifetime performance and reactor protection of LWBR. In addition, the measured test results confirmed the adequacy of the ranges for the various nuclear design parameters used in the LWBR safety analysis, with the exception that the flow coefficient of reactivity was larger than expected. The safety analysis was modified to include the effects of the larger than expected flow coefficient of reactivity without requiring any change in rated core power.

The testing showed that the calculational models can accurately predict the behavior of  $^{233}\text{U}-\text{ThO}_2$  systems with closely spaced fuel rods and movable fuel. Although extensive use was made of small critical experiments, neutron physics experiments, and high-speed computers, the predictions were made without the benefit of a full scale mock-up critical or of any similar predecessor power reactor core.

### 6.3 - THERMAL PERFORMANCE

The nuclear parameters normally used in evaluating core thermal performance are seed and blanket power sharing, power distribution among fuel assemblies, core power symmetry, and fuel assembly temperature rise. All of these parameters would require exit thermocouple measurements which were not available during the operation of the LWBR core as explained in WAPD-TM-1542, listed in Section 1A of Appendix A. Physics testing (e.g., reactivity worth measurements, symmetry measurements, and copper-nickel flux wire activations) coupled with reactor plant primary and secondary system calorimetric data

adequately compensated for the lack of thermocouples to monitor fuel assembly outlet temperature. All data confirmed the predictions of the thermal design calculations of core performance.

## 6.4 - HYDRAULIC PERFORMANCE

### 6.4.1 - Flow and Pressure Drop

Prior to initial core criticality and with the reactor plant at 531F and 2000 psia, LWBR in-core and primary-loop instrumentation was used to monitor seed and blanket assembly flow rates, core and bypass inlet flow pressure drops, and loop flow rates under four- and three-loop, fast-speed pump operating conditions. Comparison of the range of measured core flows, core pressure drop and total reactor flow\* with appropriate limiting design prediction for four-loop operation showed that: (1) all measured flow rates were above the lower limit of the predicted thermal design values, (2) measured core pressure drop was below the upper limit of the predicted structural design value, and (3) measured data were in close agreement with prediction. These test measurements provided confirmation that such LWBR hydraulic objectives as adequate steady state coolant flow rates and satisfactory pressure distribution on core structures had been attained at the beginning of core life.

The measured core flow rate trends through the LWBR operating lifetime showed that core pressure drop increased about 6 to 7 percent during the 29,047 EFPH operation of LWBR; this was consistent with the approximately 6-percent increase anticipated due to crud deposition in LWBR.

## 6.5 - REACTOR COOLANT CHEMISTRY

### 6.5.1 - Reactor Coolant Water Conditions

The LWBR plant operated with ammonium hydroxide ( $\text{NH}_4\text{OH}$ ) primary coolant chemistry control. The pH of the reactor coolant was maintained between 10.1 and 10.3 by addition of  $\text{NH}_4\text{OH}$ . Conductivity measurements were required to correspond to the measured pH values. Plant degasification was used to maintain reactor coolant total gas below 125 cc/kg, and hydrogen gas between 10

\*Sum of loop flowmeter readings.

and 60 cc/kg. The pH and conductivity levels decreased, and total gas and hydrogen levels increased with plant operation. This was the result of NH<sub>4</sub>OH depletion from core gamma flux. Reactor primary coolant samples were obtained daily and chemical analyses were performed to follow and control these parameters. Chemical additions and plant degasifications were used to maintain parameters within their specified ranges. The reactor coolant visual crud concentration was monitored by weekly sampling of the influent and effluent from the purification system ion exchangers. These analyses confirmed the low reactor coolant crud levels during steady state LWBR plant operations.

#### 6.5.2 - Base and Operational Radionuclide Levels

##### 6.5.2.1 - Base Level Fission and Activation Products

Special radiochemical testing was performed during initial LWBR power operation to characterize the reactor coolant radioactivity. This testing characterized soluble, gaseous, and crud activities. Light Water Breeder Reactor reactor coolant radioactivity was mostly water activation products (<sup>18</sup>F and <sup>13</sup>N), rather than water impurity activation corrosion products (crud) or fission products which were at low levels. All results from the initial power operation radiochemical testing met the required acceptance criteria.

##### 6.5.2.2 - Routinely Monitored Radionuclides

Selected radionuclides were monitored on a routine basis (daily or weekly) throughout the lifetime of the LWBR core. Reactor coolant degassed gross beta activity measurements were made daily during plant operation. These activities were normalized to 100-percent power and were generally in the range of  $9.0 \times 10^{-3}$  to  $2.0 \times 10^{-2}$   $\mu\text{Ci}/\text{ml}$ . The degassed gross beta activities were considered acceptable throughout core life.

Gross iodine, <sup>131</sup>I, and <sup>133</sup>I measurements normalized to 100-percent power were obtained on a weekly basis during power operations. A best fit of measured fission product data through the first 13,000 EFPH of LWBR operation indicated a natural uranium contamination level of 2.0 ppm. This value was in acceptable agreement with uranium contamination levels measured in core tubing and was within the range of fission product measurements made at LWBR startup.

All measured iodine results obtained throughout LWBR core lifetime were consistent and agreed favorably with the predicted buildup curves. No fuel element defects were evidenced in these iodine data.

## 6.6 - PLANT OPERATING EXPERIENCE

### 6.6.1 - Introduction

The LWBR core achieved criticality for the first time on August 26, 1977. The plant was then heated to intermediate temperatures (for performing zero power physics tests), then heated to operating temperature and pressure for the hot operations tests.

The LWBR Acceptance Test Program formally ended on December 2, 1977 when the President, from the Oval Office in the White House, issued the order to "Increase Light Water Breeder Reactor Power to 100% (signed) Jimmy Carter". This order was written on an "electric blackboard" and transmitted by telephone lines to a TV monitor in the Shippingport Station control room. As a historical note, December 2, 1977 was the 35th anniversary of the first self-sustaining chain reaction which was achieved under the leadership of Enrico Fermi at the University of Chicago West Stands on December 2, 1942 and the 20th anniversary of the achievement of initial criticality of the first core at the Shippingport Atomic Power Station.

LWBR was operated at a nominal coolant pressure of 2000 psia and an average coolant temperature of 531F for the first 4325 EFPH for a power rating of 72 Mw gross electric output. Starting in May 1978, a series of pressure, temperature, and power reductions was implemented to reduce the risk of fuel cladding deformation. The total gross electrical output for LWBR was logged as 2,128,943,479 kilowatt hours. The reactor was critical for a total of 35,801 hours.

The plant operated on four loops, except for some periods of three-loop operation to permit maintenance on an isolated loop. With the exception of the planned maintenance shutdowns in the Spring and Fall of each year of operation, the station was maintained mostly at constant power for extended periods.

### 6.6.2 - Maintenance

Maintenance of plant systems and components did not generally limit the ability of Shippingport Atomic Power Station with the LWBR core installed to meet the load demands of the Duquesne Light Company's power distribution system. With the exception of the planned maintenance shutdowns in the Spring and Fall of each year of operation, the Station was available for most of the calendar time. The Spring and Autumn maintenance shutdowns were scheduled during those times of the year when the system load was relatively small and the Station could best be spared. During the 5 years of operation with LWBR, there were 19 interruptions of electrical output due to protective equipment action and/or operator action. Most of these required little or no maintenance and the outage usually lasted 1 day or less. In general, operations during the lifetime of LWBR were uneventful due to the effective preventive maintenance program.

### 6.6.3 - Additional Information

WAPD-TM-1542, listed in Section 1A of Appendix A, contains a detailed discussion of LWBR operations at Shippingport.

## SECTION 7 - DEFUELING AND SHIPMENT OF THE LWBR CORE FUEL

### 7.1 - INTRODUCTION

The objective of defueling was to remove the 39 fuel modules comprising the LWBR core and transfer them to the Naval Reactors Expended Core Facility (ECF) in Idaho for analysis and evaluation of the breeding concept in a thorium-based fuel cycle and subsequent disposal.

Defueling of LWBR was a joint effort by personnel from Westinghouse Electric Corporation's Bettis Atomic Power Laboratory, which designed the reactor, and Duquesne Light Company, which had prime responsibility for operations at Shippingport.

### 7.2 - DEFUELING SAFETY

Throughout LWBR defueling, the prime consideration was personnel safety, both for the technicians performing the defueling operations and for the general public outside of the defueling area. As a part of defueling preparations, a Defueling Safety Assessment was formally issued. Safety features included careful control of personnel radiation exposure, protection against uncontrolled nuclear criticality and spread of radioactive contamination, and use of specially designed and tested defueling equipment to protect personnel from injury and to prevent damage to fuel. As a direct result of the emphasis placed on safety, all defueling operations, including disassembly of fuel modules after removal from the reactor and subsequent shipment of the modules to ECF, were completed with no serious injury to personnel, no damage to fuel or equipment, and no release of radioactive contamination to the environment.

Defueling was completed with total personnel radiation exposure approximately 40 percent of that calculated during defueling planning; no individual worker exceeded 10 percent of the permissible yearly dose of 5 Rem.

Nuclear safety was assured through several features of the defueling program. Protection against nuclear criticality was obtained by heavily borating the reactor vessel and canal water to ensure a minimum margin to criticality of 10 percent during the most reactive defueling condition. This also ensured ample margin under worst-case accident conditions.

### 7.3 - SUMMARY OF DEFUELING OPERATIONS

Defueling operations commenced with draining the reactor pit and removing the dome covering the reactor. Insulation and ventilation equipment were removed first, followed by instrumentation and piping which penetrated the closure head, then the reactor vessel closure head studs. This provided access to the welds that sealed the reactor. Cutting of these welds which sealed the control drive mechanism (CDM) motor tube vent valves, the CDM-to-housing gap, the bypass inlet flow (BIF) system, and the main closure permitted removal of head area components.

After removing head area components, such as CDMs and instrumentation, the blanket modules were detached from the closure head and lowered to the core barrel bottom plate. The closure head was then removed and stored, and the reactor pit was refilled with borated water. Borated water in the reactor vessel and water pit was used to prevent inadvertent criticality. The hold-down barrel was removed from the reactor vessel, placed into a shipping container and sent to a disposal site. The 39 fuel modules comprising the core were then removed one at a time. All seed modules were removed from the reactor first. Reflector and blanket module removal alternated as required by module-to-module clearance shipping schedules and storage space availability. Fuel removal from the reactor was performed in parallel with disassembly and shipping operations due to limited out-of-reactor storage space for the fuel.

Defueling was completed with no major problems. Two major evolutions requiring special consideration were the operations for detaching the blanket modules from the closure head and lowering them to seat on the bottom plate, and the removal of reflector and blanket modules from the reactor vessel.

During reactor assembly, the fuel assemblies, consisting of a blanket module and its mated seed module, were raised from the core barrel bottom plate and latched onto the closure head by using one tool to raise each assembly approximately 3 inches in a single continuous lift. At that time, there was clearance between modules to ensure that exposed grids on adjacent blanket modules would not hang up on each other. For module lowering at end of life,

clearance was no longer assured due to predicted radiation-induced growth and distortions. To allow the modules to be lowered without damage due to grid interference and hangup, all 12 blanket modules were lowered incrementally and simultaneously.

The same considerations affected planning for blanket and reflector module removal from the reactor. It was judged that estimated dimensional changes in fuel modules could have reduced intermodular clearances sufficiently to cause damage to modules if they were raised in a straight lift. Tools were developed to reposition adjacent modules to provide maximum clearances and to avoid obstacles. In addition, a study of potential hangups resulted in a fuel removal sequence that contributed to maximum utilization of space.

#### 7.4 - DISASSEMBLY OF LWBR FUEL MODULES

Partial disassembly of LWBR fuel modules at Shippingport, limited to removal of support and/or extension components, was necessary to allow the fuel modules to fit into the M-130 shipping containers. In each case, a lifting adapter was installed in place of the removed component to permit handling with the same equipment that was used to remove the fuel modules from the reactor. Disassembly of seed and blanket modules was performed under water in the seed/blanket disassembly stand, a large framework structure and work platform designed to clamp and support a fuel module during disassembly operations. Disassembly of reflector modules was performed after the modules were loaded into the M-130 shipping container.

#### 7.5 - LOADING AND SHIPPING OPERATIONS

Shipping operations started with receipt of an M-130 container on its railcar at Shippingport. Three containers were previously modified internally to accommodate either six seed modules, three blanket modules, or four reflector modules. Preparation of the container for receiving fuel included off-loading from the railcar, hooking the container up to a support system for initial filling with borated water, attaching an anticontamination enclosure, placing the protected container into the water in the loading area, and removing the closure head. Fuel modules were loaded into the container and

secured. Final preparations included reinstalling the closure head, removing the filled container from the water and decontaminating the exposed surfaces, reinstalling it on the railcar, and performing several operations using the support system to ensure that the shipment was in compliance with Federal Regulation 10CFR Part 71. Fuel removal from Shippingport was completed in 10 shipments to ECF.

#### 7.5.1 - Additional Information

Section 4 of Appendix A lists three reports on defueling and shipment of the LWBR core.

## SECTION 8 - END-OF-LIFE EVALUATION

### 8.1 - INTRODUCTION

After the 39 expended fuel modules were removed from the reactor vessel and shipped to the Naval Reactors Expended Core Facility in Idaho, 12 of the modules had their end plates cut off so that individual fuel rods could be removed. Some of the rods that were removed were nondestructively assayed and a few rods were destructively assayed to determine their fissile fuel content. The assayed rods were called "proof-of-breeding" (POB) rods, and the 12 modules from which they were taken were called POB modules. Some other rods, called "core examination" rods, were selected for nondestructive and destructive examination to characterize their physical attributes at end of life (EOL). In addition, nonfuel components were also selected for examination as part of this program.

### 8.2 - THE TWO-STAGE STRATIFIED RANDOM SAMPLING PLAN OBJECTIVES

#### 8.2.1 - Objectives

The sampling plan that was used to select the POB rods and modules had two stages. The first was selection of the POB modules. These modules included at least one from each of the nine different symmetric sets, or strata, of expended modules in the core. The second stage of the plan was the selection of the POB rods from the POB modules. The rods in the core were also grouped into strata, and a representative sample of POB rods was chosen from each rod stratum. The selection procedure for both rods and modules was random; hence, the name "two-stage stratified random sampling plan."

The primary objective of the two-stage stratified random sampling plan was to provide a selection of POB rods that would fairly and adequately represent the total population of rods in the core, so that the assay results for these rods could be used to estimate the total EOL loading of all the rods in the core with sufficient precision and accuracy to demonstrate that breeding had occurred. A related objective was to allocate the POB rods to the

different rod and module strata in such a way as to minimize the sampling variance in the core loading estimate -- that is, the uncertainty in the determination of the total fissile content of all 17,290 rods in the core based on measurements performed on a sample of these rods. Sufficient rods were to be chosen from each rod stratum to permit an evaluation of the degree of variability in EOL loading among the different rods of a given type. Similarly, replicate modules were to be chosen from some module strata so that information would be obtained on the module-to-module variation in loading (i.e., on the symmetry of the fuel distribution throughout the core). Finally, the sampling plan was intended to provide high confidence that breeding would be demonstrated even if it should happen that the fissile inventory ratio (FIR) proved to be smaller than best-estimate predictions.

#### 8.2.2 - Simulation Studies Used to Develop the Sampling Plan

Prior to starting assay, it was concluded that 500 fuel rods chosen for assay from 12 modules according to the two-stage stratified random sampling plan could satisfy the above objectives. This conclusion was based on simulation studies carried out using the predicted EOL loadings of all rods in the core, obtained as described in WAPD-TM-1612, listed in Section 1-H of Appendix A.

#### 8.2.3 - Selection of Twelve Proof-of-Breeding Modules

The first stage of the two-stage stratified random sampling plan was the selection of 12 POB modules from the nine different module strata present in the expended core. One POB module was selected from each of six strata, and two POB modules were chosen from each of the remaining three strata: Type III seed, Type IIIII blanket, and Type IVA reflector. Inclusion of a second POB module from these strata provided a measure of the variation of EOL loading among modules within a given stratum to confirm the expected high degree of symmetry of the core. For all strata except the Type V reflector, the number of POB modules selected was one-third of the number of modules in the core. The Type V reflector modules contained less fuel than other module types so that one module out of six was considered to be an adequate sample.

The selection of POB modules was also governed by certain geometrical constraints, which were imposed to ensure that the chosen modules would come from all parts of the core.

#### 8.2.4 - Selection of Five Hundred Proof-of-Breeding Rods

The second stage in the sampling plan was the selection of 500 POB rods from the 12 POB modules. The selection was based on the division of the core rods into different strata. All rods in a given stratum had the same physical design and had essentially identical initial loadings at BOL. For reflector rods, all of which were constructed in the same way and all had zero fissile fuel at BOL, the strata were based on the predicted EOL rod loadings.

The next step in the sampling plan was to decide how many of the POB rods to allocate to each rod stratum. The optimum allocation would be the scheme that produced the smallest sampling variance in the EOL core loading estimate. The size of the sampling variance depended on the method used to deduce the total loading for all the rods in a stratum from the assay results for the POB rods. Two methods were employed to do this. In the first method, called the stratum average (SA) method, the average measured loading for the POB rods was taken to represent the average loading of all the rods in the stratum.

The second method used to infer stratum loadings was called the linear regression (LR) method. In this method, a comparison was made between the predictions of the POB rod loadings and the measured loadings. It was assumed that the relationship between prediction and measurement could be satisfactorily represented by a straight line. This linear relationship was used to apply a correction to the average measured loading of the POB rods before multiplying by the number of rods in the stratum to get the estimated total stratum loading.

The final assay results demonstrated that the LR method could be applied to all module strata and use of the LR estimation for all modules resulted in a much smaller core loading variance than the SA method.

The final step in the sampling plan was the identification of the specific rods to be assayed. These rods were selected randomly, subject to certain geometrical constraints that were applied to ensure that all parts of each module would be adequately represented in the sample.

#### 8.2.5 - Selection of Twenty-Four Additional Rods

When the assay results showed that some individual reflector rods had up to 65 percent more fuel than predicted, it was decided that additional reflector rods should be assayed to allow their properties to be characterized more precisely. Accordingly, 20 additional rods selected from the outer rod rows of reflector module IV-9 were assayed. The results for these additional rods were consistent with the results for the rods in the original sampling plan.

In addition, the PIFAG was used to process a few fuel rods that were included in the core examination program. It was decided to perform a full-fledged assay on four of these rods because they had particularly high fuel burnup.

Thus, the total number of rods nondestructively assayed was 524. Five hundred of these were from the original sampling plan, 20 were added to aid in the analysis of the reflector data, and four were included from the core examination work.

#### 8.2.6 - Selection of Seventeen Rods for Destructive Assay

Seventeen of the POB rods were sent to Argonne National Laboratory (ANL) for destructive assay after they had been nondestructively assayed in the PIFAG. Five of these rods were seed, four were standard blanket, six were power flattened blanket, and two were reflector. These numbers are in roughly the same proportion as the distribution of fuel in the EOL core. The objective was to obtain destructive assay results on a few POB rods to establish an accurate reference against which the nondestructive results could be compared and any bias could be revealed.

#### 8.2.7 - Additional Information

Additional information on the sampling plan is contained in WAPD-TM-1612, listed in Section 1-H of Appendix A.

## 8.3 - PROOF OF BREEDING

### 8.3.1 - Introduction

The objective of the POB program was to determine the EOL fissile fuel content of the core, which together with the known BOL loading, would determine if the core were a breeder. The BOL fissile fuel content was 501.04 Kg, including about 0.4 Kg of  $^{235}\text{U}$  in addition to the  $^{233}\text{U}$ , contained in the seed and blanket parts of the core. The reflector contained no fissile fuel at BOL. The initial fissile content was known to a precision of better than 0.1 percent based on both destructive and nondestructive assay of individual fuel pellets during core manufacture.

### 8.3.2 - Sample Selection

Figure 19 identifies the locations of the 12 POB modules. The modules were chosen to give a good geometrical representation of the core. They included at least one of each distinct type (seed, blanket and reflector) and three pairs in symmetric locations (SIII-1 and III-2, BIII-2 and III-6, R IV-4 and IV-9) to provide information about core symmetry.

After selection of the modules, the POB rods were randomly selected from predetermined strata according to the strategy described in WAPD-TM-1612 (see Section 1-H of Appendix A).

As an example, Figure 20 shows a cross section of one of the blanket modules with the locations of the POB rods indicated as solid black circles within strata bounded by black lines.

The rods were randomly selected subject to the geometrical constraints to ensure that a representative sample would be chosen from all parts of the module. This procedure was typical for POB rods from all 12 modules selected for the proof of breeding experiment.



SAMPLED  
MODULE



MODULE  
NOT SAMPLED

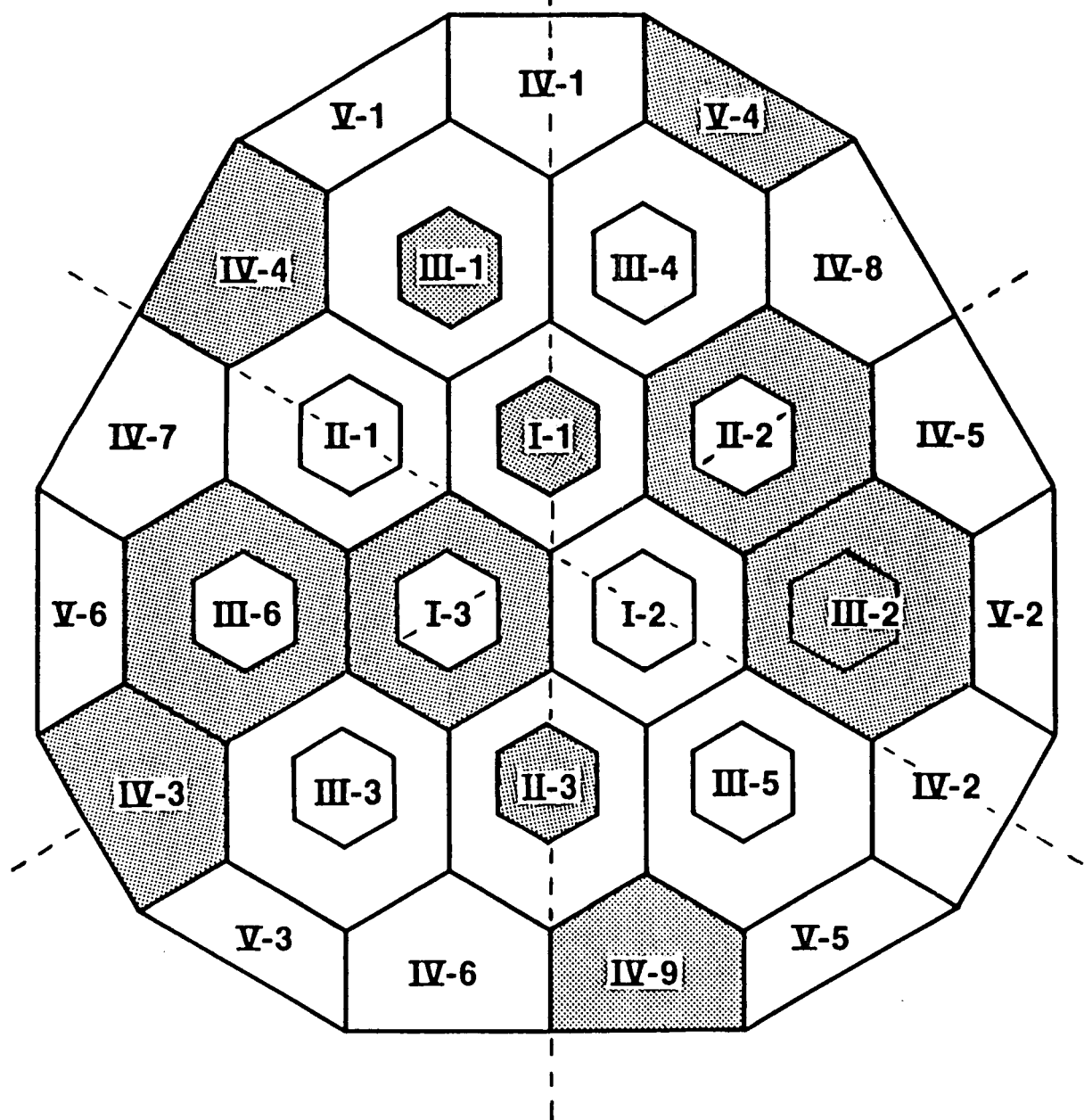


Figure 19. Sample Modules for LWBR Core

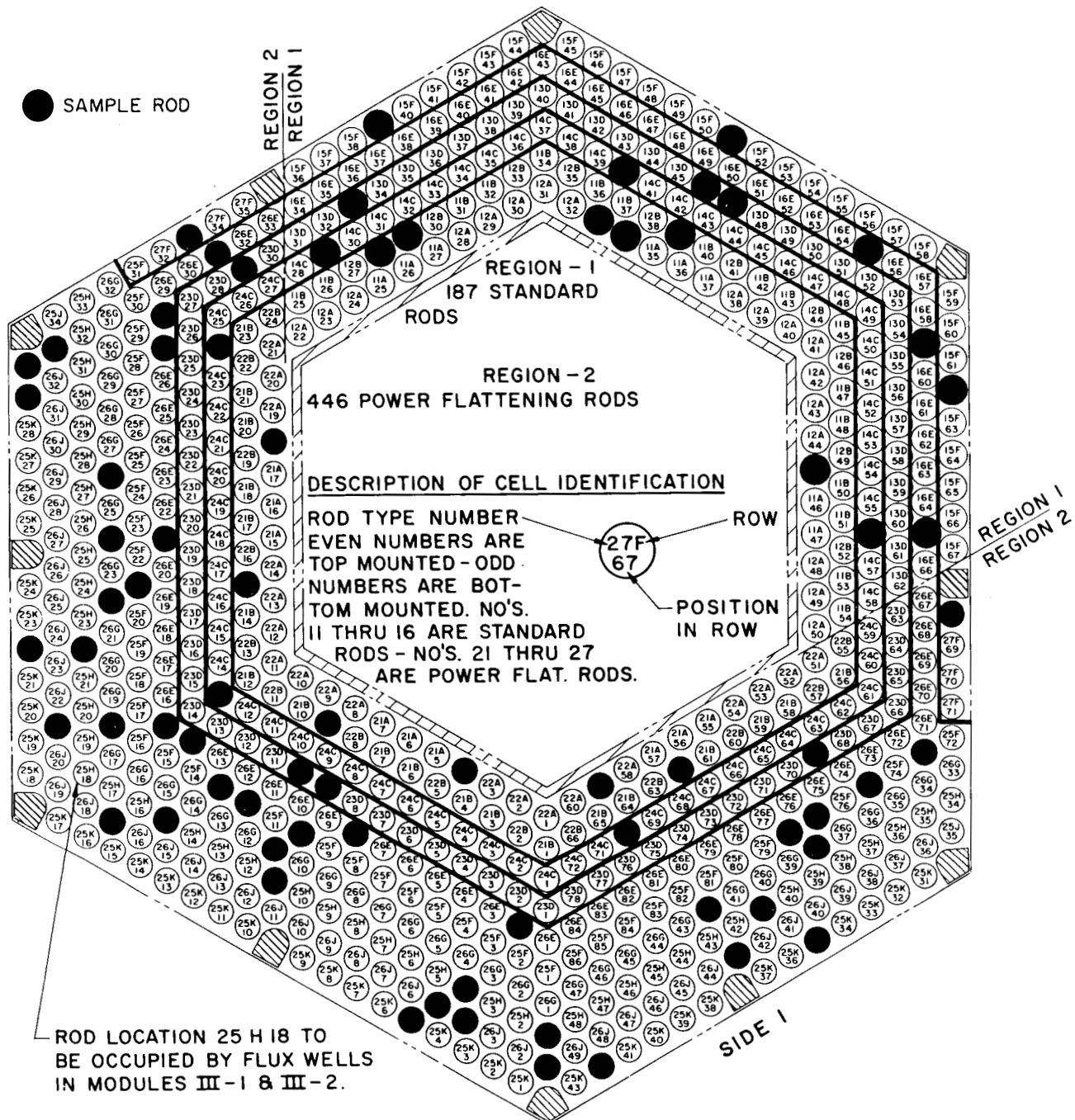


Figure 20. Rod Sampling for Blanket III-6 Modules

### 8.3.3 - Nondestructive Assay Techniques

Nondestructive assay of the 524 rods was accomplished with a specially designed assay gauge (termed PIFAG) based on the proportionality between the number of delayed neutrons coming from controlled irradiation of the residual fuel in a rod and the fuel content of the rod.

Figure 21 is a schematic diagram of the assay gauge. This gauge is described in WAPD-TM-1547 and 1555 listed in Section 1-H of Appendix A. In brief, rods passing through the source region on the left of the figure are interrogated by neutrons from four  $^{252}\text{Cf}$  sources. Delayed neutrons resulting from fissions that occur in the fuel in the source region are counted as the rod passes through the detector region.

Two different interrogation spectra were provided by means of a movable center tube. The figure shows the position of the center tube for the PIFAG configuration referred to as the thermal system. Movement of the center tube to the left brings an In-Cd liner into the source region. The liner removes the low energy portion of the interrogation spectrum and provides a configuration referred to as the epithermal system. Assay data was obtained using both systems, which were semi-independent and provided an interval check on the quality of the data.

Except for some reflector rods with small quantities of fissile fuel, individual rod loadings were obtained with a total uncertainty of less than 0.5 percent per rod at the one sigma level.

Assay work was initiated in July 1984 and completed in June 1987.

### 8.3.4 - Assay Results

#### 8.3.4.1 - General

Table 2 shows the results for all 18 regular blanket rods from Module III-6. Regular blanket rods come from the inner blanket region of the core. Blanket rods from the outer region are designated "power flattening blanket."

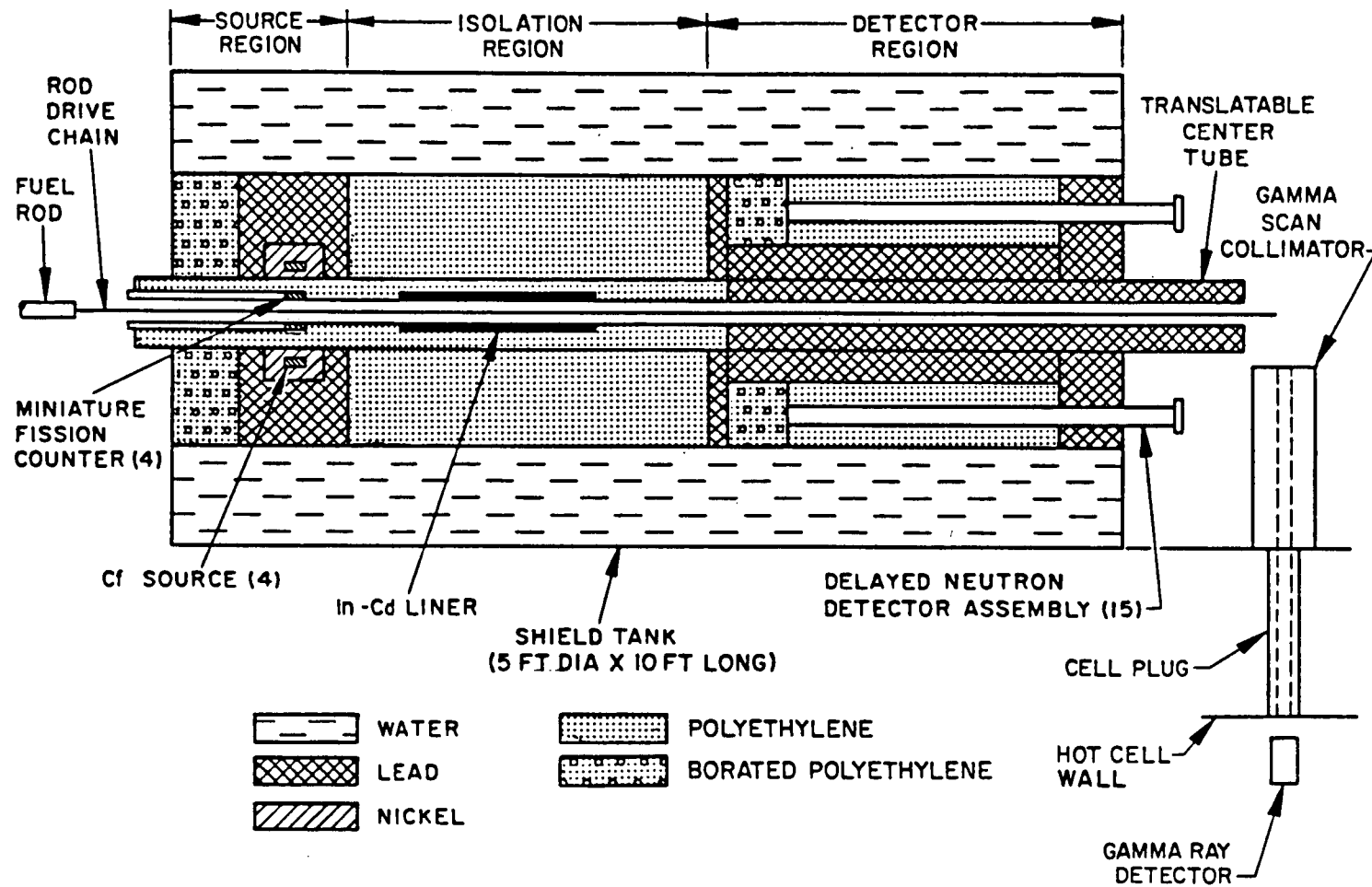


Figure 21. PIFAG Schematic Diagram

Table 2 - Regular Blanket III-6 Fissile Loadings in Grams

Cell	Predicted By PDQ	Measured PIFAG				Differences in Percent		
		Thermal		Epithermal		EPI/ THER	THER/ PDQ	EPI/ PDQ
A33	34.362	34.555	(0.24)	34.721	(0.31)	+0.48	+0.56	+1.04
A34	34.410	34.673	(0.25)	34.612	(0.34)	-0.18	+0.76	+0.59
A45	33.591	34.117	(0.23)	34.134	(0.37)	+0.05	+1.57	+1.62
B28	33.426	32.896	(0.21)	32.999	(0.28)	+0.31	-1.59	-1.28
B29	33.576	33.108	(0.23)	32.994	(0.29)	-0.34	-1.39	-1.73
B39	34.252	33.843	(0.23)	33.829	(0.31)	-0.04	-1.19	-1.23
C29	39.399	38.748	(0.22)	38.943	(0.28)	+0.50	-1.65	-1.16
C40	40.319	39.888	(0.23)	39.845	(0.33)	-0.11	-1.07	-1.18
C56	39.255	38.704	(0.21)	38.891	(0.33)	+0.48	-1.40	-0.93
D33	46.985	46.296	(0.23)	46.276	(0.28)	-0.04	-1.47	-1.51
D46	47.434	46.917	(0.25)	47.066	(0.36)	+0.32	-1.09	-0.78
D47	47.429	46.880	(0.25)	46.912	(0.37)	+0.07	-1.16	-1.09
F39	47.344	47.751	(0.23)	47.770	(0.25)	+0.04	+0.86	+0.90
F51	47.580	48.214	(0.25)	48.080	(0.33)	-0.28	+1.33	+1.05
F62	47.306	47.736	(0.23)	47.815	(0.26)	+0.17	+0.91	+1.08
E55	52.903	52.462	(0.24)	52.625	(0.28)	+0.31	-0.83	-0.53
E59	52.861	52.333	(0.26)	52.640	(0.34)	+0.59	-1.00	-0.42
E65	52.445	51.791	(0.22)	52.031	(0.27)	+0.46	-1.25	-0.79

(X.XX) = 1 Std. Dev. Uncertainty in Percent

The cell number refers to the location of a rod in the module. The PDQ loadings are predicted values that were calculated with the LWBR Nuclear Analysis model.

The PIFAG uncertainties are typically about 0.25 percent for these rods in the thermal system and a little higher in the epithermal system.

The epithermal results tended to be slightly higher than the thermal results. This was generally true for seed and blanket rods indicating a small epithermal to thermal bias. For reflector rods, the thermal values were slightly higher.

The measured loadings are within 2 percent of the predicted loadings. However, note that with the exception of the three rods in Row A and the three rods in Row F the PIFAG values are consistently lower than predicted. Note that each of the six rods for which the assay results are higher than predicted are adjacent to water channels in the core. In all cases, the nuclear

model underpredicted the loadings in rods adjacent to water channels. It is judged that this results from the difficulty in characterizing the flux gradient across a fuel-water interface in a diffusion theory code like PDQ. Diffusion coefficients and cross sections used in PDQ were obtained from infinite lattice calculations.

This characteristic was observed in all seed and blanket modules. However, in reflector modules, the measured loadings of all rods were significantly higher than predicted (up to 5.1 percent) which is believed due to a transport problem in the calculational model which fails to accurately account for neutron leakage into the reflector region.

#### 8.3.4.2 - Destructive Versus Nondestructive Results

Destructive analysis of 17 rods was performed independently by Argonne National Laboratory (ANL) to assess the accuracy of the nondestructive assay gauge. The results, discussed in detail in WAPD-TM-1612, listed in Section 1-H of Appendix A, indicated no statistical difference, at the 5 percent significance level, between the PIFAG thermal system results and the ANL results. However, a small statistically significant bias was observed between the PIFAG epithermal results and the ANL results, consistent with the previously mentioned difference between the thermal and epithermal results. Therefore, the final determination of the FIR was based solely on the higher quality thermal results.

#### 8.3.4.3 - Symmetry Results

Table 3 shows the module loadings for the three pairs of symmetrically located modules in the core. In all cases, no statistically significant difference was observed between the modules in each set, indicating very little, if any, flux tilt in the core. However, as discussed below, the individual reflector module values showed a difference consistent with a small flux tilt observed during BOL physics testing.

##### Seed III-1 and III-2

The loadings differ by  $0.20 \pm 0.17$  percent based on thermal PIFAG data and  $0.32 \pm 0.17$  percent based on the epithermal data, where the uncertainties are

Table 3 - Comparison of Module Loadings for Symmetric Modules

<u>Module</u>	<u>Module Loadings (Grams <math>\pm 1\sigma</math>)</u>		
	<u>As-Built</u>	<u>Thermal</u>	<u>Epithermal</u>
<b>S III-1</b>	<b>16517.5</b>	<b>13229.9 <math>\pm</math> 17.1</b>	<b>13256.1 <math>\pm</math> 17.1</b>
<b>S III-2</b>	<b>16556.5</b>	<b>13256.7 <math>\pm</math> 14.6</b>	<b>13298.8 <math>\pm</math> 15.3</b>
<b>Pct. Diff.</b>	<b>-0.24%</b>	<b>-0.20% <math>\pm</math> 0.17%</b>	<b>-0.32% <math>\pm</math> 0.17%</b>
<b>RB III-2</b>	<b>6629.9</b>	<b>7955.0 <math>\pm</math> 6.8</b>	<b>7954.9 <math>\pm</math> 5.8</b>
<b>RB III-6</b>	<b>6626.8</b>	<b>7951.3 <math>\pm</math> 5.3</b>	<b>7965.6 <math>\pm</math> 5.4</b>
<b>Pct. Diff.</b>	<b>-0.05%</b>	<b>0.05% <math>\pm</math> 0.11%</b>	<b>-0.13% <math>\pm</math> 0.10%</b>
<b>PFB III-2</b>	<b>23157.3</b>	<b>21516.5 <math>\pm</math> 15.0</b>	<b>21570.7 <math>\pm</math> 15.7</b>
<b>PFB III-6*</b>	<b>23170.4</b>	<b>21551.4 <math>\pm</math> 16.3</b>	<b>21575.0 <math>\pm</math> 16.6</b>
<b>Pct. Diff.</b>	<b>+0.06%</b>	<b>-0.16% <math>\pm</math> 0.10%</b>	<b>-0.02% <math>\pm</math> 0.11%</b>
<b>R IV-4</b>	<b>0.0</b>	<b>3323.8 <math>\pm</math> 14.8</b>	<b>3303.2 <math>\pm</math> 16.6</b>
<b>R IV-9</b>	<b>0.0</b>	<b>3341.9 <math>\pm</math> 7.9</b>	<b>3321.3 <math>\pm</math> 9.3</b>
<b>Pct. Diff.</b>	<b>0.0%</b>	<b>-0.54% <math>\pm</math> 0.50%</b>	<b>-0.55% <math>\pm</math> 0.58%</b>

**\*Without Flux Well Rod**

one standard deviation in the difference in module loadings. These differences are not statistically different from zero at the 5 percent significance level. Note that a difference of 0.24 percent was already present in the as-built loadings.

#### Blanket III-2 and III-6

For the RB modules, the differences in module loadings are statistically insignificant for both the thermal and epithermal data. The BOL difference was also negligible. Before making the PBF module comparison, it was first necessary to correct for the presence of a flux well in Module III-2. As for the RB modules, the differences in module loadings are statistically insignificant.

#### Reflector IV-4 and IV-9

For these modules, the loadings differ by about 0.5 percent with the uncertainties being about the same as the differences. Although statistically insignificant, the differences are in agreement with what would be predicted based on a small asymmetry of "tilt" detected in the core neutron flux distribution from EOL physics testing.

#### 8.3.4.4 - Final Results

Table 4 shows the total module loadings estimated for the modules from which the POB rods were sampled compared to calculated values.

The PIFAG results for the seed and blanket agree with the calculation to better than one percent. However, there is a definite trend, with the PIFAG results being lower than predicted. The reflector results, on the other hand, are higher than predicted. Because of the relative amount of fuel in the different regions, the larger-than-expected amount of fuel in the reflector just slightly over balances the smaller-than-expected amount in the rest of the core, as shown in Table 5.

Table 5 contains the final results for the total core fissile fuel loading and the FIR.

Table 4 - Nondestructive Assay Results for 12 LWBR Fuel Modules

<u>Fuel Module</u>	<u>Module Fissile Fuel Content, Grams</u>			<u>Percentage Differences</u>		
	<u>PIFAG Thermal</u>	<u>PIFAG Epithermal</u>	<u>Calculated</u>	<u>Epith. -Therm.</u>	<u>Therm. -Calc.</u>	<u>Epith. -Calc.</u>
SI-1(a)	12490.5 ± 18.1(b)	12514.9 ± 19.3	12571.8	.+20	-.65	-.45
SII-3	12891.1 ± 13.9	12936.0 ± 17.3	12942.0	.+35	-.39	-.05
SIII-1	13229.9 ± 17.1	13256.1 ± 17.1	13276.8	.+20	-.35	-.16
SIII-2	13256.7 ± 14.6	13298.8 ± 15.3	13276.8	.+32	-.15	.+17
BI-3	19591.1 ± 13.6	19618.0 ± 12.7	19662.8	.+14	-.36	-.23
BII-2	25697.8 ± 14.9	25737.9 ± 15.2	25786.5	.+16	-.34	-.19
BIII-2	29471.5 ± 16.4	29525.6 ± 16.7	29559.4	.+18	-.30	-.11
BIII-6	29560.0 ± 17.1	29598.0 ± 17.5	29616.8	.+13	-.19	-.06
RIV-3	3050.9 ± 14.5	3016.9 ± 12.7	2911.3	-.11	+4.80	+3.63
RIV-4	3323.8 ± 14.8	3303.2 ± 16.6	3179.7	-.62	+4.53	+3.88
RIV-9	3341.9 ± 7.9	3321.3 ± 9.3	3179.7	-.62	+5.10	+4.45
RV-4	1721.1 ± 4.5	1704.8 ± 7.6	1662.8	-.95	+3.51	+2.53

(a) Modules are identified as S(Seed), B(Blanket), or R(Reflector).

(b) One standard deviation of the estimated module loading.

Table 5 - Total Fissile Fuel Loadings and FIR for the LWBR Core

<u>Rod Type</u>	<u>No. of Rods</u>	<u>Initial Loading (Kgm)</u>	<u>EOL Loading - Kgm</u>		
			<u>PIFAG Thermal</u>	<u>PIFAG Epithermal</u>	<u>Calculated</u>
Seed	7428	198.58	155.60	156.02	156.20
Blanket	6815	302.43	312.91	313.38	313.82
Reflector	<u>3047</u>	<u>0.00</u>	<u>39.47</u>	<u>39.14</u>	<u>37.78</u>
<b>Total</b>	<b>17290</b>	<b>501.02</b>	<b>507.98</b>	<b>508.54</b>	<b>507.81</b>
<b>FIR</b>			<b><math>1.0139 \pm 0.0014</math></b>	<b><math>1.0150 \pm 0.0021</math></b>	<b>1.0135</b>
<b>FIR Best Estimate</b>			<b><math>1.0139 \pm 0.0014</math></b>		

The reflector, which contained no fuel at BOL, contained nearly 8 percent of the fuel at EOL. The fissile inventory ratio which is the ratio of fissile fuel at EOL to the amount at BOL is  $1.0139 \pm 0.0014$  based on PIFAG thermal system measurements and  $1.0150 \pm 0.0021$  based on PIFAG epithermal measurements. The uncertainties are one standard deviation and include an estimate of the bias obtained from a comparison with destructive assay data. Both values are slightly higher than the predicted value of 1.0135. Because the epithermal measurements were less precise than the thermal measurements and because it is suspected that a small bias is present in the epithermal results, the best-estimate for the FIR is judged to be the thermal value of  $1.0139 \pm 0.0014$ .

It is concluded from these results that breeding in a LWBR has been demonstrated and that the thorium/uranium-233 fuel cycle can be used in proven pressurized light water reactors to greatly extend the nation's nuclear fuel resources.

#### 8.3.5 - Additional Information

Additional information on proof of breeding is contained in the technical memoranda listed in Section 1-H of Appendix A.

### 8.4 - CORE COMPONENT EXAMINATION

#### 8.4.1 - Introduction

Detailed postoperation examination of LWBR core components was made to determine if these components had functioned in accordance with predictions or, if there was evidence of unexpected response to the stresses of reactor operation for the extended lifetime to 29,047 EFPH.

The examinations summarized in this section occurred at Shippingport and at ECF during five years (October 1982 through September 1987).

#### 8.4.2 - Major Assembly Examination

The condition of several major components from the LWBR reactor core was determined after five years of power operation. All 39 fuel modules were visually inspected immediately after being removed from the Shippingport

reactor vessel. All modules were found to be in excellent condition and no abnormalities were detected that could be attributed to core operation. In addition to visual examinations, module growth and bow were measured on selected assemblies. Module bow and growth agreed with expected values based on radiation-induced Zircaloy growth alone. There was no contribution to bowing or growth from pellet to clad interference.

Bow at EOL for the hexagonally-shaped seed fuel modules ranged from 0.010 to 0.053 inch, less than or within the predictions of 0.025 inch (best-estimate) and 0.092 inch (upper-bound) models. Bow for the blanket fuel modules, also hexagonally shaped, ranged from 0.029 to 0.100 inch, closely matching the predictions of 0.041-inch (best-estimate) and 0.130-inch (upper-bound) models. Bow for the reflector modules ranged from 0.188 to 0.239 inch, again within predictions of 0.180-inch (best-estimate) to 0.257-inch (upper-bound) models.

Outward appearances of the modules were similar to that at installation. Some oxidation and crud were noted, but there were no indications of defects or distortions. Most of the stainless steel core structural component surface areas exhibited only the magnetite corrosion surface commonly found on components in pressurized water test loops. As expected, some marks attributed to handling and shipping were found during reexamination of selected modules at the Expendable Core Facility (ECF). These marks, although of negligible depth, were easily noted by removal of the corrosion film surface.

Another area examined was the reactor vessel closure head. It was of interest because of the material composition. The closure head was among the first forged from ASTM-A-508, Class 4 material for reactor application and it performed satisfactorily in service. Visual, ultrasonic, and magnetic particle tests were performed and no defects were found. The nondestructive tests performed on the closure head were an ultrasonic probe of the material and a magnetic particle test of the fillet weld at the bolting flange.

Examinations of structurals forming the guide path for the movable fuel at Shippingport were also performed. As part of an evaluation of a one-time occurrence of an anomalous slow scram by one module during periodic testing,

videographs of the guide path and guide path components (compression sleeve and guide tube extension) for the module having the slow scram were compared to those of the guide path of a module having no unusual characteristics. This was done in order to seek a mechanical source for binding or interference. No differences were found between the two guide paths.

Two observations were made:

1. Crud was found to be deposited in several components such that an imprint of the adjacent component was made. Images of the blanket modules were left on the reflector module shells. Features of the seed modules were found inside the guide tube extension and inside the compression sleeve.
2. Mottled surface appearances of fuel rods (nodular white corrosion product) varied with the type of fuel pellets. Boundaries between binary and thoria fuel were seen in the deshelled seed module exam. Dark bands at the interfaces between pellets were noted on the blanket rods.

In general, all external examinations showed that the LWBR components were in excellent condition at end of core life. The results indicated there was no degradation detrimental to core operation.

#### 8.4.3 - Additional Information

Additional information on major assembly examination is contained in WAPD-TM-1602, listed in Section 1-E of Appendix A.

### 8.5 - NONDESTRUCTIVE EXAMINATION OF LWBR FUEL RODS

#### 8.5.1 - Introduction

Spent modules were shipped from Shippingport to the Naval Reactors ECF in Idaho Falls, Idaho for detailed examination. The examinations were performed, in part, to assess support structure and fuel rod performance and to provide a data base for evaluation of design procedures. The program included examinations of entire modules as well as individual components (fuel rods, grids, bolts, etc.). The purpose of this section is to present results of in-bundle

and out-of-bundle EOL nondestructive examinations of LWBR fuel rods that were performed to evaluate fuel rod dimensional stability, cladding and fuel pellet integrity, Zircaloy cladding corrosion, and fuel rod crud buildup.

#### 8.5.2 - Examinations Performed

In-bundle examinations included visual examination of each module, rod spacing and bow measurements, and pull force measurements. In-bundle spacing and bow were determined by digitizing 5X video recordings of fuel rods in seven of the 39 LWBR fuel modules. Up to 10,000 spacing measurements and 10,000 rod centerline position measurements were obtained for a single fuel module. Pull forces were measured for all rods removed from spent fuel modules. Measured pull forces were monitored at 0.1 to 0.4-inch increments during rod pull and were compared with limits to assure that fuel rod cladding was not overstressed during removal. The data was also used for analysis of sliding friction and comparisons between rods.

Out-of-bundle examinations included measurement of fuel rod length, diameter, plenum ovality, cladding wear, free-hanging bow, and oxide thickness in the rod examination gage (REX) (see WAPD-TM-1610, listed in Section 1-D of Appendix A) specifically designed for examination of LWBR fuel rods. Ultrasonic probes on the REX were also used to screen fuel rods for defects (e.g., partial or through cracks). Nineteen fuel rods were examined with the REX.

Approximately 40,000 diameter measurements per rod were obtained with the REX. Measured diameters were used to determine the axial variation of average fuel rod diameter and cladding ovality. Approximately 1000 oxide thickness measurements per rod were obtained with the REX. Measured oxide thickness was used to study the axial and radial variation of oxide thickness for individual rods and for comparison between rod types.

An orbiting profilometer on the REX was used to determine fuel rod plenum ovality and wear mark depth and volumes. The gage provided surface radial and angular position around the circumference of a fuel rod relative to a fixed coordinate system. Approximately 2500 measurements of the cladding surface were used to determine the depth and volume of an individual wear mark.

Approximately 2000 measurements of cladding surface position were used to characterize plenum ovality for a single rod.

Fuel rod free-hanging bow was determined by digitizing 5X video recordings with the rod suspended in the REX. End-of-life (EOL) free-hanging bow measurements were obtained for comparison with similar measurements obtained during fuel rod fabrication and for calculation of EOL in-bundle bow of fuel rods.

Out-of-bundle examinations also included neutron radiography of the fuel rods and crud characterization and crud thickness measurements by Argonne National Laboratory-West (ANL-W) and gamma scan of the fuel rods using the production irradiated fuel assay gage (PIFAG) at ECF (see WAPD-TM-1555 and 1614, listed in Section 1-H of Appendix A). Neutron radiography was used to determine pellet integrity, fuel stack length, and to search for spaces between pellets (in-stack axial gaps). Gamma scans were also used to determine fuel stack lengths and to search for in-stack axial gaps. Measured fuel stack lengths were used to calculate fuel stack length changes for comparison with predictions. Crud examinations were performed to determine elemental and isotopic components of the LWBR crud, to determine axial variation of crud thickness, and for comparison among rod types.

#### 8.5.3 - Examination Results and Conclusions

Conclusions drawn from these examinations can be summarized as follows:

1. Rod length and diameter change measurements and fuel stack length measurements indicate that pellet-cladding interaction for seed and blanket fuel rods was less than anticipated based on irradiation test results and analyses. Rod length increases were less than best-estimate predictions. Fuel stack length was greater than best-estimate predicted values. Cladding diameter shrinkage was less than CYGRO best-estimate predictions. The smaller length increases resulted in greater than predicted rod end to baseplate clearances, thereby permitting coolant free flow through the baseplate holes.

2. Fuel geometry indicated that fuel pellet temperatures were less than expected. Fuel pellet end faces were still clearly dished after 30,000 EFPH operation. Blanket pellet end tapers were not distorted by pellet hourgassing at peak power locations. This conclusion is supported by results of fission gas measurements presented in WAPD-TM-1606, listed in Section 1-D of Appendix A.
3. LWBR fuel pellets were dimensionally stable. Gamma scan and neutron radiography of 35 rods revealed no axial gaps greater than 0.030 inch. Cracks were observed in as many as 41 percent of pellets in a rod. Some cracks were wide enough to indicate fuel separation, but all pieces remained in place. No pellets were crumbled or gave any indication of risk to cladding integrity.
4. Cladding wear at the grid contact points was low. A maximum wear depth of only 0.0014 inch was measured. Only 2.2 percent of the rod-to-grid contact points visually examined for wear had an appearance warranting examination with the orbiting profilometer. Half of the locations examined had depths less than 0.0005 inch. The absence of large cladding wear indicates that fuel rods were adequately restrained by the AM-350 support grids. Low cladding wear substantiated statistical predictions of cladding wear, which indicated excessive wear of LWBR fuel rods was unlikely.
5. As expected, RXA seed cladding was freestanding. The maximum measured ovality for cladding was only 0.0017 inch over the plenum and 0.0044 inch over the fuel stack. Fuel-cladding clearances remained in seed rods throughout lifetime. Diameter profiles gave no indications of ridging or restricted shrinkage.
6. Deformation of unsupported, nonfreestanding cladding in the plenum region of blanket rods was small. Less than expected cladding elongation and fuel stack shrinkage resulted in smaller unsupported cladding lengths in fuel rod plena. The maximum measured plenum ovality was only 0.0038 inch. This ovality was comparable to best-estimate predicted plenum ovality of 0.006 inch for the limiting blanket fuel

rod with a 1.5-inch best-estimate unsupported cladding length. Low blanket plenum ovalities support statistical predictions of blanket cladding ovality, which indicated that collapse of unsupported cladding was unlikely.

7. Nonfreestanding cladding blanket and reflector rods shrank onto the pellets and assumed pellet shapes as predicted. Diameter profiles of blanket rods showed grooves at pellet end tapers and reflector rod profiles showed ridges caused by the untapered pellets. All grooves were within predicted maximums. The maximum measured ridge for a reflector rod was 1.4 mils compared to a worst-case predicted value of 1.1 mils.
8. Cladding ovality over the fuel stack was less than 0.005 inch for all rods. Ovality was most common at the end thoria fuel locations in blanket rods. The cladding apparently had not fully crept onto the fuel at these low power, low fluence locations.
9. Power depression at grid elevations was evident in measured profiles of rod diameter and surface oxide thickness. Variations in rod surface color occurred on some rods at grid levels and at pellet interfaces, caused by temperature-sensitive formation of oxide.
10. Examination of rod-to-rod spacing for one seed module indicated that the 95/95 tolerance interval for seed fuel rod channel closure was 50 percent or less for the central spans. No indications of rod-to-rod contact were observed. This was consistent with statistical analyses of rod-to-rod spacing. The minimum measured rod-to-rod spacing was 0.010 inch.
11. Examination of rod-to-rod spacings in 5 blanket modules indicated that the 95/95 tolerance interval for standard blanket channel closure was 48 percent or less for the peak power spans and 59 percent or less at all other spans. The 95/95 tolerance interval for power flattening fuel rod closure was 48 percent or less. One near contact condition (0.002 inch rod-to-rod spacing) was observed. Examination of the rods involved did not reveal any degradation in performance.

12. Examination of rod-to-rod spacing in one reflector module after base-plate severing indicated that the 95/95 tolerance interval for reflector channel closure was 39 percent or less. No near contact conditions were observed.
13. Measurement of fuel rod in-bundle bow indicated that module bow was the primary contributor to fuel rod bow. The maximum bow between grids measured was 0.020 inch, 0.027 inch, and 0.029 inch for seed, blanket, and reflector rods, respectively. These bows are well below worst-case estimates of fuel rod bow. Calculations of in-bundle bow for the four spans near the fixed ends of rods from free-hanging bow data yielded peak bows of 0.0148 inch, 0.0183 inch, and 0.015 inch for seed, blanket, and reflector rods. These calculated bows are well below worst-case estimates of fuel rod bow. A 0.0248-inch bow was calculated for the span nearest the free end of one blanket rod. This bow was larger than expected.
14. There was no evidence of fuel rod binding in the AM-350 support grids. Pull forces for all rods removed were well below disassembly limits. Residual grid spring force was generally high at the end grid and low for the central grids.
15. Although there was no evidence of fuel rod defects, ultrasonic inspection of 12 fuel rods indicated that some LWBR fuel rods may have had significant cladding flaws. Three of the 12 rods examined had internal crack indications in excess of 0.010 inch. However, metallographic examination of two of these indications showed no indication of cladding cracks.
16. Crud measurements on 3 rods indicated that crud buildup was low, although some crud could have been removed by rod handling. The maximum measured diametral crud thickness was only 0.00048 inch. As expected, crud for the seed rod and blanket fuel rod examined was heavier near the ends versus the central 60 percent of the rod. Contrary to expectations, crud for the reflector rod examined was

heavier in the middle of the rod. Crud thicknesses on the reflector rod were less than for the seed and blanket rod.

17. Detailed visual examination of 19 fuel rods in the REX and cursory examination of about 1100 rods during rod removal did not reveal any indications of fuel rod failure or other unusual conditions (e.g., collapsed sections, etc.). A wide variation in rod surface appearance was observed. Appearance (from black-and-white video pictures) of rods in proximity to one another varied from uniform white to speckled to uniform gray.
18. Corrosion oxide film thickness profiles were as expected for PWR fuel rods, i.e., highest at the high power, binary fueled regions with pronounced thinning at the support grid levels and at the top and bottom of the binary fuel stack. Measured thicknesses were in reasonable agreement with values calculated with a model based on cladding surface temperature, fast flux, and exposure time.

Overall, LWBR fuel rod performance was excellent. Examinations indicated that the rods sustained no defects (i.e., breached cladding), no major cladding deformations, and little wear during operation for 29,047 EFPH. Models for predicting fuel rod performance were found to be slightly over-conservative. Limiting observations were generally well below worst-case predictions. In many instances, average observations were less than best-estimate predictions. For the most part, the model conservatism can be attributed to an over estimate of pellet-cladding interaction. These examinations confirmed the expected performance behavior of the thorium/uranium-233 fuel system.

#### 8.5.4 - Additional Information

Additional information on the nondestructive examination of fuel rods may be found in WAPD-TM-1605, listed in Section 1-D of Appendix A.

## 8.6 - DESTRUCTIVE EXAMINATION OF LWBR FUEL RODS

### 8.6.1 - Introduction

This section describes the results of destructive examination of 12 LWBR fuel rods at end of life. The general appearance of the rods and their microstructural and chemical condition following core operation to 29,047 EFPH was characterized. The effect of core operation on Zircaloy-4 cladding corrosion, hydriding, and iodine and cesium content was evaluated. Similarly, fuel microstructure (including grain size and porosity changes), iodine and cesium content, and in some cases depletion were assessed.

Destructive examinations of fuel rods were performed both at Argonne National Laboratory-West (ANL-West) in Idaho Falls, Idaho, and at Argonne National Laboratory-East (ANL-East) in Argonne, Illinois. After the rods were nondestructively examined in the Rod Examination Station (REX) at the Expended Core Facility (ECF), the rods were shipped to ANL-West, where they were neutron radiographed and punctured to obtain fission gases. The neutron radiography procedure and examination findings are given in WAPD-TM-1605 (see Section 1-D of Appendix A).

The approximately 10-foot long rods were cut in half to facilitate handling and were shipped to ANL-East. Samples were cut from each rod half; some of the samples were shipped back to ANL-West for examination for iodine and cesium content and for fuel depletion while all other examinations were performed at ANL-East. Results of these examinations are summarized below.

### 8.6.2 - Iodine and Cesium Analysis of the Fuel and Cladding

Stress corrosion cracking of metallic components, such as the Zircaloy-4 cladding, has historically been a problem concerning reactor safety and fuel performance. Iodine and cesium have been identified as possible corrosive agents causing stress corrosion cracking. Under reactor conditions, fission product iodine can react with Zircaloy. Measurement of fission product iodine and cesium inventories in the fuel rod samples was performed to determine the fraction of these nuclides that migrate to the gap region and into the cladding. (The gap region was defined as the fuel-cladding gap, fuel cracks, and

the interconnected, open porosity in the fuel.) The quantity of fission products  $^{129}\text{I}$  and  $^{137}\text{Cs}$  in the fuel-cladding gap and, separately, dissolved in the fuel and cladding were determined for two seed fuel rods and two standard blanket fuel rods.

Fission products  $^{129}\text{I}$  and  $^{137}\text{Cs}$  deposited in the gap were determined by immersing the fuel and cladding, separately, in 2N HCl for 30 minutes. Ultrasonic vibration was applied to aid in dissolving any iodine and cesium deposits from the cladding surface only. Fuel particles remaining in the cladding and fuel wash solution were removed by filtration. After diluting the solution to a know volume, and aliquot was taken for  $^{137}\text{Cs}$  measurement by gamma-ray spectroscopy. The remaining solution was analyzed for  $^{129}\text{I}$  by adding carrier iodine and separating the iodine by solvent extraction. The separated iodine was precipitated as palladium iodide ( $\text{PdI}_2$ ) and counted for  $^{129}\text{I}$  with a calibrated lithium-drifted germanium detector.

The  $^{129}\text{I}$  and  $^{137}\text{Cs}$  inventory in samples of  $\text{ThO}_2$  and  $\text{ThO}_2\text{-UO}_2$  fuel was determined after comminution and dissolution of the powdered fuel samples in HBr-HF solution containing carrier iodine. Cesium-137 and  $^{129}\text{I}$  were determined from the dissolver solution in the same manner as for the gap wash solutions.

To determine the fission product  $^{129}\text{I}$  and  $^{137}\text{Cs}$  inventory in the cladding, the cladding was first washed, dried, weighed, and measured to calculate the inside surface area. A one-gram sample of cladding was dissolved in a HCl-HF mixture containing carrier iodine. The dissolver solution was diluted to a know volume and an aliquot was taken for  $^{137}\text{Cs}$  analysis. The cesium and iodine inventories were then obtained in the same manner as for the gap wash solutions.

#### 8.6.3 - Tensile Testing of the Cladding

Tensile tests were performed on RXA cladding from the seed region and on SRA cladding from the standard blanket and reflector regions. Seven- to eight-inch long sections were cut from the fuel rod to be tested and the fuel was removed, leaving the cylindrical cladding intact. Cladding sample locations along the length of the rod were selected between support grid levels to

ensure that the gage length surface was free from wear marks. Four fuel rods (two seed, one standard blanket, and one reflector) were tested at room temperature. Three fuel rods (two seed and one reflector) were tested at 500F to determine elevated temperature mechanical properties. Heat lamps were used to achieve the elevated test temperature. Elevated temperature tests at end of life were conducted at 500F rather than the 700F temperature used for beginning of life because annealing of radiation damage in Zircaloy occurs at temperatures above about 500F. Difficulty in separating fuel from blanket cladding precluded testing of additional blanket rods.

Tensile tests were conducted in-cell on an Instron machine at a strain rate of 0.058 inch/inch of gage per minute for room temperature and elevated temperature testing, respectively. Mechanical properties measured and reported were 0.2 percent offset yield strength, the ratio of ultimate strength to yield strength, percent elongation in a 2-inch gage length upon rupture, and percent reduction in area.

#### 8.6.4 - Summary and Conclusions

Performance of the LWBR Zircaloy-4 clad thorium oxide/uranium-233 oxide fuel rods during core life to 29,047 EFPH was excellent. No conclusive or direct evidence of fuel rod failure was observed; the possibility of cladding defects in two seed modules after defueling the core was noted. The level of hydriding in the fuel rod Zircaloy cladding was lower than predicted and did not limit core performance. Specific results and conclusions are summarized below:

1. Fission gas (xenon and krypton) release from LWBR fuel to the plenum region was very small, less than 0.2 percent of total gas generated and within best-estimate predictions. Light water breeder reactor fuel rods, therefore, operated at low fuel temperatures, below 2580F. Microstructural features, such as fuel grain size and porosity, confirmed this observation.
2. Fuel pellets remained cylindrical and essentially intact within the rods. Axial and circumferential cracks were observed in the fuel pellets, but the basic shape was maintained. The extent of cracking

was limited. Fuel chips were not observed, and pellet fragments were not dislocated axially as observed in some irradiation test rods. Hence, PCI due to dislodged fuel sections or chips was minimized.

3. Axial expansion of the pellet ends into the end dishes did not occur to any measurable extent. End dishes were observed in neutron radiographs of all rod types. Longitudinal cross sections through the end-dish regions confirmed that the dish depth had not changed measurably from as-built dimensions. Pellet-cladding interaction and cladding ridging (diametral expansion) at pellet ends, therefore, were minimized by this low axial expansion.
4. Fuel porosity remained small in size in the binary fuel pellets at burnups below 20,000 MWD/MT. Fission gas bubbles (porosity) became more evident in the grain boundaries at higher depletions.
5. No central coring of the fuel was encountered.
6. Large grained fuel was not observed. The ASTM grain size varied from 2.6 to 6.0. Grain size was larger at the edge of the blanket fuel pellets by an average of 1.15 ASTM grain size but was larger in the center of the seed fuel pellets by an average of 0.5 ASTM grain size. Lack of significant grain growth confirmed that the LWBR fuel operated at low temperatures (below 2580F) and was stable.
7. Cladding in the seed region remained freestanding (separated from contact with the fuel) as designed. The pellets were free to slide inside the cladding. Pellet-cladding interaction was not significant in the seed fuel rods; cladding strains due to PCI, therefore, were low.
8. Cladding in the blanket region was in tight contact with the cladding and was not free to slide. This was expected since the cladding was designed to be nonfreestanding and significant grooving was observed in nondestructive fuel rod diameter measurements in the blanket region. This indicated that high local cladding strains due to axial expansion (ridging) at pellet ends were not realized.

9. Cladding in the one reflector region rod examined, which contained thoria fuel only, was separated from the fuel by a small gap of 1 to 2 mils.
10. The hydrogen content in the Zircaloy-4 cladding increased moderately from the as-fabricated level of 45 ppm maximum to approximately 100 ppm in the seed and blanket fuel rods. Hydrogen pickup in the reflector cladding (fabricated to the same standards as the seed and blanket cladding) was very small with an average measured hydrogen content of 34 ppm, well below the as-fabricated maximum of 45 ppm. Measured values were well below predicted levels for all rods examined.
11. The zirconium hydrides in the cladding were oriented in the preferred circumferential direction parallel to the rod surface, which minimized the potential for surface cracks. No massive hydrides were observed. Lack of hydrogen embrittlement was beneficial to fuel rod performance.
12. A uniformly even and essentially unbroken cladding oxide layer was observed on the waterside surface of all fuel rods examined. The oxide thickness ranged from approximately 0.05 mil for cladding with the thinnest oxide layer to 1.75 mils for cladding with the thickest oxide layer. For fast neutron fluences to approximately  $40 \times 10^{20} \text{ n/cm}^2$ , oxide thickness for the RXA seed cladding and the SRA blanket cladding (over binary fuel) was comparable. Above this fluence level, the SRA cladding experienced greater oxide thickness than RXA cladding. The results for the maximum measured oxide thickness are in reasonable agreement with the CHORT model predictions.
13. No oxide was observed on the cladding I.D. (fuel side) surface.
14. The potential for iodine-induced stress corrosion cracking of the Zircaloy-4 cladding in LWBR fuel rods was not significant. Essentially no iodine was detected in the fuel-cladding gap or on the cladding inner surface. Only iodine dissolved in the fuel was detected.

15. Low levels of the fission product  $^{137}\text{Cs}$  were observed on the cladding I.D., at about 0.1 weight percent.
16. The inner (fuel-side) surface of seed and blanket cladding was covered with a thin film and a coating of fine nodules (about 0.5 micron to 5 microns across). Both the film and nodules consisted primarily of thorium and zirconium. The inner surface of the nonfreestanding blanket cladding had circumferential rings consisting of fuel particles; only isolated patches of fuel particles were observed on the freestanding seed cladding.
17. Mechanical strength of the LWBR Zircaloy-4 cladding at EOL behaved as expected. Both the SRA and RXA cladding increased in strength as a function of neutron fluence. The SRA cladding, having higher yield and ultimate strength than RXA cladding at BOL, remained higher in strength throughout the core life.
18. Inconel X-750 plenum springs and Type 348 stainless steel plenum sleeves remained structurally sound during core life. Some relaxation of spring free lengths from BOL was experienced, but positive spring force was maintained throughout core operation based on comparison of spring free lengths with plenum lengths under load. No cracks or other degraded conditions were observed.
19. The fuel rod cladding-to-end stem weld remained structurally sound with no evidence of cracking or hydriding.
20. The solid Zircaloy-4 end stem components which were in contact with the nickel-bearing Alloy 600 baseplates in the seed and reflector regions did not show evidence of embrittlement due to high hydrogen content. The hydrogen content was very low, 25 to 50 ppm.
21. Performance of the Zircaloy-4 fuel rod fasteners which attached the fuel rods to either top or bottom baseplates was good. The hydride content of 150 to 200 ppm in the seed region and 350 to 400 ppm in the reflector region was higher than in the cladding, as expected.

Local regions of higher hydride (to 1000 ppm) were observed in several seed fasteners at locations of apparently greater contact pressure with the Inconel-600 baseplate. The low (20 ppm) hydride content in the blanket region indicated that the presence of the chromium-plated washers performed as designed. Hydride content in the blanket region rod fasteners did not increase above as-fabricated levels. All fasteners performed as designed.

#### 8.6.5 - Additional Information

Detailed information on the EOL destructive examination of LWBR fuel rods is contained in WAPD-TM-1606, listed in Section 1-D of Appendix A.

### 8.7 - EXAMINATION OF LWBR GRIDS AND OTHER MODULE STRUCTURAL COMPONENTS

#### 8.7.1 - Introduction

The purpose of this section is to document the EOL examinations performed on structural components removed from the LWBR core. The components examined included fuel rod grids, bolts, screws, tubes, shafts, posts, shells, fuel rod nuts and washers, shear keys, and struts. Visual inspections were performed to assess structural integrity and surface condition of the above components. Seal block bolts, baseplate bolts, and guide tube extension bolts had dye penetrant inspections performed. Metallography was performed to assess potential cracking, corrosion buildup, and microstructural condition of many of the above components, which constituted a range of materials: AM-350 stainless steel, Zircaloy-4, Alloy X-750, Alloy 600, Type 348 stainless steel, and 30Cr-10Si-Ni braze.

#### 8.7.2 - Components and Materials Selected for EOL Examination and Examination Results

##### 8.7.2.1 - Grids

End-of-life examinations were specified for two sections of LWBR seed grid that were representative of the peak fluence regions of the core. Two seed grid sections approximately 2 inches wide, 4 inches long, and 1.75 inches high were removed by the Module Disassembly Apparatus (MDA) (an underwater milling machine) for detailed examination.

The following examinations were performed to characterize performance of AM-350 stainless steel and 30Cr-10Ni-Fe braze as core materials:

1. Visual inspections for qualitative assessment of corrosion.
2. Metallography for quantitative assessment of corrosion and characterization of microstructure.
3. Metallography for qualitative assessment of weld joint and brazed joint integrity.
4. Measurement of spring force to assess stress relaxation.

The following examinations were performed to characterize grid mechanical performance:

1. Visual inspections for qualitative assessment of crud deposition.
2. Measurement of cell pitch (distance centerline-to-centerline) to assess grid stability.
3. Measurement of spring intrusions into adjacent grid cells to assess dimensional stability of the grid springs (potential interference with rods in adjacent cells).
4. Measurement of grid cell panel proximity to a nominal diameter (BOL) fuel rod to assess changes in grid dimensions.
5. Measurement of free spring position (undeflected position) and spring force measurements to assess ability to confine fuel rods.

Visual inspections included examination of integrity and corrosion appearance of grid sheet metal, braze material, spot welds and heat affected zones (HAZ) on boundary strap end plates, springs, and dimples. Integrity is defined as absence of cracks, crevice corrosion, pitting, fretting, or wear.

Stress relaxation measurements involved measuring free spring positions and forces for a range of spring deflections. Stress relaxation of the grid springs was an important characteristic in selecting AM-350 stainless steel as a grid material because the ability to maintain a minimum seed spring force of 0.8 pound on the fuel rods was required to prevent accelerated flow-induced

vibratory wear of fuel rod cladding. Strict limits on BOL grid dimensions were set for: (a) free spring position, (b) proximity, (c) spring intrusion, and (d) cell pitch to ensure adequate grid stability and performance throughout core life. End-of-life measurements of these parameters were specified to determine the effect of core performance on these grid parameters. The precision of BOL measurements and manufacturing tolerances of the various grid dimensions dictated the precision required for EOL measurements.

#### 8.7.2.2 - Results of Examinations of Grids

The AM-350 stainless steel grids were dimensionally stable through EOL. Some variations in grid pitch were observed. Adequate panel proximities and intruded spring clearances were maintained. Grid springs relaxed yet maintained adequate force on fuel rods through EOL to prevent accelerated vibratory cladding wear. Surface oxide of AM-350 appeared at grain boundaries up to 0.2 mil deep in agreement with prediction. Two unusual pockets of oxide were observed on the backside of two grid dimples, however, no cracks were observed. Fuel rod contact surfaces on springs and dimples behaved well. Grid surfaces were covered by a thin uniform layer of crud. Joints brazed with 30Cr-10Si-Ni exhibited minor corrosion and cracking but remained rigid. Spot welds and HAZs did not show any signs of cracking or unusual corrosion.

#### 8.7.2.3 - Bolts, Screws, and Washers

Light water breeder reactor bolts, screws, and washers were chosen for visual examination, fluorescent penetrant testing for cracks, and metallography on selected specimens. Stress corrosion cracking was a specific concern for Inconel X-750 and Inconel-600 bolts. Corrosion and hydriding were the primary concerns for examination of Zircaloy-4 shell screws. Chromium-plated blanket washers, used to separate the Zircaloy-4 blanket rod fuel nuts from contact with Inconel-600 baseplates (nickel-enhancement of hydrogen pickup in Zircaloy), were examined to assess performance. Examination of LWBR fuel rod nuts are discussed in WAPD-TM-1606, listed in Section 1-D of Appendix A.

#### 8.7.2.4 - Results of Examination of Bolts, Screws, and Washers

The following are results of examinations of bolts, screws, and washers:

1. Bolts made of Alloy X-750, Inconel-600, AM-350, and 17-4 PH did not crack or show any unusual corrosion behavior.
2. Zircaloy-4 module shell screws had hydrides up to 150 ppm and oxide thicknesses up to 1 mil. No cracking occurred.
3. A chromium-coated 17-4 PH washer which separated Zircaloy-4 fuel rod nuts from Inconel baseplates showed minor wear of the bearing surface.

#### 8.7.2.5 - Plates and Shells

Partial disassembly of fuel modules at ECF permitted visual access to internal surfaces of structural plates and shells. Inconel-600 baseplates and cover plates from a blanket module were selected for inspection. Zircaloy-4 shells were slit lengthwise and examined after removal from a seed and reflector module. Crud deposition and grid-to-shell contact were items of concern. Reflector shell dimensions were measured to assess module bow.

#### 8.7.2.6 - Results of Examinations of Plates and Shells

Results of examinations of plates and shells include the following:

1. Inconel-600 baseplates and cover plates were clean and crud-free.
2. Internal surfaces of Zircaloy-4 module shells showed some flow patterns and selective crud deposition. Growth of a reflector shell was consistent with module bow measurements.

#### 8.7.2.7 - Tubes

A reflector flux thimble tube, Type 348 stainless steel, failed during the last six months of operation of LWBR. Visual and metallographic examinations were performed to determine the cause of failure. The reflector flux thimble guide tube was also examined. Activation levels were measured from samples cut from the reflector flux thimble tube, a blanket flux thimble tube,

and a BIF supply tube. Estimates were made of the thermal neutron activating fluxes from which fission average fast neutron fluxes were estimated.

#### 8.7.2.8 - Results of Examinations of Tubes

A Type 348 stainless steel reflector flux thimble failed due to a combination of corrosion and erosion.

#### 8.7.2.9 - Shear Keys and Struts

The shear keys and shear key struts were structural assemblies which connected the blanket bottom baseplate to the guide tube (see Figure 5). Visual examination of two 17-4 PH stainless steel shear keys and two Inconel-600 shear key struts was performed to assess the condition of the components following core operation to 29,047 EFPH.

#### 8.7.2.10 - Results of Examination of Shear Keys and Struts

The 17-4 PH shear keys and Inconel-600 shear key struts experienced minor crud buildup and surface corrosion which was inconsequential to performance.

#### 8.7.2.11 - Posts and Shafts

Zircaloy-4 module support posts of all three module types were examined visually. Blanket support post lengths were measured to assess growth. A seed support shaft and balance piston were examined for crud buildup and wear which had potential effects on module scram behavior.

#### 8.7.2.12 - Results of Examinations of Posts and Shafts

The following indicate results from examinations of posts and shafts:

1. Growth of Zircaloy blanket support posts agreed with prediction.
2. A seed support shaft and balance piston did not show any abnormal wear or crud buildup. Satisfactory scram capability was confirmed.

#### 8.7.3 - Additional Information

Additional detailed information on examination of structural components may be found in WAPD-TM-1607, listed in Section 1-G of Appendix A.

(Intentionally Blank)

## SECTION 9 - LONG TERM FUEL STORAGE

### 9.1 - INTRODUCTION

Long term fuel storage was the last major phase of the LWBR Development Program. The objective of this phase was to package and transport all LWBR fuel from the Expended Core Facility (ECF) to the Idaho Chemical Processing Plant (ICPP) for long-term underground dry storage. The process consisted of preparation of a loaded fuel storage liner (to remove the water and seal the contents), placing the dewatered liner into a submerged shipping cask, removal of the cask from the water pit, and shipment. These operations were all performed in the ECF water pits.

### 9.2 - FUEL SHIPMENT OPERATIONS

The fuel shipment process was comprised of the following operations: (1) Peach Bottom shipping cask receipt and water pit installation; (2) fuel storage liner transfer to the liner closure station; (3) fuel storage liner closure; (4) fuel storage liner drying, inert gas backfill, and leak testing; (5) fuel storage liner loading into the Peach Bottom cask; (6) Peach Bottom cask removal from the water pit; and (7) Peach Bottom cask shipment.

Upon receipt of the empty Peach Bottom cask (a cylindrical, lead shielded shipping container with an interior space 26 inches in diameter and 159 inches in length) at the ECF high bay, the cask shipping cover was removed. Radiological surveys of the cask were performed to confirm that no unacceptable surface contamination was present and that radiation levels were acceptably low. After removal of the cask crushblocks and the shipping tie-down hardware, horizontal handling equipment was installed on the cask. The cask was lifted from the transport trailer and was placed horizontally in the downender support structure located adjacent to the ECF water pits. The lift adapter plate was bolted to the top of the cask. The primary vertical handling rigging, consisting of the primary spreader beam, wire ropes, and pear links, was installed. The cask was then upended to the vertical position, lifted from the downender, and lowered into the cask underwater support structure

at the bottom of the water pit used for disposal operations. Removal of the cask top closure lid utilizing the lift adapter plate was the final step in preparation for receipt of a fuel storage liner.

All spent LWBR fuel was stored in open, stainless steel, fuel storage liners located within the fuel storage racks submerged in water pits. To initiate liner closure operations, the loaded storage liner was transferred from the storage racks to the liner closure station head installation port. Concurrently, the storage liner closure head was fitted with metallic O-rings. The liner closure head was lowered into the water and onto the liner body. With the closure head properly installed, all closure head bolts were torqued to seal the closure head to storage liner interface. The liner lift adapter was then installed, and the liner was transferred from the liner closure station head installation port to the liner closure station dewatering port for dewatering operations. These ports were rectangular steel work stations installed under water in the water pits and designed to support specific operations.

Five fluid processes were necessary to meet the requirements for long-term storage of the LWBR fuel. The storage liners required water blowdown, air circulation, vacuum drying, neon backfill, and pressure/leak testing. All fuel liner dewatering processing was performed, monitored, and controlled by the dewatering support system and its associated mechanical tooling. Storage liner blowdown removed the bulk water from within the storage liner. Dry air circulation removed several pounds of remaining residual water, which reduced the burden on the vacuum-drying process. Vacuum drying, which required approximately 22 hours of vacuuming and soaking operations, finally dried the storage liner. Neon gas backfill provided the inert atmosphere desirable for long-term storage, while pressure and leak testing verified the integrity of the storage liner seals.

With the loaded fuel storage liner dried and sealed, the storage liner was transferred under water to the Peach Bottom cask. The liner was inserted into the cask cavity through the top opening and the cask top closure lid was reinstalled. The cask vertical redundant rigging, consisting of the primary

rigging and the redundant rigging A-frame and independent wire rope, was attached. The loaded cask was then lifted out of the water pit. Clean water was used to flush and clean the exterior of the cask and rigging as they exited the water pit. Once the cask internals were drained, the cask was transferred to the downender and rotated to the horizontal position. Prior to loading the cask onto the trailer, radiological surveys were performed to verify that the cask was externally radiologically clean. Horizontal rigging was utilized to transfer the cask to the trailer, followed by the attachment of the shipping tie-down hardware, crushblocks, and the cask shipping cover.

A total of 48 fuel shipments were made; these shipments were comprised of the following: 39 liners with LWBR spent fuel modules, seven liners with individual fuel rods, one liner with a spare unirradiated LWBR seed module, and one liner with intact and remnants of irradiation test rods. The seven fuel rod liners accommodated the rods removed from the modules for examination purposes, the unirradiated calibration rods used to verify the calibration of proof-of-breeding equipment, and the rods from the modules disassembled for fuel rod grid removal and for in-bundle fuel rod gap examinations.

### 9.3 - IDAHO CHEMICAL PROCESSING PLANT FACILITY AND FUEL STORAGE

The Idaho Chemical Processing Plant (ICPP) constructed the LWBR Fuel Storage Facility to store the LWBR fuel in dry underground storage vaults. The ICPP is located within the Idaho National Engineering Laboratory (INEL), 5 miles from ECF. The tractor trailer hauling the loaded Peach Bottom cask traversed this distance at a maximum allowable speed of 15 miles per hour. Fifty storage vaults were provided for the irradiated fuel and one vault for the unirradiated spare seed module. Each vault was designed to hold one storage liner. The main advantages for placing LWBR fuel in underground storage vaults were: (1) built-in shielding from radioactivity and adequate shielding for criticality safety; (2) dry fuel storage; (3) fuel isolation from the environment; (4) ease of monitoring; (5) fuel retrieval capabilities; (6) low manpower requirements; (7) low capital cost; and (8) previous satisfactory experience with dry vault storage of other nuclear fuel.

The dry storage vaults were fabricated from carbon steel pipe. The storage vaults for the irradiated fuel were arrayed in two rows, with 25 vaults in each row. The two rows were constructed on 30-foot centers, with each vault within each row spaced on 10-foot centers. The storage vault for the unirradiated fuel was isolated from the irradiated fuel vaults. A reinforced concrete slab was constructed around each vault to provide a working surface and laydown area. Each vault consisted of a smaller-diameter lower section which held the fuel storage liner and an upper section which contained a concrete shielding plug. The lower section was approximately 30 inches in diameter and 15 feet, 10 inches long, and the upper section was approximately 36 inches in diameter and 4 feet long. A crushblock was placed in the bottom of the storage vault to absorb energy and prevent damage to the fuel storage liner in the unlikely event of an accidental drop. Each storage vault is periodically inspected and the storage vault contents are monitored for the presence of liquid water and fission gas to assure vault integrity.

Upon receipt of the LWBR fuel at ICPP, the tractor trailer carrying the loaded Peach Bottom cask was positioned adjacent to the designated storage vault. Two pieces of equipment were utilized by ICPP to prepare the cask for storage liner removal; these were the cask support pedestal and the cask centering and shielding device. The cask support pedestal was positioned on the storage vault concrete slab laydown area. This pedestal allowed the cask bottom closure lid bolts to be removed while the cask was seated vertically on its bottom closure lid on the pedestal. The cask centering and shielding device was placed on the top of the open storage vault. This device centered the cask over the vault opening and shielded ICPP personnel during storage liner insertion into the vault.

The cask was lifted from the trailer by a mobile crane rigged to the cask upper trunnions through a lifting yoke. The cask was placed vertically on the cask support pedestal and transferred to the vault by the mobile crane and lifting yoke. The cask was inserted into the centering and shielding device and the lift rigging was removed.

With the cask properly aligned over the vault opening, the liner was lowered to the bottom of the vault. During storage liner insertion into the storage vault, shielding was provided by the Peach Bottom cask and the centering device. When the storage liner was seated within the vault, the empty cask was returned to the support pedestal for bottom lid installation, then reloaded onto the shipping trailer for return to ECF. The vault was sealed by installing the concrete shield plug, lid gasket, and lid.

#### 9.3.1 - Additional Information

WAPD-TM-1601 (listed in Section 1-E of Appendix A) discusses the preparation of the expended LWBR fuel for long term storage.

(Intentionally Blank)

## SECTION 10 - SUMMARY OF ADVANCED WATER BREEDER APPLICATIONS WORK

### 10.1 - INTRODUCTION

The Advanced Water Breeder Applications (AWBA) Program, established in 1976, was a part of the Department of Energy's Water Cooled Breeder Program.

To build on the successful design and operation of the Shippingport breeder core (LWBR) and to provide the technology to implement this concept for improved fuel utilization, Bettis Atomic Power Laboratory developed three self-sustaining breeder concepts, and Knolls Atomic Power Laboratory (KAPL) developed one concept for commercial-sized plants of 900 to 1000 Mw(e) net. The first of the breeder concepts, called the "scale-up" concept, used the same fuel assembly and control system designs as the Shippingport core. This concept was developed to identify and resolve any potential technical concerns related to extrapolating the small Shippingport LWBR to a larger commercial-size core. The second Bettis concept employed movable thoria finger rods (analogous to the poison rods of commercial cores) for reactivity control, rather than the large movable fuel assemblies of the scale-up concept. This concept, which employed fuel management with annual refueling shutdowns, provided reduced power peaking factors. The third Bettis concept, a batch loaded concept, incorporated significant advances: it utilized smaller fuel assembly sizes compatible with present commercial reprocessing plant disassembly (shearing) equipment, was capable of being assembled remotely using high-radiation level recycle fuel, and provided additional margin for breeding in the equilibrium cycle. The fourth breeder concept, developed by KAPL, incorporated a stationary seed-blanket core arrangement plus movable thoria shim rods in combination with a typical commercial PWR reactivity control system. These concepts are described briefly in the following sections.

To provide the initial fuel load for a commercial breeder, prebreeders would be necessary; these reactors would use enriched ordinary uranium ( $^{238}\text{U}$  and  $^{235}\text{U}$ ) and  $\text{ThO}_2$  to produce electrical energy, while also producing  $^{233}\text{U}$  from the thorium. After sufficient  $^{233}\text{U}$  had been accumulated to fuel a self-sustaining breeder core, no further prebreeder operation would be necessary to support the breeder, and no further mining of uranium ore would be required.

The prebreeder could be in a separate reactor plant, or the initial prebreeder and subsequent breeder reactors could be integrated into a single plant concept. The AWBA work included the development of conceptual designs for such commercial-sized prebreeder cores.

## 10.2 - ADVANCED BREEDER CONCEPTS

### 10.2.1 - LWBR Scale-Up Concept

The first large core self-sustaining breeder concept investigated by the AWBA Project was designated the LWBR "scale-up." This concept was based and relied on proven technology. The scale-up concept consisted of 141 interior fuel assemblies, identical in mechanical design to the three central modules of the Shippingport LWBR core. These fuel assemblies were surrounded by a region containing fuel rods with relatively high fissile loadings that served to flatten the radial power distribution. The 7-foot high active core was surrounded by a reflector region containing thoria-fueled rods that reduced the loss of neutrons due to leakage and enhanced the breeding capability of the core. The core was sized to fit within a reactor vessel of 279-inch inside diameter. The technical feasibility of the vessel was based on a design study made by a subcontractor having expertise in design and manufacture of reactor vessels. Because movable fuel was used for reactivity control, soluble boron was not required for normal operation or normal cold shutdown and would be needed only for cold shutdown with the most reactive seed assembly stuck at the hot operating height for a shutdown period greater than 100 hours. All fuel rods were bolted to base plates (approximately half to the bottom base-plate and half to the top) to eliminate any potential for axial displacement of fuel rods.

The LWBR scale-up concept was a batch-loaded concept which produced a net output of 900 Mw(e) and achieved a nominal lifetime of about 3.5 years at an assumed 75-percent load factor. The minimum lifetime, assuming a 1-percent underreactive core, would be slightly greater than 3 years. In addition, as was demonstrated in the Shippingport LWBR, the lifetime of the scale-up could be extended by operating at reduced power levels following the end of full power reactivity lifetime. For example, the scale-up concept could operate

for an additional 9 months at 70-percent power while generating 630 Mw(e). Thus, an operating utility would have wide flexibility in scheduling the time for shutting down for refueling.

The scale-up concept bred in all cycles from the initial to the equilibrium fuel cycle. The Fissile Inventory Ratio (FIR) of the concept, defined as the total fissile inventory at the end of the cycle (assuming all  $^{233}\text{Pa}$  has decayed to  $^{233}\text{U}$ ) divided by that at the beginning of the cycle was 1.017 for the initial cycle and 1.005 for the equilibrium cycle. The breeding performance degraded as fuel was recycled until the equilibrium cycle was attained because the breeder was assumed to be initially fueled from a segregated fuel prebreeder, which provided a high  $^{233}\text{U}$  content mixture. Recycle of the fuel decreased the relative  $^{233}\text{U}$  content and increased the content of  $^{235}\text{U}$ , which produced fewer neutrons per absorption and, hence, reduced the number of neutrons available for conversion of  $^{232}\text{Th}$  to  $^{233}\text{U}$ . Since the minimum FIR was 1.005, the total losses during the recycle of the irradiated breeder fuel had to be kept to less than 0.5 percent for the scale-up concept to be a net breeder in all fuel cycles from the initial to the equilibrium.

Analyses provided a high degree of confidence that breeding would occur in the scale-up concept. The scale-up core thermal performance was satisfactory and the core complied with the structural criteria of the ASME Code, Section III, and with the safety requirements of the Code of Federal Regulations. Since the scale-up concept required little advancement in technology beyond that used to build and operate the Shippingport LWBR core, very little further research and development would be necessary on the reactor design if it were to be used as a commercial energy source.

#### 10.2.2 - Movable Thoria Finger Rod Controlled Breeder Concept

The primary reason for developing a movable thoria finger rod controlled, self-sustaining breeder conceptual design was to reduce fuel rod power peaking factors from those that occur in designs controlled by large movable fuel assemblies. The reduction in peaking factors resulted from not having large portions of the core movable relative to one another, as they are in a movable fuel assembly controlled design. Reduced peaking factors allowed a higher

average power without exceeding local limits. This gain could be utilized as increased reactor power or as a smaller core and reactor vessel for the same power.

The movable thoria finger rod controlled breeder concept had a power rating of 1000 Mw(e). The core was designed to operate as a fuel managed core where one-third of the core is replaced annually; this assumes a 75-percent load factor. The active core consisted of 211 hexagonal fuel assemblies and 42 peripheral half-hexagonal blanket assemblies. Axial and radial thoria reflector blankets surround the active core region and captured neutrons which would otherwise be lost through leakage. These reflector regions enhanced the breeding performance of the concept. All modules employed Zircaloy fuel rod support grids to minimize neutron losses. The entire core fitted into a reactor vessel having a 256-inch inside diameter.

A unique aspect of this concept was that during operation above 50 percent of full power, reactivity control was accomplished by the motion of assemblies consisting of 18 control rods containing thoria ( $\text{ThO}_2$ ) in about 65 percent of the active fuel assemblies in the core. These control rods were large in diameter (1.2 inches) and contained duplex pellets having an outer thoria annulus and an inner zirconia region. The size and number of the control rods were selected to provide sufficient reactivity worth to allow swing-load operation of the core, to provide the desired cycle lifetime of 1 year at an assumed load factor of 75 percent, and to provide structural integrity of the finger rod and its guide tube under the limiting condition of one stuck finger rod.

The remainder of the active core fuel assemblies each contained 36 movable poison rods which were similar in composition, size, and function to control rods used in commercial PWR cores. These poison rods were fully withdrawn from the core under normal operating conditions and provided sufficient reactivity worth to assure hot core shutdown when all rods were inserted. Soluble boron was not required for normal operation and would be used only for sustained steady state operation at less than 50-percent power and for cold core shutdown.

The finger rod controlled breeder concept was calculated to have an FIR of 1.03 in the initial cycle and greater than 1.01 in the equilibrium cycle. Analyses indicated that the core would perform satisfactorily under normal and accident conditions and that the concept would meet the structural criteria of Section III of the ASME Code and the safety requirements of the Code of Federal Regulations.

#### 10.2.3 - Advanced Movable Fuel Breeder Concept

Having shown by the scale-up concept that extrapolation of the Shippingport LWBR to a commercial size reactor was feasible, an advanced concept incorporating logical extensions of LWBR technology was designed to achieve better performance.

Like the scale-up concept, the self-sustaining advanced movable fuel breeder (AMFB) used movable fuel assemblies for reactivity control. The AMFB, however, had a higher power rating than the scale-up, had a significantly longer lifetime than the scale-up, and provided a greater margin for breeding in the equilibrium cycle.

The AMFB concept was a batch-loaded core consisting of 121 seed assemblies, 240 blanket assemblies, and 42 peripheral half-blanket assemblies. Seed fuel rods were smaller in diameter and had higher fissile loadings than blanket rods. The outer ring of blanket and half-blanket assemblies contained fuel rods of higher fissile loadings than the interior blanket assemblies to flatten the core radial power distribution. Surrounding the 10-foot high active core was a thoria-fueled reflector region that reduced neutron leakage and improved breeding performance. All modules employed Zircaloy fuel rod support grids to minimize neutron losses. The core fitted within a 266-inch inside diameter reactor vessel.

The AMFB produced a net output of 1000 Mw(e) and had a nominal full power lifetime for the initial cycle of about 5 years at a 75-percent load factor. Like the scale-up concept, its lifetime could be extended by further operation at less than full power. It had an initial cycle FIR of 1.03 and an equilibrium cycle FIR slightly greater than 1.01. Use of soluble boron was not

required for either normal operation or cold shutdown with the most reactive seed assembly stuck at the hot operating position.

A major difference between the AMFB concept and the scale-up concept was that the AMFB seed assemblies were not encased in Zircaloy shells. Eliminating this Zircaloy component not only reduced the amount of Zircaloy in the active core, but also permitted an increase in the seed fuel rod diameter and an enlargement of the seed fuel rod array. These changes increased the fuel-to-coolant ratio which, in turn, resulted in an improved FIR and a longer core lifetime. Calculations evaluating the structural and vibrational characteristics of the shell-less seed assembly have shown it to be acceptable. A second major difference was the reduction in size of the blanket assemblies. The AMFB seed and blanket assemblies were of the same hexagonal shape and size, approximately the same size as commercial reactor fuel assemblies. With its taller core, the AMFB produced more power than the scale-up concept (1000 versus 900 Mw(e)).

As in the scale-up concept, all fuel rods in the AMFB were anchored to prevent any sudden axial displacement, but the rods were all attached to the fuel assembly bottom baseplate by a simple connector. This method of attachment, by facilitating the remote fabrication of the fuel assembly, reduced radiation exposure from the highly radioactive recycled breeder fuel, minimized initial fuel rod bow, and eliminated the need to have free ends of fuel rods facing upstream into the coolant flow. All fuel rod support grids, either stamped piece or machined, were made of Zircaloy; this gave a significant improvement in FIR compared with Shippingport LWBR and the scale-up concept, both of which used AM-350 stainless steel grids. No orificing of fuel assemblies was required since the hydraulic resistances of the seed, blanket, and reflector assemblies had been balanced by selection of fuel rod sizes, fuel rod spacing, and number of grids. Use of a fuel assembly support structure, similar to that used in commercial cores, to support blanket assemblies (rather than suspension from the vessel head as in the Shippingport LWBR and the scale-up concept) simplified refueling.

It was judged that the AMFB concept would meet the structural criteria of Section III of the ASME code. Fuel rod, hydraulic, and heat transfer calculations indicated that margin existed to meet the safety requirement of the Code of Federal Regulations.

#### 10.2.4 - Seed-Blanket Prebreeder/Breeder System Concept

The key features of the KAPL breeder concept included: (1) using a reactivity control system which minimized the amount of movable fuel required, and (2) combining the prebreeder and breeder functions into a single reactor plant. Like the Shippingport LWBR, the scale-up concept, and the AMFB, the seed-blanket breeder contained seed regions and blanket regions to help control reactivity; however, unlike those concepts, the seed and blanket regions were completely stationary, being built into the fuel assembly lattice.

The seed-blanket breeder core consisted of 163 fuel assemblies of two types, each type containing regions of seed fuel rods and blanket fuel rods. Seed fuel rods were smaller in diameter and had higher fissile loadings than the blanket fuel rods which contained only thoria fuel pellets. Fuel rods were positioned by machined Zircaloy spacer-grids. One type of fuel assembly contained a movable poison control rod group analogous to poison control rods in commercial PWRs: the other type of fuel assembly contained a movable thoria shim rod group. The thoria shim rods had a small diameter, being more like the poison control rod fingers in size than like the large-diameter thoria fingers described above for the thoria finger controlled breeder concept. The 12-foot high active core was surrounded by a thoria fueled reflector-blanket region to reduce neutron leakage and improve breeding performance. The core fitted within a 206-inch diameter reactor vessel.

The seed-blanket breeder produced a net output of 964 Mw(e) with a nominal cycle length of 2.5 years for its batch-loaded core, assuming a 75-percent load factor. The equilibrium cycle FIR was 1.01.

The reactivity control system of the seed-blanket breeder involved poison control rod groups in the core and soluble boron in the coolant, which were used just as in a commercial PWR. However, the seed-blanket core arrangement minimized core lifetime reactivity variation so that for most of a core cycle

at near full-power equilibrium operating conditions, the soluble boron in the coolant could be reduced to lower concentrations, and the thoria shim rods could be used to trim core reactivity, thereby improving breeding performance. The seed-blanket breeder concept was intended for base-load electric generation capacity. Although swing-load operation could be performed, the additional use of soluble boron and poison rods would degrade breeding.

The seed-blanket breeder core was predicted to have nuclear and thermal performance comparable to a large commercial PWR, and would meet all safety requirements.

#### 10.2.5 - Additional Information

Appendix B lists all reports published as part of the AWBA program.

## APPENDIX A - PUBLISHED LWBR TECHNICAL MEMORANDA

This Appendix is divided into the following sections:

1. DEVELOPMENT AND DESIGN

- A. Core Design and Testing
- B. Neutronics and Mathematics Development
- C. Thermal and Hydraulics Development
- D. Fuel Elements, Fuel Pellets, and Cladding Development
- E. Mechanical and Structural Development
- F. Materials
- G. Grids Development
- H. Proof of Breeding Development

2. MANUFACTURING

- A. Fuel Pellets and Cladding
- B. Fuel Rods
- C. Grids
- D. Fuel Assemblies

3. RADIOLOGICAL CONTROLS

4. INSTALLATION, DEFUELING, AND SHIPMENT OF EXPENDED FUEL

5. SUMMARY

Report No.	Title
<b>1. <u>DEVELOPMENT AND DESIGN</u></b>	
<b>A. <u>Core Design and Testing</u></b>	
WAPD-TM-1143	"Light Water Breeder Reactor Movable Fuel Hydraulic Balancing System," July 1979.
WAPD-TM-1208	"Design of the Shippingport Light Water Breeder Reactor," January 1979.
WAPD-TM-1326	"Summary of the Nuclear Design and Performance of the Light Water Breeder Reactor (LWBR)," June 1979.
WAPD-TM-1331	"Summary of the Fuel Rod Support System (GRIDS) Design for LWBR," February 1979.
WAPD-TM-1336	"Results of Initial Nuclear Tests on LWBR," June 1979.
WAPD-TM-1385	"Summary of the Thermal Evaluation of LWBR," March 1980.
WAPD-TM-1386	"Summary of the Hydraulic Evaluation of LWBR," April 1981.
WAPD-TM-1388	"Summary of the Control Drive Mechanism Design and Performance for LWBR," January 1983.
WAPD-TM-1409	"Design Features of the Light Water Breeder Reactor (LWBR) which Improve Fuel Utilization in Light Water Reactors," August 1981.
WAPD-TM-1421	"Nuclear Analysis and Performance of the Light Water Breeder Reactor (LWBR) Core Power Operation at Shippingport," April 1984.
WAPD-TM-1437	"The Determination of Statistically Based Design Limits Associated with Engineering Models," February 1980.
WAPD-TM-1455	"Reactor Physics Experimental Program for the Light Water Breeder Reactor (LWBR) at Shippingport," December 1981.
WAPD-TM-1455 Addendum	"Reactor Physics Test Program for the Light Water Breeder Reactor (LWBR) at Shippingport," December 1983.

Report No.	Title
<b>1. DEVELOPMENT AND DESIGN (Cont)</b>	
<b>A. Core Design and Testing (Cont)</b>	
WAPD-TM-1542	"Shippingport Operations with the Light Water Breeder Reactor Core," March 1986.
WAPD-TM-1546	"Light Water Breeder Reactor Flow Coefficient of Reactivity," June 1987.
<b>B. Neutronics and Mathematics Development</b>	
WAPD-TM-518	"SUMOR, A FORTRAN-IV Program for the Philco 2000 for Neutron Resonance Cross Sections Including Level-Interference and Exact Doppler Broadening," November 1967.
WAPD-TM-521	"X-Ray Line Broadening: Its Solution and Application through the use of a Digital Computer," November 1965.
WAPD-TM-601	"Measured Natural Neutron Source in $U_{233}O_2-ZrO_2-ThO_2$ ," April 1967.
WAPD-TM-606	"Xenon Spatial Stability in Large Seed-Blanket Reactors," April 1967.
WAPD-TM-609	"A Simple Method to Improve the Efficiency of $\Sigma_a/\Sigma_T$ Estimator in Certain Monte Carlo Programs," October 1966.
WAPD-TM-610	"A Variational Principle for the Neutron Diffusion Equation Using Discontinuous Trial Functions," October 1966.
WAPD-TM-611	"The Graphic Display of Numerical Data," April 1966.
WAPD-TM-612	"Protactinium-233 Resonance Integral Measurements," September 1967.
WAPD-TM-613	"Integral Measurement of the Epithermal Neutron Capture-to-Fission Cross Section Ratios of U-233 and U-235," June 1967.
WAPD-TM-614	"Small U-233 Fueled Seed and Blanket Critical Experiments," November 1967.

Report No.	Title
1. <u>DEVELOPMENT AND DESIGN (Cont)</u>	
B. <u>Neutronics and Mathematics Development (Cont)</u>	
WAPD-TM-615	"Relative Reaction Rates in Seed-Blanket Slab Assemblies with Hydrogen-to-Thorium Ratio of 0.51, 1.55, and 5.1," December 1966.
WAPD-TM-617	"A Method of Including Epithermal Neutron Scattering by Bound Protons in Combined Slowing-Down/Thermal Calculations by Monte Carlo," October 1966.
WAPD-TM-621	"Annular Seed-Blanket Reactor Critical Experiments," February 1967.
WAPD-TM-622	"Measurement of the Effective Resonance Integral of 30 Mil Thorium Wire Relative to the Integral of an Infinite Dilution," March 1967.
WAPD-TM-625	"Measurement of Change in $\alpha$ and Fission Rate with Temperature for U-235," August 1967.
WAPD-TM-627	"Measurement of the Effective Resonance Integral and Doppler Coefficient of Thorium Oxide Rods," December 1966.
WAPD-TM-632	"Critical Dimensions of $U_{235}$ Aqueous Systems Containing $U_{238}$ or $Th_{232}$ ," September 1966.
WAPD-TM-638	"Neutron Leakage Effects on the Fast Advantage Factor in a Seed-Blanket Assembly," April 1967.
WAPD-TM-667	"Fission Spectrum Averaged Cross Section Measurement for $Be^9$ , (n, 2n) Reaction," January 1968.
WAPD-TM-670	"Effective Cadmium Cutoff Energies for Finite Cylindrical Filter with Finite Size Detectors," November 1967.
WAPD-TM-672	"Calculational Method for Thermal Disadvantage Factor," September 1967.
WAPD-TM-673	"Variational Calculation of Complex Natural Modes of Xenon Oscillation," September 1967.

Report No.	Title
<b>1. <u>DEVELOPMENT AND DESIGN (Cont)</u></b>	
<b>B. <u>Neutronics and Mathematics Development (Cont)</u></b>	
WAPD-TM-675	"A Simple Method to Incorporate Heterogeneous and Doppler Broadening Effects in the MUFT-5 Resonance Treatment," July 1967.
WAPD-TM-690	"Numerical Comparison of Neutron Transport Approximation for Application at Energies above 0.8 Mev," April 1968.
WAPD-TM-691	"An Evaluation of the Neutron Reaction Cross Sections and Fission Spectrum of U <sub>233</sub> for ENDF/B," December 1969.
WAPD-TM-695	"Natural Modes of the Xenon Problem with Temperature and Control Feedback," May 1967.
WAPD-TM-733	"Interface Conditions for Few Group Equations with Flux Adjoint Weighted Constants," January 1968.
WAPD-TM-736	"Combined Space-Time Synthesis with Axially Discontinuous Trial Functions," October 1967.
WAPD-TM-760	"Integral Measurements of Neutron Capture and Fission in U-233," August 1968.
WAPD-TM-761	"DAFT1 - A FORTRAN Program for Least Squares Fitting of 0.0253 eV Neutron Data for Fissile Nuclides," February 1968.
WAPD-TM-768	"PUN-1 - A FORTRAN IV Program for the Evaluation of Unresolved Resonance Integrals and Related Multigroup Cross Sections," March 1969.
WAPD-TM-771	"Extremum Variational Principles for the Monoenergetic Transport Equation with Arbitrary Adjoint Source," February 1969.
WAPD-TM-772	"An Evaluation of ETA for U-233 at 0.025 Ev Using the RECAP-4c Monte Carlo Program," September 1968.
WAPD-TM-773	"Gaussian Quadrature for Certain Integrals with Weight Function EXP (-X <sup>2</sup> )," January 1970.

Report No.	Title
1. <u>DEVELOPMENT AND DESIGN (Cont)</u>	
B. <u>Neutronics and Mathematics Development (Cont)</u>	
WAPD-TM-804	"Measurements of Neutron Fluctuations, Absolute Detector Efficiency, and Natural Neutron Source Strength in a Lattice of Slightly Enriched UO <sub>2</sub> Rods in Light Water," June 1968.
WAPD-TM-811	"REDUX: A FORTRAN IV Program for Calculation of Statistical Parameters from Count Samples Measured in Reactor Fluctuation Experiments," September 1969.
WAPD-TM-814	"Neutron Capture in Protactinium-233," December 1969.
WAPD-TM-830	"Transmission Measurement of the Cf-252 Fission Neutron Spectrum," March 1969.
WAPD-TM-837	"Integral Measurements of the Protactinium-233 Neutron Capture Cross-Section," June 1970.
WAPD-TM-877	"JITER - A FORTRAN IV Program for the Computation, from One Dimensional Modal Kinetics Models, of Statistical Parameters Measured in Reactor Fluctuation Experiments," June 1969.
WAPD-TM-878	"Monte Carlo Eigenfunction Iteration Strategies that are and are not Fair Games," September 1969.
WAPD-TM-893	"Approximate J( $\theta$ , $\beta$ ) Function," August 1969.
WAPD-TM-915	"A Measurement of Neutron Spatial Distribution in a Water Moderated Thorium Oxide Rod Lattice," February 1970.
WAPD-TM-931	"A Study of Physics Parameters in Several Water-Moderated Lattices of Slightly Enriched and Natural Uranium," March 1970.
WAPD-TM-932	"A Comparison of Thermal Neutron Activation Measurements and Monte Carlo Calculations in Light Water Moderated Uranium Cells," March 1970.
WAPD-TM-935	"GRAMP - A Program to Generate Reich-Moore Parameters for Multilevel Unresolved Resonance," May 1970.

Report No.	Title
1. <u>DEVELOPMENT AND DESIGN (Cont)</u>	
B. <u>Neutronics and Mathematics Development (Cont)</u>	
WAPD-TM-938	"On the Use of Effective Delayed Neutron Fractions for Few-Group Space-Time Analysis," April 1970.
WAPD-TM-941	"A Versatile Eigenvalue Method for Calculating $B_i$ With BE-21," April 1970.
WAPD-TM-959	"On the Use of Space-Synthesis With Energy Group Collapsing," April 1970.
WAPD-TM-960	"Notes on Nuclear Reactor Kinetics," July 1970.
WAPD-TM-968	"Space Time Method for Movable Fuel Problems," December 1970.
WAPD-TM-971	"An Evaluation of the Radiative Neutron Capture Cross Sections of Thorium-232 for the Range 0.0 ev to 15 Mev," December 1970.
WAPD-TM-978	"A New Static Flux Synthesis Model for Movable Material Reactor Problems," November 1970.
WAPD-TM-991	"Spatial Distribution of the Indium Activation in Water Using a Californium-252 Source," March 1971.
WAPD-TM-997	"Analysis of the Fission Neutron Spectrum of U-233 and Criticality Computations for Homogeneous U-233 - $H_2O$ Spheres and Cylinders," June 1972.
WAPD-TM-1052	"Revision of the Thermal Parameters of $U^{233}$ ," September 1972.
WAPD-TM-1062	"An Energy Dependent Spatial Mesh Approximation for Neutron Group Diffusion Problems," June 1973.
WAPD-TM-1072	"The Cf-252 Fission Neutron Spectrum From 0.5 to 13 MeV," December 1973.
WAPD-TM-1073	"Total Cross Section Measurements with a CF-252 Time of Flight Spectrometer," April 1973.
WAPD-TM-1076	"On the Use of Residuals for the Estimation of Error in Approximate Synthesis Solution," June 1973.

Report No.	Title
1. <u>DEVELOPMENT AND DESIGN (Cont)</u>	
B. <u>Neutronics and Mathematics Development (Cont)</u>	
WAPD-TM-1089	"Measurement and Analysis of Parameters in Tight Th <sub>232</sub> - U <sub>235</sub> and Th <sub>232</sub> - U <sub>233</sub> Lattices Moderated with D <sub>2</sub> O," January 1974.
WAPD-TM-1090	"Study of the ThO <sub>2</sub> Doppler Effect in a Tight U <sub>235</sub> O <sub>2</sub> - ThO <sub>2</sub> Lattice Moderated with D <sub>2</sub> O," January 1974.
WAPD-TM-1101	"U-233 Oxide-Thorium Oxide Detail Cell Critical Experiments," July 1974.
WAPD-TM-1109	"Calculation of the Interaction of the 23.45 ev and 21.78 ev Resonances of <sup>232</sup> Th in a ThO <sub>2</sub> Rod," January 1974.
WAPD-TM-1117	"BMU Series of U-233 Fueled Critical Experiments," January 1975.
WAPD-TM-1129	"The U-233 Fission Neutron Spectrum From 0.8 to 10 MeV," December 1973.
WAPD-TM-1132	"Thermal Scattering Cross Sections of U <sub>233</sub> and Th <sub>232</sub> ," March 1974.
WAPD-TM-1137	"BH-99 - A Program for the Statistical Analysis of Data Based on the Extreme Value Distribution," August 1973.
WAPD-TM-1141	"Spatial Distribution of the Indium Activation in a Water Moderated Thorium Oxide Rod Lattice Using a <sup>252</sup> Cf Source," September 1974.
WAPD-TM-1182	"Measurements and Calculations of Heavy Isotopes in Irradiated Fuels and of U-233 Fission Product Poisoning," July 1974.
WAPD-TM-1183	"Decay Heating Measurements and Calculations for Irradiated <sup>235</sup> U, <sup>233</sup> U, <sup>239</sup> Pu, and <sup>232</sup> Th," July 1974.
WAPD-TM-1204	"Absorption Cross Section Measurements for Cf-252 Spontaneous Fission Neutrons," June 1975.

Report No.	Title
<b>1. DEVELOPMENT AND DESIGN (Cont)</b>	
<b>B. Neutronics and Mathematics Development (Cont)</b>	
WAPD-TM-1217	"Monte Carlo Analysis of Direct Measurements of the Thermal Eta (0.025 eV) for U-233 and U-235," April 1975.
WAPD-TM-1218	"Monte Carlo Analysis of Thermal Spectrum Averaged Measurements of Eta of U-233 and U-235," April 1975.
WAPD-TM-1232	"A Monte Carlo Analysis of a Direct Measurement of the Average Neutron Yield from Spontaneous Fission of Cf-252," November 1976.
WAPD-TM-1247	"The Measurement of Boron-10 Lined and Counter Characteristics in an Irradiated Fuel Environment," January 1977.
WAPD-TM-1259	"The Reactivity Perturbation Assay of Irradiated Fuel Rods," October 1976.
WAPD-TM-1266	"PDQ-8 Reference Manual," May 1978.
WAPD-TM-1267	"RCP01 - A Monte Carlo Program for Solving Neutron and Photon Transport Problems in Three Dimensional Geometry with Detailed Energy Description," August 1978.
WAPD-TM-1268	"RCPL1 - A Program to Prepare Neutron and Photon Cross Section Libraries for RCP01," August 1978.
WAPD-TM-1279	"The Measurement of Thorium Absorption Cross Section Shape Near Thermal Energy," November 1976.
WAPD-TM-1288	"Monte Carlo Simulation Using the Meter System with Applications to LWBR," February 1977.
WAPD-TM-1314	"The Calculational Model Used in the Analysis of Nuclear Performance of the Light Water Breeder Reactor (LWBR)," August 1978.
WAPD-TM-1316	"ASBLT - A System of DATATRAN Modules Which Process Core Fuel Loading for Use in As-Built Calculations," February 1979.

Report No.	Title
1. <u>DEVELOPMENT AND DESIGN (Cont)</u>	
B. <u>Neutronics and Mathematics Development (Cont)</u>	
WAPD-TM-1365	"Spatial Distribution Measurements of Fission Neutrons in Water as an Oxygen Data Test," February 1978.
WAPD-TM-1370	"Effect of Simulated Thermal Shield Motion on Nuclear Instrument Response - Measurements and Calculations," August 1979.
WAPD-TM-1550	"Breed - A CDC 7600 Computer Program for the Automation of Breeder Reactor Design Analysis," March 1985.
WAPD-TM-1622	"The Light Water Breeder Reactor Neutron Noise Monitoring Program," September 1987.
C. <u>Thermal and Hydraulic Development</u>	
WAPD-TM-428	"FLOT-1: Flow Transient Analysis of a Pressurized Water Reactor During Flow Coastdown," April 1968.
WAPD-TM-466	"Critical Heat Flux Tests on a Coolant Channel Simulating a Closely Spaced Lattice of Rods," March 1969.
WAPD-TM-568	"WATER: A Large Range Thermodynamic and Transport Water Property FORTRAN-IV Computer Program," December 1966.
WAPD-TM-680	"A Digital Computer Program for Nuclear Reactor Design Water Properties," July 1967.
WAPD-TM-693	"ACT-1: A Digital Program for the Analysis of the Containment Transient During a Loss of Coolant Accident in LWB," May 1967.
WAPD-TM-800	"FLASH-3: FORTRAN IV Program for the Simulation of Reactor Plant Transients in Space and Time," July 1968.
WAPD-TM-840	"FLASH-4: A Fully Implicit FORTRAN IV Program for the Digital Simulation of Transients in a Reactor Plant," March 1969.

Report No.	Title
<b>1. <u>DEVELOPMENT AND DESIGN (Cont)</u></b>	
<b>C. <u>Thermal and Hydraulic Development (Cont)</u></b>	
WAPD-TM-918	"Thermal and Hydraulic Effects of Crud Deposited on Electrically Heated Rod Bundles," September 1970.
WAPD-TM-1013	"Critical Heat Flux and Pressure Drop Tests with Parallel Upflow of High Pressure Water in Bundles of Twenty 0.25 and 0.28 Inch Diameter Rods," January 1975.
WAPD-TM-1070	"HOTROD: A Computer Program for the Subchannel Analysis of Coolant Flow In Rod Bundles," November 1973.
WAPD-TM-1154	"Effect of Axial Locations of Spacers and Hot Spots on the CHF Power of Rods," September 1978.
WAPD-TM-1155	"Critical Heat Flux and Pressure Drop Tests with Vertical Upflow of Water in a 20-Rod Bundle of 0.695-inch Diameter Rods," February 1977.
WAPD-TM-1156	"Development and Manufacture of Electrically Heated Coaxial Rods," August 1976.
WAPD-TM-1162	"Critical Heat Flux and Pressure Drop Tests with High Pressure Water in a Bundle of 0.571- and 0.526-Inch Diameter Rods with a Non-Uniform Radial and Axial Heat Flux Distribution," September 1976.
WAPD-TM-1170	"Critical Heat Flux and Pressure Drop Tests with Parallel Upflow of High Pressure Water in Bundles of Twenty-Nine 0.301 Inch Diameter Rods with a Non-Uniform Radial and Axial Heat Flux Distribution," January 1975.
WAPD-TM-1199	"Flow Patterns in High Pressure Two-Phase Flow - A Visual Study of Water in a Uniformly Heated 4-Rod Bundle," November 1975.
WAPD-TM-1211	"WASP2 - A FORTRAN IV Computer Program for Calculating Water Properties Used in Reactor Safety Analysis," June 1976.
WAPD-TM-1227	"Hydraulic Pressure Pulses with Structural Flexibility: Test and Analysis," April 1976.

Report No.	Title
---------------	-------

1. DEVELOPMENT AND DESIGN (Cont)

C. Thermal and Hydraulic Development (Cont)

WAPD-TM-1249 "FLASH 6: A FORTRAN IV Computer Program for Reactor Plant Loss of Coolant Accident Analysis," July 1976.

WAPD-TM-1249 Addendum "FLASH-6: A FORTRAN IV Computer Program for Reactor Plant Loss of Coolant Accident Analysis," April 1977.

WAPD-TM-1253 "Summary of Several Hydraulic Tests in Support of the Light Water Breeder Reactor Design," May 1979.

WAPD-TM-1290 "Pressure Pulse Test Results and Qualification of the FLASH-34 Flexible Structural Member Model With a Surge Tank Attached to the Test Vessel," August 1977.

WAPD-TM-1296 "FLASH-6 Simulation of Top Injection Emergency Core Cooling Heat Transfer Tests," May 1977.

WAPD-TM-1375 "Hydraulic Pressure Pulses with Elastic and Plastic Structural Flexibility: Test and Analysis," March 1978.

WAPD-TM-1419 "Critical Heat Flux Experiments with a Local Hot Patch in an Internally Heated Annulus," February 1979.

WAPD-TM-1450 "FLASH 6 Simulation of Semiscale Blowdown Data, NRC Standard Problems 2 and 3," September 1979.

WAPD-TM-1479 "Hydro-Mechanical Stability of Slip-Fit Joints in the Light Water Breeder Reactor Vessel," September 1982.

D. Fuel Elements, Fuel Pellets, and Cladding Development

WAPD-TM-514 "CYGRO - Stress Analysis of the Growth of Concentric Cylinders," October 1965.

WAPD-TM-514 Addendum 1 "CYGRO-1 - Stress Analysis of the Growth of Concentric Cylinders," July 1966.

WAPD-TM-547 "CYGRO-2 A FORTRAN IV Computer Program for Stress Analysis of the Growth of Cylindrical Fuel Elements With Fission Gas Bubbles," November 1966.

WAPD-TM-569 "GLUB-1: A FORTRAN IV Digital Computer Program for Waterlogged Fuel Element Analysis," November 1966.

Report No.	Title
1. <u>DEVELOPMENT AND DESIGN (Cont)</u>	
D. <u>Fuel Elements, Fuel Pellets, and Cladding Development (Cont)</u>	
WAPD-TM-570	"Behavior of Gaseous Fission Product in Oxide Fuel Elements," October 1966.
WAPD-TM-574	"Irradiation Performance Capabilities of Oxide Fuel Rods: X-1-u Test of Two 100-Inch Long Highly Rated Annular $ZrO_2 + UO_2$ Fuel Rods," September 1966.
WAPD-TM-583	"Comparisons with Experiment of Calculated Dimensional Changes and Failure Analysis of Irradiated Bulk Oxide Fuel Test Rods Using the CYGRO-1 Computer Program," September 1966.
WAPD-TM-583 Addendum 1	"A Procedure for Analysis of Zircaloy-Clad Bulk Oxide Rods Using the CYGRO-1 Computer Program," April 1967.
WAPD-TM-585	Properties of Zircaloy-4 Tubing," December 1966.
WAPD-TM-586	"Thermal Conductivity of Bulk Oxide Fuels," April 1967.
WAPD-TM-587	"Mechanical Properties of Oxide Fuels," October 1967.
WAPD-TM-591	"Deformation and Collapse of Fuel Rod Cladding Due to External Pressure," January 1967.
WAPD-TM-593	"Examination of a Failed Rod Operating with Molten $UO_2-ZrO_2-CaO$ Fuel," December 1966.
WAPD-TM-595	"Evaluation of the Irradiation Performance of Zircaloy-4 Clad Test Rod Containing Annular $UO_2$ Fuel Pellets (Rod 79-19)," December 1966.
WAPD-TM-596	"Evaluation of the Irradiation Behavior of a Zircaloy-4 Clad Rod Containing Low Density - $UO_2$ Fuel Pellets," January 1968.
WAPD-TM-618	"FIGRO - FORTRAN IV Digital Computer Program for the Analysis of Fuel Swelling and Calculation of Temperature in Bulk-Oxide Cylindrical Fuel Elements," December 1966.

Report No.	Title
<b>1. <u>DEVELOPMENT AND DESIGN (Cont)</u></b>	
<b>D. <u>Fuel Elements, Fuel Pellets, and Cladding Development (Cont)</u></b>	
WAPD-TM-618 Addendum 1	"FIGRO - A CDC-6600 Computer Program for the Analysis of Fuel Swelling and Calculation of Temperature in Bulk-Oxide Cylindrical Fuel Elements," October 1967.
WAPD-TM-618 Addendum 2	"FIGRO (Addendum II) - A CDC 6600 Computer Program for the Analysis of Fuel Swelling and Calculation of Temperature in Bulk-Oxide Cylindrical Fuel Elements," April 1970.
WAPD-TM-628	"Behavior of an Intentionally Defected Fuel Rod Which Ruptured During Irradiation (Rod Bett 79-64D)," July 1969.
WAPD-TM-629	"Irradiation Behavior of Zircaloy-Clad Fuel Rods Containing Dished-End UO <sub>2</sub> Pellets," July 1967.
WAPD-TM-630	"Short-Term Irradiation of Zircaloy-4 Clad Fuel Rod Containing Low-Density or Annular ZrO <sub>2</sub> -UO <sub>2</sub> Ceramic Fuel Pellets; X-1-t Test," June 1968.
WAPD-TM-631	"Performance of Fuel Rods Having 97 Percent Theoretical Density UO <sub>2</sub> Pellets Sheathed in Zircaloy-4 and Irradiated at Low Thermal Ratings," July 1968.
WAPD-TM-649	"A Continuum Dilatation Model for Creep Swelling of Ceramic Nuclear Fuels with Applications," September 1967.
WAPD-TM-651	"Fracture of Cylindrical Fuel Rod Cladding Due to Plastic Instability," April 1967.
WAPD-TM-652	"An Analysis of Transient Clad Strains in Cylindrical Fuel Elements Including the Effects of Oxide Pellet Cracking (STRIPE)," February 1970.
WAPD-TM-664	"Observations on the Irradiation Behavior of Zircaloy-4 Clad Rod Container Low Density ThO <sub>2</sub> -5.3 w/o UO <sub>2</sub> Pellets," December 1969.
WAPD-TM-687	"Analysis of In-Pile Creep Measurements of Bulk Oxide Fuels," May 1967.
WAPD-TM-714	"Effect of Cladding Ovality and Diametral Creep on Fuel Rod Support Systems," December 1970.

Report No.	Title
1. <u>DEVELOPMENT AND DESIGN (Cont)</u>	
D. <u>Fuel Elements, Fuel Pellets, and Cladding Development (Cont)</u>	
WAPD-TM-726	"Elastic Analysis of Thermal Gradient Bowing in Rod-Type Fuel Elements Subjected to Axial Thrust," January 1968.
WAPD-TM-755	"A Non-Linear Continuum Creep Model for the Swelling of Ceramic Nuclear Fuels," April 1968.
WAPD-TM-756	"Estimated Creep Properties of Zircaloy During Neutron Irradiation," May 1968.
WAPD-TM-757	"A Procedure for Calculation of Steady-State Temperature in Zircaloy-Clad, Bulk-Oxide Fuel Elements Using the FIGRO Computer Program," November 1969.
WAPD-TM-758	"The In-Pile Thermal Conductivity of Selected ThO <sub>2</sub> -UO <sub>2</sub> Fuels at Low Depletions," May 1969.
WAPD-TM-770	"Inelastic Bowing of Multispan Fuel Rods Subjected to Axial Thrust and Temperature Gradients," September 1968.
WAPD-TM-777	"Radiation Transfer Across a Spherical Pore in a Linear Temperature Gradient," February 1969.
WAPD-TM-794	"Analysis of Void Migration, Clad Collapse, and Fuel Cracking in Bulk Oxide Fuel Rods," July 1968.
WAPD-TM-805	"Release of Fission Gases from Oxide Fuels," July 1969.
WAPD-TM-807	"The Porosity Correction Factor for Thermal Conductivity of Porous Materials," February 1970.
WAPD-TM-847	"ROBOT - A Computer Program to Solve the Bowing Problem in Rod-Type Fuel Elements," July 1969.
WAPD-TM-850	"Gas Release from Thoria - Base Oxide Fuel Pellets," April 1971.
WAPD-TM-851	"Some Studies on the Oxidation States of Fission Product Iodine (I129) in Irradiated UO <sub>2</sub> ," July 1969.
WAPD-TM-869	"The Characteristics of the Zircaloy-4 Tubing in LWBR Fuel Rods," November 1979.

Report No.	Title
<b>1. <u>DEVELOPMENT AND DESIGN</u> (Cont)</b>	
<b>D. <u>Fuel Elements, Fuel Pellets, and Cladding Development</u> (Cont)</b>	
WAPD-TM-900	"High Temperature Deformation and Burst Characteristics of Recrystallized Zircaloy-4 Tubing," January 1970.
WAPD-TM-901	"In-Pile and Unirradiated Thermal Conductivity of a Single Fired $\text{ThO}_2 + 10\text{ w/o UO}_2$ ," February 1970.
WAPD-TM-908	"Thermal Conductivity of Polycrystalline Thoria and Thoria-Urania Solid Solutions," December 1972.
WAPD-TM-909	"Corrosion of Oxide Nuclear Fuels in High Temperature Water," February 1970.
WAPD-TM-940	"Comparison of Dimensional Changes in Fuel Rods with Predictions Under Cyclic Conditions of Power and System Pressure," March 1970.
WAPD-TM-942	"BUBL-1 - A Statistical Fuel Swelling and Fission-Gas Release Model," September 1970.
WAPD-TM-961	"CYGRO-3 - A Computer Program to Determine Temperatures, Stresses and Deformations in Oxide Fuel Rods," March 1970.
WAPD-TM-962	"A Fuel Swelling Model Based on Chemical Reaction Rate Theory and Incorporating Re-Solution Effects," July 1971.
WAPD-TM-973	"In-Pile Dimensional Changes of Zircaloy-4 Tubing Having Low Hoop Stresses," July 1971.
WAPD-TM-975	"The Plane-Stress Yield Loci for Zircaloy-4 Tubing, Estimated from Knoop Hardness," May 1971.
WAPD-TM-979	"Analysis of the Transient Capability of Rod-Type Fuel Elements," December 1970.
WAPD-TM-980	"Review of Mechanisms for Swelling and Gas Release of Oxide Fuel Rods," October 1970.
WAPD-TM-986	"In-Pile Dimensional Changes of $\text{ThO}_2\text{-UO}_2$ Fuel Rods with Nonfree Standing Cladding," November 1970.

Report No.	Title
1. <u>DEVELOPMENT AND DESIGN (Cont)</u>	
D. <u>Fuel Elements, Fuel Pellets, and Cladding Development (Cont)</u>	
WAPD-TM-1048	"Iodine Stress Corrosion Cracking of Zircaloy-4 Tubing," February 1974.
WAPD-TM-1059	"Re-Solution Effects and Fission Gas Swelling in UO <sub>2</sub> ," June 1973.
WAPD-TM-1060	"Plastic Anisotropy of Polycrystalline Zircaloy," February 1976.
WAPD-TM-1086	"Inelastic Column Buckling of Internally Pressurized Tubes," April 1973.
WAPD-TM-1092	"Effects of Thermal Gradients in Oxide Fuels," March 1973.
WAPD-TM-1094	"Post Irradiation Recovery of Irradiation Damage," August 1973.
WAPD-TM-1104	"The Relationship Between Failure Strains in Burst Tests on Zircaloy Tubing and Wall Thickness Eccentricity," January 1973.
WAPD-TM-1124	"Fission Gas Swelling and Long Range Migration at Low Temperatures," January 1974.
WAPD-TM-1126	"Thermal Analysis of Zircaloy-Clad Fuel Rod End Cap Weldments," November 1973.
WAPD-TM-1148	"Fission Product Iodine in Thoria/Urania Oxides," February 1979.
WAPD-TM-1149	"Halogen Stress Corrosion Cracking of Zircaloy-4 Tubing," July 1974.
WAPD-TM-1153	"A Computer Simulation of the Redistribution of Alkaline Earth Fission Products in Fuel Rods Containing Oxide Fuel," October 1974.
WAPD-TM-1157	"HYDIZ-A 2-Dimensional Computer Program for Migration of Interstitial Solutes of Finite Solubility in a Thermal Gradient," June 1974.

Report No.	Title
<b>1. <u>DEVELOPMENT AND DESIGN (Cont)</u></b>	
<b>D. <u>Fuel Elements, Fuel Pellets, and Cladding Development (Cont)</u></b>	
WAPD-TM-1203	"An Analysis of Iodine Stress Corrosion Cracking of Zircaloy-4 Tubing," February 1976.
WAPD-TM-1236	"Fission Product Distribution in Oxide Fuels," December 1976.
WAPD-TM-1243	"Some High Temperature Mechanical Properties of Internally Pressurized Zircaloy-4 Tubing," February 1976.
WAPD-TM-1248	"The Effects of Internal Surface Flaws, Iodine Concentration and Temperature on the Stress Corrosion Cracking Behavior of Zircaloy-4 Tubing," February 1976.
WAPD-TM-1250	"Flow-Induced Vibrational Wear Behavior of Zircaloy Clad Simulated Fuel Rods in a Grid Support System," March 1987.
WAPD-TM-1255	"A Study of the Compaction Parameters Affecting Cracks in High Density Thorium Oxide Fuel Pellets," September 1980.
WAPD-TM-1263	"High Strain Rate Tensile Tests of Zircaloy at 550°F," February 1976.
WAPD-TM-1270	"Free-Hanging Bow Measurements of LWBR Fuel Rods," March 1979.
WAPD-TM-1272	"Sources of Internal Hydriding in Unirradiated Thoria-Fueled Zircaloy Rods," February 1979.
WAPD-TM-1300	"The CYGRO-4 Fuel Rod Analysis Computer Program," July 1977.
WAPD-TM-1311	"Grain Growth in Thoria and Thoria-Base Fuel Pellets," January 1976.
WAPD-TM-1313	"The Susceptibility of Unirradiated Recrystallized Zircaloy-4 Tubing to Stress Corrosion Cracking," December 1977.

Report No.	Title
1. <u>DEVELOPMENT AND DESIGN (Cont)</u>	
D. <u>Fuel Elements, Fuel Pellets, and Cladding Development (Cont)</u>	
WAPD-TM-1320	"Low Strain Diameter Expansion of Internally Pressurized Zircaloy-4 Tubing at High Temperatures," March 1978.
WAPD-TM-1322	"Corrosion of Zircaloy-4 Tubing in 680°F Water," December 1978.
WAPD-TM-1324	"Effect of Fuel Chips on Cladding Stress in Zircaloy Clad Oxide Fuel Rods," November 1978.
WAPD-TM-1338	"Cladding Deformation into Pellet End Voids," September 1981.
WAPD-TM-1339	"Analysis of Cladding Deformation Over Plenum Axial Gaps in Zircaloy Clad Fuel Rods," December 1982.
WAPD-TM-1340	"Properties of Thoria and Thoria-Urania: A Review," June 1978.
WAPD-TM-1345	"Densification Related Pellet Diameter Shrinkage in Low Burnup Thoria-Base Fuels," September 1978.
WAPD-TM-1347	"Fuel Rod-Grid Interaction Wear; In-Reactor Tests," November 1979.
WAPD-TM-1348	"The Friction Grip Endclosure - A Means for Increasing the Fatigue Life of Fuel Rod End Welds," March 1983.
WAPD-TM-1350	"Fission Gas Release From ThO <sub>2</sub> and ThO <sub>2</sub> -UO <sub>2</sub> Fuels," August 1978.
WAPD-TM-1350 Addendum 1	"Fission Gas Release and Grain Growth in ThO <sub>2</sub> -UO <sub>2</sub> Fuel Irradiated at High Temperature," July 1979.
WAPD-TM-1350 Addendum 2	"Fission Gas Release From High Burnup ThO <sub>2</sub> and ThO <sub>2</sub> -UO <sub>2</sub> Fuels Irradiated at Low Temperature," May 1982.
WAPD-TM-1369	"A Model for Incorporating Fuel Swelling and Clad Shrinkage Effects in Diffusion Theory Calculations," March 1980.

Report No.	Title
1. <u>DEVELOPMENT AND DESIGN (Cont)</u>	
D. <u>Fuel Elements, Fuel Pellets, and Cladding Development (Cont)</u>	
WAPD-TM-1387	"Summary of the Fuel Element Design for LWBR," October 1987.
WAPD-TM-1393	"Cladding Corrosion and Hydriding in Irradiated Defected Zircaloy Fuel Rods," August 1985.
WAPD-TM-1394	"Iodine and Cesium in Oxide Fuel Pellets and Zircaloy-4 Cladding of Irradiated Fuel Rods," March 1979.
WAPD-TM-1397	"Evaluation of Coolable Geometry Adequacy of the LWBR Core During a Loss-of-Coolant Accident (LOCA)," June 1985.
WAPD-TM-1404	"Ex-Reactor Deformation of Externally Pressurized Short Lengths of Fuel Rod Cladding," May 1979.
WAPD-TM-1411	"Stress Corrosion Cracking and Surface Pitting Tests of NiCrFe Alloy Bolts," February 1983.
WAPD-TM-1412	"Corrosion and Hydriding Performance Evaluation of Three Zircaloy-2 Clad Fuel Assemblies After Continuous Exposure in PWR Cores 1 and 2 at Shippingport, PA," January 1980.
WAPD-TM-1412 Addendum	"Corrosion and Hydriding Performance Evaluation of Three Zircaloy-2 Clad Fuel Assemblies After Continuous Exposure in PWR Cores 1 and 2 at Shippingport, PA (Addendum)," January 1984.
WAPD-TM-1431	"Metallographic Standards for Estimating Hydrogen Content of Zircaloy-4 Tubing," February 1982.
WAPD-TM-1495	"A Model for the Oxidation of Zirconium-Base Alloys," May 1981.
WAPD-TM-1501	"A Model for the Transition in the Oxidation of Zirconium Base Alloys," October 1981.
WAPD-TM-1505	"WADER-A Computer Program for Waterlogging Analysis of Defected Fuel Rods," August 1982.

Report No.	Title
1. <u>DEVELOPMENT AND DESIGN (Cont)</u>	
D. <u>Fuel Elements, Fuel Pellets, and Cladding Development (Cont)</u>	
WAPD-TM-1509	"Thermal Tests to Investigate Stability of Externally Pressurized Zircaloy-4 Tubing Over Axial Gaps," July 1982.
WAPD-TM-1514	"A Fracture Mechanics Analysis of Iodine Stress Corrosion Crack Propagation in Zircaloy Tubing Used to Clad Oxide Pellet Fuel Rods," April 1983.
WAPD-TM-1530	"The High-Temperature Ex-Reactor Thermal Conductivity of Thoria and Thoria-Urania Solid Solutions," December 1982.
WAPD-TM-1548	"In-Pile and Out-of-Pile Corrosion Behavior of Thoria-Urania Pellets," January 1987.
WAPD-TM-1603	"Light Water Breeder Reactor Fuel Element Performance Characteristics for Extending Core Life," October 1987.
WAPD-TM-1604	"Internal Hydriding in Defected Zircaloy Fuel Rods - A Review," September 1987.
WAPD-TM-1605	"End-of-Life Nondestructive Examinations of Light Water Breeder Reactor Fuel Rods," October 1987.
WAPD-TM-1606	"End-of-Life Destructive Examination of Light Water Breeder Reactor Fuel Rods," October 1987.
WAPD-TM-1608	"Primary Disassembly of Light Water Breeder Reactor Modules for Core Evaluation," October 1987.
WAPD-TM-1609	"Light Water Breeder Reactor Rod Removal System," October 1987.
WAPD-TM-1610	"Light Water Breeder Reactor Module and Rod Examination Systems," October 1987.
WAPD-TM-1611	"Light Water Breeder Reactor Core Evaluation Operations at ECF," October 1987.
BMI-1775	"Fabrication, Characterization, and Thermal-Property Measurement of ZrO <sub>2</sub> ," June 1966.

Report No.	Title
1. <u>DEVELOPMENT AND DESIGN (Cont)</u>	
D. <u>Fuel Elements, Fuel Pellets, and Cladding Development (Cont)</u>	
BMI-1789	"Thermal Stability of Zirconia and Thoria Based Fuels," January 1967.
BMI-X-10274	"Thermal Diffusivity Measurement of Irradiated Oxide Fuels," February 1970.
E. <u>Mechanical and Structural Development</u>	
BMI-X-10210	"Fabrication, Characterization, and Thermal Property Measurements ThO <sub>2</sub> -UO <sub>2</sub> Fuel Materials," October 1967.
BMI-X-447	"Final Report on Hot-Hardness Measurements on ThO <sub>2</sub> -UO <sub>2</sub> Pellets," August 1967.
WAPD-TM-620	"Sizing of Zircaloy Structural," February 1967.
WAPD-TM-697	"Large Deflection Theory for Inelastic Stresses and Strains," August 1967.
WAPD-TM-712	"A Numerical Method for Determining Strain Distributions in a Plastic or Creeping Material Under Incremental Loading," September 1967.
WAPD-TM-731	"GAPL-1, A Computer Program for the Plastic Stress Analysis of a Horizontal Plate with Pressure Loading Above and Deflection Restraints Below," January 1970.
WAPD-TM-791	"GAPL-3: A Computer Program for the Inelastic Large-Deflection Stress Analysis of a Thin Plate, or Axially Symmetric Shell with Pressure Loading and Deflection Restraints," June 1969.
WAPD-TM-890	"BUSHL - A Computer Program for the Inelastic Buckling of Shells of Revolution under External Pressure and Axial Compression," March 1971.
WAPD-TM-926	"DUZ-2 - A Program for Solving Axisymmetric and Plane Elastic-Plastic Problems on the CDC-6600," September 1970.
WAPD-TM-956	"A Method of Analysis for the Creep-Buckling of Tubes Under External Pressure," October 1970.

Report No.	Title
<b>1. DEVELOPMENT AND DESIGN (Cont)</b>	
<b>E. Mechanical and Structural Development (Cont)</b>	
WAPD-TM-983	"Pore Motion in Solids Resulting from Applied Stresses," February 1971.
WAPD-TM-984	"Improved First Order Analysis of the Plastic Stability of Diffuse Patches in Tubes and Sheets," August 1973.
WAPD-TM-1081	"MATUS: A Three-Dimensional Finite Element Program for Small-Strain Elastic Analysis," March 1973.
WAPD-TM-1134	"A Method for Measurement of Relative Differences in Thermal Expansion Coefficients," June 1978.
WAPD-TM-1140	"BESTRAN - A Technique for Performing Structural Analyses," February 1975.
WAPD-TM-1187	"MDSFP - A Computer Program for Elastic Solution of Three Dimensional Structures by the Finite Element Method," February 1979.
WAPD-TM-1349	"Forces in Bolted Joints: Analysis Methods and Test Results Utilized for Nuclear Core Applications," March 1981.
WAPD-TM-1383	"ACCEPT: A Three-Dimensional Finite Element Program for Large Deformation Elastic-Plastic Creep Analysis of Pressurized Tubes," March 1980.
WAPD-TM-1384	"Finite Deformation Analysis of Continuum Structures with Time-Dependent Anisotropic Elastic Plastic Behavior," March 1980.
WAPD-TM-1538	"Probabilistic Alternatives to Worst Case Analysis: Illustrated by a Linear Approximation for the Clearance between Reactor Core Assembly Structures," January 1984.
WAPD-TM-1601	"Preparation of LWBR Spent Fuel for Shipment to ICPP for Long Term Storage," October 1987.

Report  
No.

Title

1. DEVELOPMENT AND DESIGN (Cont)

E. Mechanical and Structural Development (Cont)

WAPD-TM-1602 "End-of-Life Light Water Breeder Reactor Component Examinations at Shippingport Atomic Power Station and Module Visual and Dimensional Examinations at Expended Core Facility," October 1987.

F. Materials

WAPD-316 "Optical Absorption Spectra of UO<sub>2</sub> and Its Solid Solutions," June 1967.

WAPD-TM-472 "Thermal Expansion and Preferred Orientation in Zircaloy," November 1965.

WAPD-TM-500 "The Effects of Heat Treatment on the Corrosion and Hydrogen Absorption Characteristics of a Zirconium-Niobium-Copper (Zr + 2.5% NB + 0.5% Cu) Alloy," March 1966.

WAPD-TM-519 "Angular Values Between Crystallographic Planes in Zirconium Used in Transmission Electron Microscopy," November 1965.

WAPD-TM-533 "The Corrosion and Hydrogen Pickup of Electron Beam Welded Nickel-Free Zircaloy-2 and Zircaloy-4," March 1966.

WAPD-TM-544 "The Effect of Silicon on the Corrosion and Hydrogen Absorption Characteristics of Zircaloy-4 and Nickel-Free Zircaloy-2," April 1966.

WAPD-TM-590 "Recovery and Recrystallization Kinetics of Cold Worked Zircaloy-4 Plate and Tubing," February 1968.

WAPD-TM-644 "Electron Probe Microanalysis of Irradiated Materials Using a Small Sample Approach," May 1967.

WAPD-TM-746 "Radiation Enhanced Relaxation in Zircaloy-4 and in a Zirconium +2.5 w/o Niobium +0.5 w/o Copper Alloy," May 1968.

WAPD-TM-754 "Further Studies Defining the Aqueous Corrosion Performance of a Zirconium Niobium Copper Alloy," April 1970.

Report No.	Title
1. <u>DEVELOPMENT AND DESIGN (Cont)</u>	
F. <u>Materials (Cont)</u>	
WAPD-TM-759	"Hydrogen Behavior in Zirconium Based Alloys," June 1968.
WAPD-TM-782	"Effects of Pressure Upon the Corrosion of Zircaloy-4," October 1968.
WAPD-TM-906	"The Influence of Prior Corrosion History Upon the Hydrogen Pickup by Zircaloy During Subsequent Exposure in Hot Water," December 1970.
WAPD-TM-943	"Phenomenological Model of In-Pile Stress Relaxation," August 1971.
WAPD-TM-972	"The Corrosion of LWBR Zircaloy Endcap Weldments," February 1973.
WAPD-TM-1027	"Irradiation Creep Based on Dislocation Climb," February 1973.
WAPD-TM-1043	"High Temperature, Time-Dependent Deformation in Internally Pressurized Zircaloy-4 Tubing," October 1974.
WAPD-TM-1049	"Corrosion Properties of NiCrFe Alloy 718 and Nicrobraz-50 (BNi-7)," June 1973.
WAPD-TM-1066	"Viscoelastic Analysis of In-Pile Stress Relaxation," March 1973.
WAPD-TM-1077	"Microstructural Observations on Nickel-Chromium-Iron Alloy 718," January 1973.
WAPD-TM-1123	"Irradiation Induced Primary Creep," April 1974.
WAPD-TM-1192	"Base Materials Property Study of NiCrFe Alloy 718," July 1975
WAPD-TM-1214	"Mechanical Properties of ASTM A-508 Class 4 Steel Used in the LWBR Closure Head and Support Flange," July 1978.
WAPD-TM-1269	"Out-of-Pile Corrosion of Zircaloy Fasteners Containing Non-Pickled Threads," February 1979.

Report No.	Title
------------	-------

---

1. DEVELOPMENT AND DESIGN (Cont)

F. Materials (Cont)

WAPD-TM-1392 "Out-of-Pile Hydriding and Thermal Relaxation of Reactor Fasteners Using Zircaloy Components - The Rem-120 Test," January 1980.

WAPD-TM-1396 "External Pressure Test and Deformation Evaluation of a Zircaloy-4 Hexagonal Shell," January 1984.

WAPD-TM-1426 "Out-of-Pile Accelerated Hydriding of Zircaloy Fasteners," October 1979.

WAPD-TM-1440 "Corrosion and Hydriding of Irradiated Zircaloy Fuel Rod Cladding," September 1982.

WAPD-TM-1517 "A Model for the In-Pile Transition in the Oxidation of Zirconium Based Alloys," March 1982.

WAPD-TM-1536 "Irradiation Growth of Zircaloy," November 1982.

WERL-1114-3 "Hydrogen Accumulation Rates Within Thick-Walled Tubes of Fe-Cr and Fe-Cr-Ni Alloys During Exposure to High-pH, High Temperature, Pressurized Water Containing Dissolved Hydrogen," June 1967.

G. Grids Development

WAPD-TM-1028 "Mechanical and Metallurgical Characteristics of Ni Cr Fe Alloy 718 Joints Brazed with Ni-13 w/o Cr-10 w/o P Filler Metal," October 1974.

WAPD-TM-1063 "Brazing Fixture Materials for Fabrication of AM-350 Fuel Rod Support Grids," August 1976.

WAPD-TM-1131 "Decarburization of AM-350 Stainless Steel LWBR Fuel Rod Support Grids," February 1977.

WAPD-TM-1164 "Fuel Rod/Support Grid Scratching and Friction," October 1979.

WAPD-TM-1184 "The Development of a Corrosion Resistant Brazing Filler Metal for Use in Fabricating LWBR Fuel Rod Support Grids," September 1978.

Report  
No.

Title

1. DEVELOPMENT AND DESIGN (Cont)

G. Grids Development (Cont)

WAPD-TM-1406 "Radiation Induced Dimensional Changes of AM-350 Stainless Steel," August 1982.

WAPD-TM-1607 "End-of-Life Examinations of Light Water Breeder Reactor Grids and Other Module Structural Components," October 1987.

H. Proof of Breeding Development

WAPD-TM-1088 "The Delayed Neutron Pellet Assay Gage," November 1974.

WAPD-TM-1256 "Conceptual Evaluation of Nondestructive Assay of  $^{233}\text{UO}_2$ - $\text{ThO}_2$  Fuel Rods," January 1979.

WAPD-TM-1368 "The Nondestructive Assay of  $\text{UO}_2$ - $\text{ThO}_2$  Fuel Pellets Using the Delayed Neutron Pellet Assay Gage," June 1979.

WAPD-TM-1414 "Design and Operation of a Pilot Irradiated Fuel Assay Gage," June 1982.

WAPD-TM-1547 "Production Irradiated Fuel Assay Gauge Neutron Detection: Description and Testing," April 1986.

WAPD-TM-1555 "Testing of a Production Irradiated Fuel Assay Gauge," July 1986.

WAPD-TM-1612 "Proof of Breeding in the Light Water Breeder Reactor," October 1987.

WAPD-TM-1614 "Use of Production Irradiated Fuel Assay Gage for Determination of the LWBR Fissile Inventory Ratio," September 1987.

2. MANUFACTURING

A. Fuel Pellets and Cladding

WAPD-TM-576 "Fabrication of High and Low Density  $\text{ThO}_2$  Fuel Pellets," December 1966.

Report No.	Title
2. <u>MANUFACTURING (Cont)</u>	
A. <u>Fuel Pellets and Cladding (Cont)</u>	
WAPD-TM-577	"Fabrication of Fuel Pellets from Pot Process Denitrated ThO <sub>2</sub> Powder," July 1966.
WAPD-TM-578	"Fabrication of Solid, Annular, and Dished-End Ceramic Fuel Pellets," May 1967.
WAPD-TM-581	"Fabrication of Fuel Pellets from Sol-Gel Powders," November 1966.
WAPD-TM-582	"Removal of Iron and Boron During Fabrication of Ceramic Fuel Pellets," June 1966.
WAPD-TM-589	"Fractional Factorial Experiment in Fabricating Thoria Fuel Pellets," February 1967.
WAPD-TM-607	"Single Sinter Process for Manufacturing UO <sub>2</sub> -ZrO <sub>2</sub> and UO <sub>2</sub> -ThO <sub>2</sub> Fuel Pellets - A Feasibility Study," December 1966.
WAPD-TM-608	"Fabrication of Low Density Annular UO <sub>2</sub> -ZrO <sub>2</sub> Fuel Pellets," December 1966.
WAPD-TM-721	"Fabrication of Low Density Urania-Thoria Fuel Pellets," June 1968.
WAPD-TM-751	"Hot Pressing Behavior of Sintered Low Density Pellets UO <sub>2</sub> , ZrO <sub>2</sub> -UO <sub>2</sub> , ThO <sub>2</sub> , and ThO <sub>2</sub> -UO <sub>2</sub> ," May 1969.
WAPD-TM-789	"Planetary Ball Milling as a Method of Comminuting Presintered Thoria-Urania Granules," April 1969.
WAPD-TM-843	"Surface Diffusion Measurements in ThO <sub>2</sub> , UO <sub>2</sub> , and ThO <sub>2</sub> -UO <sub>2</sub> ," July 1969.
WAPD-TM-860	"Development of a Powder Milling Technique for Making High Density ThO <sub>2</sub> -UO <sub>2</sub> Pellets," September 1978.
WAPD-TM-880	"Effect of Carbowax Binder and Dextrose Additive on the Microstructure, Density and Open Porosity of Thoria Urania Fuel Pellets," November 1969.
WAPD-TM-1051	"The Homogenization of ThO <sub>2</sub> -UO <sub>2</sub> ," December 1972.

Report No.	Title
2. <u>MANUFACTURING (Cont)</u>	
A. <u>Fuel Pellets and Cladding (Cont)</u>	
WAPD-TM-1172	"The Chemical and Spectrochemical Production Analysis of ThO <sub>2</sub> and <sup>233</sup> UO <sub>2</sub> -ThO <sub>2</sub> Pellets for the Light Water Breeder Reactor Core for Shippingport," June 1975.
WAPD-TM-1200	"The Design and Installation of the Operational Chemistry Facility in Support of LWBR Binary ( <sup>233</sup> U) Fuel Production," May 1979.
WAPD-TM-1226	"LWBR Automated Fuel Rod Loading Verification Gage System," February 1979.
WAPD-TM-1230	"Thorium Oxide Powder Properties which are Important to ThO <sub>2</sub> and ThO <sub>2</sub> -UO <sub>2</sub> Fuel Pellet Fabricating," January 1976.
WAPD-TM-1231	"Thorium Oxide Granule and Compact Properties which are Important to ThO <sub>2</sub> and ThO <sub>2</sub> -UO <sub>2</sub> Fuel Fabrication," January 1976.
WAPD-TM-1288	"Monte Carlo Simulation Using the METER Program with Applications Related to LWBR," February 1977.
WAPD-TM-1289	"Development and Control of the Process for the Manufacture of Zircaloy-4 Tubing for LWBR Fuel Rods," January 1981.
WAPD-TM-1308	"Thoria Powder Process Development," October 1979.
WAPD-TM-1377	"Methods for Assessing Homogeneity in ThO <sub>2</sub> -UO <sub>2</sub> Fuels," June 1978.
WAPD-TM-1410	"Techniques for Chamfer and Taper Grinding of Oxide Fuel Pellets," October 1981.
WAPD-TM-1422	"Uranium-233 Purification and Conversion to Stabilized Ceramic Grade Urania for LWBR Fuel Fabrication," October 1980.
B. <u>Fuel Rods</u>	
WAPD-TM-579	"Fuel Rod End-Closure Welding," October 1966.

Report No.	Title
2. <u>MANUFACTURING</u> (Cont)	
B. <u>Fuel Rods</u> (Cont)	
WAPD-TM-588	"Fabrication of Fuel Rods Containing U-233 Pelletized Oxide Fuels," February 1967.
WAPD-TM-1130	"Detection of Radioactive Surface and Weld Contamination ( $\text{ThO}_2$ and $^{233}\text{UO}_2$ ) on Light Water Breeder Reactor Fuel Rods Using Alpha Ionization Detectors," March 1978.
WAPD-TM-1226	"LWBR Automated Fuel Rod Loading Verification Gage System," February 1979.
WAPD-TM-1228	"Ultrasonic Testing of Nuclear Fuel Rod Welds and Clad," February 1979.
WAPD-TM-1235	"Fuel Rod Welding," February 1979.
WAPD-TM-1239	"The Inspection of Assembled LWBR Fuel Rods for Internal Dimensions and Pellet Integrity Utilizing In-Motion Radiography," February 1979.
WAPD-TM-1278	"The Fabrication and Loading of Fuel Rods for the Light Water Breeder Reactor," March 1986.
WAPD-TM-1315	"Loading Assurance Methods Used in the Manufacture of the Light Water Breeder Reactor," September 1987.
C. <u>Grids</u>	
WAPD-TM-580	"Investigation of Integral Fuel Rod Spacer Fabrication Techniques," December 1966.
WAPD-TM-1063	"Brazing Fixture Materials for Fabrication of AM-350 Fuel Rod Support Grids," August 1976.
WAPD-TM-1131	"Decarburization of AM-350 Stainless Steel LWBR Fuel Rod Support Grids," February 1977.
WAPD-TM-1184	"The Development of A Corrosion Resistant Brazing Filler Metal for Use in Fabricating LWBR Fuel Rod Support Grids," September 1978.

Report  
No.

Title

2. MANUFACTURING (Cont)

C. Grids (Cont)

WAPD-TM-1297 "Brazing of AM-350 Stainless Steel LWBR Fuel Rod Support Grids," February 1979.

D. Fuel Assemblies

WAPD-TM-1317 "Fabrication of Seed, Blanket, and Reflector Fuel Assemblies for the Light Water Breeder Reactor," May 1981.

3. RADIOLOGICAL CONTROL

WAPD-TM-1273 "A Model to Estimate the Local Radiation Doses to Man from the Atmospheric Release of Radionuclides," April 1977.

WAPD-TM-1274 "A Model to Estimate Radiation Dose Commitments to the World Population from the Atmospheric Release of Radionuclides," February 1978.

WAPD-TM-1275 "AIRWAY - A FORTRAN Computer Program to Estimate Radiation Dose Commitments to Man From the Atmospheric Release of Radionuclides," June 1979.

WAPD-TM-1285 "Radiological Control Aspects of the Fabrication of the Light Water Breeder Reactor Core," May 1979.

4. INSTALLATION, DEFUELING, AND SHIPMENT OF EXPENDED FUEL

WAPD-TM-1342 "The Installation of the Light Water Breeder Reactor at the Shippingport Atomic Power Station," May 1983.

WAPD-TM-1551 "Defueling of the Light Water Breeder Reactor at the Shippingport Atomic Power Station," October 1987.

WAPD-TM-1552 "Light Water Breeder Reactor Fuel Module Disassembly at the Shippingport Atomic Power Station," October 1987.

WAPD-TM-1553 "Shipment of the Light Water Breeder Reactor Fuel Assemblies from the Shippingport Atomic Power Station to the Expend Core Facility (Idaho)," October 1987.

Report  
No. \_\_\_\_\_

Title \_\_\_\_\_

5. SUMMARY

WAPD-TM-1600 "Water Cooled Breeder Program Summary Report," October 1987.

APPENDIX B - SUMMARY OF PUBLISHED AWBA TECHNICAL MEMORANDA

Report No.	Title
WAPD-TM-1287	"Analysis of the Boron Pile Measurement of the Average Neutron Yield per Fission of $^{252}\text{Cf}$ ," August 1977.
WAPD-TM-1293	"In-pile Intragranular Densification of Oxide Fuels," October 1977.
WAPD-TM-1299	"Analysis of Homogeneous U-233 and U-235 Critical Assemblies with ENDF/B-IV Data," October 1977.
WAPD-TM-1300	"The CYGRO-4 Fuel Rod Analysis Computer Program," July 1977.
WAPD-TM-1304	"A Model to Predict Swelling, Gas Release, and Densification in Oxide Fuels," June 1978.
WAPD-TM-1305	"In-pile Temperature Dependence of the Yield Strength and Growth of Zircaloy," March 1978.
WAPD-TM-1306	"Post Irradiation Recovery of Growth in Zircaloy," December 1977.
WAPD-TM-1307	"Monte Carlo Analyses of TRX Slightly Enriched Uranium- $\text{H}_2\text{O}$ Critical Experiments with ENDF/B-IV and Related Data Sets," December 1977.
WAPD-TM-1310	"Three Core Concepts for Producing Uranium-233 in Commercial Pressurized Light Water Reactors for Possible Use in Water-Cooled Breeder Reactors," December 1979.
WAPD-TM-1365	"Spatial Distribution Measurements of Fission Neutrons in Water as an Oxygen Data Test," February 1978.
WAPD-TM-1371	"Fuel Utilization Potential in Light Water Reactors with Once-Through Fuel Irradiation," July 1979.
WAPD-TM-1376	"Irradiation Testing of Internally Pressurized and/or Graphite Coated Zircaloy-4 Clad Fuel Rods in the NRX Reactor," November 1978.
WAPD-TM-1378	"Early-in-Life Performance of Short Rod Duplex Pellet Screening (D-1) Test," November 1979.

Report No.	Title
WAPD-TM-1380	"Design Concept for a 900 Mw(e) Scale-Up of the 60 Mw(e) Shippingport LWBR," October 1982.
WAPD-TM-1443	"Fission Gas Release from Oxide Fuels at High Burnups," February 1981.
WAPD-TM-1446	"A Procedure for Obtaining Neutron Diffusion Coefficients from Neutron Transport Monte Carlo Calculations," August 1981.
WAPD-TM-1449	"Integral Testing of Thorium and U-233 Data for Thermal Reactors," June 1979.
WAPD-TM-1451	"Critical Heat Flux Tests with High Pressure Water in an Internally Heated Annulus with Alternating Axial Heat Flux Distribution," September 1979.
WAPD-TM-1456	"Review of Thorium-U-233 Cycle Thermal Reactor Benchmark Studies," March 1980.
WAPD-TM-1460	"Irradiation Performance of Duplex Fuel Pellet Test Rods Depleted to $9 \times 10^{20}$ fissions/cm <sup>3</sup> of Compartment D-1 Test," January 1982.
WAPD-TM-1462	"Critical Heat Flux Experiments in a Circular Tube with Heavy Water and Light Water," May 1980.
WAPD-TM-1467	"Swelling and Gas Release in Oxide Fuels During Fast Transients," February 1981.
WAPD-TM-1468	"A Successive Collision Calculation of Resonance Absorption," July 1980.
WAPD-TM-1469	"Treatment of Epithermal Binding Effects on Neutron Spectra in Transport Theory," March 1982.
WAPD-TM-1470	"Monte Carlo Analyses of Simple U-233O <sub>2</sub> -ThO <sub>2</sub> and U-235 O <sub>2</sub> -ThO <sub>2</sub> Lattices with ENDF/B-IV Data," September 1980.
WAPD-TM-1472	"A Thermomechanical Theory of Materials Undergoing Large Elastic and Viscoplastic Deformation," November 1980.
WAPD-TM-1475	"Critical Heat Flux Experiments in an Internally Heated Annulus with a Non-Uniform, Alternate High and Low Axial Heat Flux Distribution," February 1981.

Report No.	Title
WAPD-TM-1476	"Fabrication of Thin Wall Annular Pellets," May 1982.
WAPD-TM-1477	"Thorium-Uranium Resonance Overlap Effects Attributable to Nuclear Data Uncertainties," March 1981.
WAPD-TM-1480	"Monte Carlo Analysis of Pu-H <sub>2</sub> O and UO <sub>2</sub> -PuO <sub>2</sub> -H <sub>2</sub> O Critical Assemblies with ENDF/B-IV Data," April 1981.
WAPD-TM-1481	"Irradiation Performance of Long Rod Duplex Fuel Pellet Bundle Test - LDR Test," April 1982.
WAPD-TM-1482	"Monte Carlo Analysis of the Slightly Enriched Uranium - D <sub>2</sub> O Critical Experiment LTR11A," November 1981.
WAPD-TM-1487	"Conversion Performance Characteristics of Light Water Moderated Lattices as a Function of Fuel-to-Coolant Volume Ratio," October 1981.
WAPD-TM-1491	"Preliminary Design and Manufacturing Feasibility Study for a Machined Zircaloy Triangular Pitch Fuel Rod Support System (Grids)," July 1981.
WAPD-TM-1492	"Experimental Results of the Irradiation of Long Rod Duplex Pellet Screening Tests in the NRX Reactor (NLDR-1 Test)," July 1982.
WAPD-TM-1493	"Large Light Water Breeder Reactor Vessel Design Study," June 1982.
WAPD-TM-1498	"A Finite Element Procedure for Calculating Three Dimensional Inelastic Bowing of Fuel Rods," May 1982.
WAPD-TM-1499	"Nuclear Calculational Model Used in the Design of the 900 Mw(e) LWBR Scale-Up Concept," October 1982.
WAPD-TM-1504	"The CYGR05 Fuel Rod Analysis Computer Program," October 1982.
WAPD-TM-1505	"WADER - A Computer Program for Waterlogging Analysis of Defected Fuel Rods," August 1982.
WAPD-TM-1506	"Compaction of AWBA Fuel Pellets Without Binders," August 1982.
WAPD-TM-1507	"Co-Compaction of Duplex Fuel Pellets - A Feasibility Report," October 1982.

Report No.	Title
WAPD-TM-1508	"The Characterization of Commercial Thorium Oxide Powders," May 1982.
WAPD-TM-1512	"Potential of Duplex Fuel in Prebreeder, Breeder, and Power Reactor Designs: Test and Analyses," September 1982.
WAPD-TM-1513	"Review of Physics Critical Experiments Using the Thoria Fuel System," July 1982.
WAPD-TM-1515	"Chemical Milling of Zircaloy Tubing to Produce Integral OD Spiral Finned Tubes," February 1982.
WAPD-TM-1518	"PACER - A Monte Carlo Time Dependent Spectrum Program for Generating Few Group Diffusion Theory Cross Sections," September 1982.
WAPD-TM-1519	"Conceptual Design of a Movable Thoria Finger Rod Controlled Light Water Breeder Reactor," October 1982.
WAPD-TM-1520	"Further Experimental Results of the Irradiation of Long Rod Duplex Pellet Screening Tests in the NRG Reactor (NLDR-2/3/4 Tests)," October 1982.
WAPD-TM-1522	"Comparison of Duplex Pellet Fuel Rod Performance to Calculations Using Specified CYGR05 Materials Properties and Procedures," October 1982.
WAPD-TM-1524	"Fabrication of High Density ThO <sub>2</sub> Fuel Pellets from Freeze-Dried Granular Feed," August 1982.
WAPD-TM-1526	"Feasibility Demonstration of Using Wire Electrical Discharge Machining, Abrasive Flow Honing, and Laser Spot Welding to Manufacture High Precision Triangular Pitch Zircaloy-4 Fuel Rod Support Grids," May 1982.
WAPD-TM-1527	"ROBOT-3 - A Computer Program to Calculate the In-Pile Three-Dimensional Bowing of Cylindrical Fuel Rods," October 1982.
WAPD-TM-1528	"Critical Heat Flux and Pressure Drop in an Internally Heated Annulus with an Exterior Conducting Wall," October 1982.
WAPD-TM-1529	"In-Reactor Tests of Externally Pressurized, Short, Unsupported Lengths of Zircaloy Tubing," October 1982.

Report No.	Title
WAPD-TM-1531	"Initial and Equilibrium Cycle Evaluations of Conversion and Loading Performance in Light Water Moderated Lattices as a Function of Fuel-to-Coolant Volume Ratio," October 1982.
WAPD-TM-1532	"The Advanced Water Breeder Applications Work - A Summary," October 1982.
WAPD-TM-1534	"Design Concept of an Advanced Light Water Breeder Reactor Controlled by Movable Fuel," October 1982.
WAPD-TM-1535	"Loss-of-Coolant Accident Evaluations for Advanced Pressurized Water Breeder Reactor Designs," October 1982.
KAPL-4107	"Fuel Utilization Potential in Light Water Reactors with Once-Through Fuel Irradiation Using Various Reactivity Control Methods," November 1978.
KAPL-4154	"Comparison of Two Thorium Fuel Cycles for Use in Light Water Prebreeder/Breeder Reactor System," May 1983.
KAPL-4155	"Conceptual Design of a 1000 M <sub>W</sub> Light Water Moderated Prebreeder/Breeder Reactor System Based on the Seed-Blanket Principle," May 1983.
KAPL-4156	"Local Heat Transfer Where Heated Rods Touch in Axially Flowing Water," May 1983.
KAPL-4157	"Assessment of the Accident Response of a Light Water Moderated Breeder Reactor System," May 1983.
KAPL-4158	"Core Subchannel Thermal-Hydraulic Analysis Methods and Critical Heat Flux Margin in Light Water Breeder Reactors," May 1983.
KAPL-4159	"Thorium Shim Rod Design for a Light Water Reactor," May 1983.
KAPL-4160	"Ultrasonic Thermometry Development for In-Situ Measurement of Nuclear Fuel Temperatures," November 1982.
KAPL-4162	"A High Resolution In-Situ Ultrasonic Corrosion Monitor," December 1982.